

Faculty of Metallurgy and Materials Engineering
VŠB-Technical University of Ostrava

Dissertation

**BIOSYNTHESIS OF METALLIC NANOPARTICLES AND THEIR
APPLICATIONS**

by

Mgr. Adam Schröfel

Materials Science and Engineering

Supervisor: Prof. RNDr. Čapková Pavla, DrSc.

Storrs, Connecticut, USA

March 2012

ABSTRACT

Since the beginning of the century, biosynthesis and biofabrication of the metallic nanoparticles (NPs) have become important methods for nanomaterial preparation. They represent different approaches in comparison with the chemical or physical methods. Although biosynthetic methods have certain limitations, they can be useful in a wide spectrum of application and supplement chemical and physical methods. This dissertation reviews their utilization from sensing and medicinal applications to catalysis and biosorption.

Novel synthesis of gold and silver based bionanocomposites by biologically driven processes employing two diatom strains (*Navicula atomus*, *Diadesmis gallica*) is introduced. Transmission electron microscopy (TEM) and electron diffraction analysis (SAED) revealed a presence of metallic nanoparticles in the experimental suspension of the diatom culture mixed with tetrachloroaurate and silver nitrate. Fabricated bionanocomposite was successfully modified to form magnetically responsible material. Scanning electron microscopy (SEM) and TEM showed that the nanoparticles were associated with the diatom frustules and extracellular polymeric substances (EPS) excreted by the diatom cells. Nature of the metallic nanoparticles was confirmed by X-ray diffraction studies.

Catalytic activity has been proved by the reduction of 4-nitrophenol in presence of NaBH_4 . Bionanocomposite also exhibits the ability to inhibit bacterial growth. Disk diffusion test and minimal inhibition concentration assessment were performed for more detailed description of biocomposite antibacterial properties.

KEYWORDS

biosynthesis; nanoparticles; catalysis; precious metal; antimicrobial agent; magnetic modification; ferrofluid; diatom

AUTHOR DECLARATION

The work submitted in this dissertation is the result of my own investigation, except where otherwise stated.

It has not already been accepted for any degree, and is also not being concurrently submitted for any other degree.

Adam Schröfel

DECLARATION OF CO-AUTHORSHIP

Declaration in each element of the dissertation.	Co-authors
1. Formulating the scientific idea based on theoretical assumptions to be clarified, including formulation of the question to be answered through analytical work and research plans.	Adam Schröfel Pavla Čapková (supervisor)* Gabriela Kratošová (consultant, advisor)*
2. Planning of experiments and analyses, design of the experimental methods in a way that the questions asked under point 1 can be expected to be answered.	Adam Schröfel Gabriela Kratošová*
3. Involvement in analytical work with respect to the concrete experimental studies and investigations. <ul style="list-style-type: none"> Biosynthesis experiments, Sample handling Light Microscopy Scanning Electron Microscopy Transmission Electron Microscopy XRD diffraction ICP-AES, AAS Catalysis experiments, HPLC Antimicrobial assays Magnetic modification and VSM measurements 	Adam Schröfel Markéta Bohunická ¹ Jiří Vaněček ² , Martina Tesařová ² , Adam Schröfel Ivo Vávra ³ , Adam Schröfel Anna Dobija ⁴ , Marta Grzesiak ⁴ Jana Seidlerová*, Šárka Tomisová* Adam Schröfel, Kateřina Horská ⁵ , Pavlína Karlová ⁶ Kateřina Rosenbergová ⁷ Ivo Šafařík ⁵ , Ondřej Životský*, Adam Schröfel
4. Presentation and discussion of the results.	Adam Schröfel

*VŠB-TU in Ostrava

¹Faculty of Science, University of South Bohemia

²Biology Centre, ASCR, Institute of Parasitology, Laboratory of Electron Microscopy

³Slovak Academy of Science, Institute of Electrical Engineering

⁴Polish Academy of Science, Institute of Catalysis and Surface Chemistry

⁶Institute of Chemical Technology Prague

⁵Global Change Research Center, Academy of Science of CR, Institute of Nanobiology and Structural Biology

⁷Faculty of Veterinary Medicine, University of Veterinary and Pharmaceutical Sciences Brno

ACKNOWLEDGEMENT

Thanks are due first to my supervisor, Prof. Pavla Čapková, for her great insights, perspectives, and guidance.

My sincere thanks go to my valued colleague, Dr. Gabriela Kratošová, for her support, insightful comments and constructive criticisms at different stages of my research. I am grateful to her for holding me to a high research standard.

I am grateful to Ivo Vávra and Gabriela Kratošová for introducing me to the world of electron microscopy.

Many thanks to my cello professors Rudolf Weiss and Jan Hališka. They enabled me to have also my "research hobby" besides of playing the cello...

I would also like to express my gratitude to my parents who made me what I am today.

Lastly, I should thank many individuals, friends and colleagues who have not been mentioned here personally in making this educational process a success. I could not have made it without your supports.

TABLE OF CONTENTS

A) AIMS OF DISSERTATION.....	1
B) SCIENTIFIC BACKGROUND AND STATE OF THE ART	2
1. Introduction	2
2. Biological methods of nanoparticle synthesis	2
3. Applications of biogenous metallic nanoparticles	4
3.1. Biosorption, bioremediation and biorecovery	4
3.2. Catalysis applications	6
3.2.1. Biofabricated palladium nanoparticles in organic and inorganic catalysis	6
3.2.2. “BioPd(0)” and “bioPt(0)” as a fuel cells electro-catalysts.....	10
3.2.3. 4-nitrophenol reduction catalysts	13
3.2.4. Other heterogeneous catalysis reactions	14
3.3. Medical applications.....	15
3.3.1. Antimicrobial applications	16
3.3.1.1. Antibacterial activity	16
3.3.1.2. Antifungal and combined activity	20
3.3.1.3. Antiviral activity	22
3.3.1.4. Antibacterial fabrics and cloth	23
3.3.1. Cancer treatment and drug delivery applications.....	24

3.3.2. Biocompatibility	26
3.3.3. Other medical applications	27
3.4. Electrochemical and sensing applications	27
3.4.1. Sensors	28
3.4.2. Electrochemical applications and properties	29
3.5. Optical, bio-imaging, bio-labeling applications	31
3.6. Magnetic applications	33
3.7. Further applications and properties	35
4. Diatoms	36
C) EXPERIMENTAL PART	38
1. Materials and Methods	38
1.1. Diatom strains and cultures	38
1.2. Diatoms Biosynthesis Experiments	38
1.3. UV-VIS Analyses and Light Microscopy (LM)	39
1.4. Elemental analysis	40
1.5. Transmission Electron Microscopy (TEM) and Scanning Electron Microscopy (SEM)	40
1.6. Image analysis	40
1.7. X-ray diffraction (XRD)	40
1.8. Magnetic modification	41
1.9. Catalytic Study	41
1.10. Antimicrobial Study	42
2. Results and Discussion	43

2.1. Nanoparticle biosynthesis – bionanocomposite formation.....	43
2.1.1. Gold based bionanocomposite formation.....	43
2.1.2. Silver based bionanocomposite formation	43
2.2. Elemental Analysis and XRD Study	45
2.3. Light Microscopy	48
2.4. TEM.....	50
2.5. SEM.....	55
2.5.1. SEM analysis of NA_Au and DG_Au	56
2.5.2. SEM analysis of magnetically modified BNC	58
2.6. Possible mechanism of nanoparticle biosynthesis.....	59
2.7. Magnetization Measurements.....	60
2.8. Catalysis – 4-NP reduction	62
2.9. Antimicrobial assessment.....	67
D) CONCLUSIONS.....	69
E) LIST OF FIGURES.....	72
F) LIST OF TABLES.....	75
G) LIST OF ABBREVIATIONS.....	76
H) REFERENCES	78
I) AUTHORS PUBLICATIONS:	101

A) AIMS OF DISSERTATION

Specific goals of the dissertation are to:

- write a literature review in the metallic nanoparticle biosynthesis field
- develop protocol for biosynthesis of noble metal nanoparticles employing algae
- produce and characterize functional silica based bionanocomposite containing noble metal nanoparticles and diatom frustules
- adjust and modify the material for further usage
- prove the material efficiency and functionality in application

B) SCIENTIFIC BACKGROUND AND STATE OF THE ART

1. Introduction

“Green” approaches toward nanotechnology research have become widely used in last few years. Inspiration by nature and processes inside the living organisms can produce new opportunities and perspectives for many branches of research in nanotechnology. Particularly, synthesis of NPs and nanostructures can easily benefit from the use of nature processes found in cells. The right attitude towards the world of biomolecules, functional groups, enzymes and other important factors leads to a large number of advantages compared to common chemical and physical methods.

Scientific interest in NPs originates from their unique and variable properties. They create a link between properties of bulk material and individual atoms or molecules. The same materials exhibit different properties when studied at the nanoscale compared to the bulk materials. For instance, NPs have a much larger surface area, higher reactivity, and different chemical properties compared to their respective bulk materials. Also, the size of NPs is similar to the wavelength of light. This results in unique optical properties of NPs such as transparency.

New applications of metallic NPs are taking place in varied areas such as electronics, coating technologies, packaging, cosmetics, biosensing, medicine, and will be discussed in corresponding sections.

2. Biological methods of nanoparticle synthesis

Because of certain limitations of current physical and chemical methods, there is an increasing need to develop approaches which will be high-throughput, energy saving, occur under normal conditions, and environmentally benign. Consequently, researchers have turned to biological systems for inspiration. Bioprocesses mediated by living organisms (employing their cells, enzymes, transport chains etc.) therefore became important for metallic NP

synthesis. For this purpose, we have a vast variety of organisms in nature such as viruses, bacteria, yeast, fungi, algae, plants and plant products at our disposal.

The ability to form inorganic materials by using many different organisms either intra- or extracellularly has been well known for almost 30 years.¹ Many biotechnological applications, such as the remediation of toxic metals by the reduction to zero-valent metal nanoparticles, employ bacteria.² Therefore, many microorganisms (e.g. fungi, bacteria) have been found as possible nanofacilities for NP fabrication. These nature-derived processes contributed and led to development of relatively new biosynthesis methods for fabrication of nano- and microscale inorganic materials by microbes and other living organisms.³ Until now, a large number of both unicellular and multicellular organisms have been known to produce metallic NPs.⁴

Biosynthesis of NPs is becoming an emerging consequence of an overlap between nano- and biotechnology. In the last few years it has received attention due to its potential to develop environmentally benign technologies in material science. But in fact, NP biosynthesis is still a “chemical” approach inside of a living organism. Living cells are extremely complex systems with thousands of molecules. These molecules have varied functional groups (such as hydroxyl, amine etc.) each of which can facilitate metal reduction. Therefore, it is extremely difficult to map a specific location and process directly responsible for NP growth. This uncertainty can result in specific drawbacks while using biosynthesis methods. The resulting matter is usually a mixture of cells (cell debris) and NPs, accompanied by thousands of metabolic products and other molecules. It is sometimes very complicated to separate these tiny product particles from the cell debris. Moreover, the surrounding matrix and capping proteins contribute to NP stability⁵ and can influence their properties. Among the other disadvantages is the toxicity of precursors (such as AgNO₃) to the target organisms. Therefore, this does not allow the usage of higher concentrations of the salts resulting in lower capacity and yield.

In this section, I provide a brief overview of the current research worldwide on the use of organisms such as bacteria, cyanobacteria and actinomycetes (prokaryotes), as well as algae, yeast, fungi and plants (eukaryotes) in the biosynthesis of metal NPs with emphasize on their applications.

3. Applications of biogenous metallic nanoparticles

Regarding the broad scope of current research, we can divide these applications into several groups. The following division is based primarily on the usage of biofabricated NPs (even though the chemical composition and source organisms will be mentioned too).

3.1. Biosorption, bioremediation and biorecovery

Different organisms have ability to change metal oxidation state and concomitantly deposit resulting metal compounds and zero-valent metals on the cell surface or inside their cells. The biomass of common organisms (including algae, fungi, bacteria, actinomycetes, yeast etc.) along with some biopolymers and biowaste materials. have been known to bind precious metals.

In particular, recovery of precious metals like gold, silver, palladium, and platinum is becoming more appealing due to their increasing market prices and various industrial applications. Conventional technologies (e. g. ion exchange, chemical binding, surface precipitation) which have been developed for the recovery of such metals are neither efficient nor economically attractive. Biosorption represents a biotechnological innovation as well as a cost effective tool for recovery of precious metals from aqueous solutions. In particular, the microbial mechanisms involved in the biosorption and bioaccumulation processes have been extensively studied in natural environments. Researchers have recently gained interest in the applications of microbe–metal interactions in biotechnology, nanotechnology or material engineering. The connection between the recently discovered ability of NP biosynthesis and the thoroughly investigated biosorption is apparent. There is an abundance of suitable and high quality literature in the field of biosorption⁶⁻¹⁰. I will discuss some examples and current trends of metallic NPs biosorption applications, specifically with regard to their application for metal bioaccumulation and recovery, soil and water treatment, and waste remediation (see Table 1). Additionally, the NPs formation and ion bioreduction process will be described. For more exhaustive analysis of biosorbed and biofabricated palladium and platinum catalysts see section 3.2.

As an instance of noble metal biorecovery, Chakraborty¹¹ described experiments of gold bioaccumulation with two diatom strains. These unicellular brown algae are one of the most abundant organisms both in marine and fresh water ecosystems on Earth. Due to a low detection limit and also with regard to biosorption of other radioactive heavy metals in previous studies, gold radionuclide ¹⁹⁸Au was used. In a subsequent study,¹² AuNP formation process was described and comparison in biorecovery abilities between prokaryotic and eukaryotic algal genera was performed. Gold biosorption and bioreduction with another brown alga *Fucus vesiculosus* was also reported¹³, describing pH dependence and stages of the bioreduction process. Results of these studies indicate that live algal biomass may be a viable cost effective process for biorecovering gold.

Table 1. Biosorption applications

NP	Organism used	Application	Reference
Au	<i>Nitzschia obtusa</i> , <i>Navicula minima</i>	bioaccumulation	Chakraborty et al. 2006 ¹¹
Au	<i>Lyngbya majuscula</i> , <i>Spirulina subsalsa</i> , <i>Rhizoclonium</i> <i>hieroglyphicum</i>	bioaccumulation, biorecovery	Chakraborty et al. 2009 ¹⁴
Au	<i>Fucus vesiculosus</i>	bioaccumulation, biorecovery	Mata et al. 2009 ¹³
Ag	<i>Pleurotus platypus</i>	biosorption	Das et al. 2010 ¹⁵
Pt	<i>E. coli</i>	biosorption, biorecovery by incineration	Won et al. 2010 ¹⁶
Au	<i>Sargassum sp.</i>	biosorption, biorecovery by incineration	Sathiskumar et al. 2010 ¹⁷
Ag	<i>Saccharomyces cerevisiae</i>	As(V) removal	Selvakumar et al. 2011 ¹⁸
Ag	<i>Aeromonas sp. SH10</i>	silver-containing wastewater treatment	Zhang et al. 2007 ¹⁹
MnO ₂	<i>Bacillus sp.</i> (MTCC10650)	Mn bioremediation	Sinha et al. 2011 ²⁰

Bioaccumulation of silver ions Ag(I) from aqueous solution is reported by Das et al.¹⁵, accompanied with kinetics studies and thermodynamic calculations on sorption of silver ions on gilled macrofungus *Pleurotus platypus*. This paper represents a modern and innovative

approach for the study of interactions between biomass and metal ions. Zhang et al.¹⁹ demonstrated the potential use of gram-negative, facultative anaerobic bacteria *Aeromonas* SH10 in silver-containing wastewater treatment due to its high silver biosorption ability. The biomass was proven to strongly absorb and turn into AgNPs Ag^+ and $[\text{Ag}(\text{NH}_3)_2]^+$ ions. The maximum uptake of $[\text{Ag}(\text{NH}_3)_2]^+$ was $0.23 \text{ g(Ag).g}^{-1}$ (cell dry weight).

A concrete example of platinum recovery is presented by Won et al.¹⁶ by means of biosorption and subsequent incineration of polyethyleneimine (PEI) modified biomass (prepared by attaching PEI onto the surface of inactive *E. coli* biomass). Wastewater containing platinum used for the recovery study was obtained from an industrial laboratory for inductively coupled plasma (ICP). Recovery efficiency of platinum in ash after incineration was over 98.7%. A similar study with gold solution and easily accessible biomass of *Sargassum sp.*¹⁷ confirms recovery efficiency of more than 90%.

Since ground water contamination by arsenic has been a major problem in a lot of Asian regions,¹⁸ a very promising solution to this problem comes from a study by Selvakumar et al. involving the development of adsorbent containing silver nanoparticles for As(V) removal. Silver reducing capabilities of a novel yeast strain of *Saccharomyces cerevisiae* was used in this paper.

A heavy metal resistant strain of *Bacillus sp.* (MTCC10650) is reported²⁰ to exhibit the bioaccumulation of manganese (in form of MnO_2 NPs) simultaneously to its remediation.

3.2. Catalysis applications

Based on the basic knowledge of inorganic catalysis, noble metal NP catalysts are very attractive when compared to bulk catalyst – they have a high surface to volume ratios and their surface atoms are very active.

3.2.1. Biofabricated palladium nanoparticles in organic and inorganic catalysis

The first large group of biosynthesized nanomaterials with catalytic activity is represented by palladium NPs (Table 2). This topic is also described more in detail by recent review by De Corte et al.²¹ Baxter-Plant et al.^{22,23} reported usage of cell surface of three different

species of *Desulfovibrio* (G⁻ sulfate-reducing bacteria) for manufacturing the novel bioinorganic catalyst via reduction process of Pd(II) to Pd(0). Although the presence of reducing agent is necessary (e.g. in form of H₂) for the Pd(0) genesis, reduction process is critically influenced by the bacteria presence and we can indicate this biosorption process as a biosynthesis. On the other hand, reduction in the absence of cells does not lead to the formation of Pd(0) NPs.²⁴ This catalyst on “palladised cells” was used for reductive dehalogenation of chlorophenol (CP) and selected polychlorinated biphenyl (PCB) types. The same organism was used for dehalogenation of the other environmentally prevalent PCBs and polybrominated diphenyl ether.²⁵ The versatility of “bioPd” catalyst is also demonstrated in various reactions including dehalogenation of flame retardants such polybrominated diphenyl ether (PBDE) or tris(chloroisopropyl)phosphate (TCPP). Authors also compare effectiveness between biocatalyst, chemically reduced Pd(II) and commercial Pd(0) catalysts. Although chemically reduced Pd(II) and commercial Pd(0) were more effective debromination agents, “bioPd” dechlorinated TCPP was five times more effective than using commercial Pd(0) catalyst.²⁶

Using of *Desulfovibrio desulfuricans* in comparison with other bacterial strains has been also demonstrated: Redwood et al.²⁷ reported comparison of catalytic efficiency of and *Rhodobacter sphaeroides* in dehalogenation of PCBs and pentachlorophenol. Gram negative (G⁻) and Gram positive (G⁺) bacterial strains *D. desulfuricans* and *Bacillus sphaericus* took place as Pd(II) reducing agent for catalysis of itaconic (methylene succinic) acid.²⁸ Remarkably, the same research group published experiments in non-aqueous solvents (methanol). Specifically, experiments leading to hydrogenations of 4-azidoaniline hydrochloride and 3-nitrostyrene, and hydrogenolysis (reductive debromination) of 1-bromo-2-nitrobenzene were conducted.²⁹

Another type of G⁻ bacteria, *Shewanella oneidensis*, was also used for biofabrication of Pd(0) catalyst (with H₂, formate, lactate, pyruvate or ethanol as electron donors) for dehalogenation purpose.³⁰ The obtained bioPd(0) NPs had the ability to reductively dehalogenate PCB congeners in aqueous and sediment matrices from anonymous industrial plant. Moreover, the aforementioned paper offers a comparison with commercially available palladium powders. Further studies of *S. oneidensis* show differences between catalytic reactivity of Pd(0) crystals formed on viable or non-viable biomass. The relatively large and

densely covering Pd(0) crystals (non-viable biomass) exhibited high catalytic reactivity towards hydrophobic molecules such as polychlorinated biphenyls. In contrast, the smaller and more dispersed nanocrystals on a viable bacterial carrier were catalytically active towards anionic pollutant perchlorate.³¹

S. oneidensis bacterial strain was also used for removal of the pesticide lindane (γ -hexachlorocyclohexane or γ -HCH) by catalytic reduction of γ -HCH to benzene (as more efficient than with commercial powdered Pd(0))³². The same study introduces a membrane reactor technology suitable for dechlorination of γ -HCH polluted wastewater at a low-flux synthetic dialysis membrane. Similar implementation of membrane reactor was introduced for degradation process of diatrizoate - iodinated contrast media (ICM). Although currently applied techniques such as advanced oxidation processes exhibit only limited removal efficiencies of ICM, work by Hennebel et al.³³ showed that membrane contactors with encapsulated biogenic NPs can be effective for contaminated water treatment. A similar study from the same group of scientists reported usage of membrane reactors in the treatment of secondary effluents of sewage treatment plants.³⁴

The topic of reactor technology for “bioPd” catalysts is further pursued in works dealing with dechlorination of trichlorethylene (TCE) in a pilot-scale membrane reactor³⁵ and dechlorination of TCE by encapsulated palladium NPs in a fixed bed reactor.³⁶ Polyurethane cubes empowered with “bio-Pd” were implemented in a fixed bed reactor for the treatment of water containing TCE. This study showed that the influent recycle configuration resulted in a cumulative removal of 98% TCE after 22 h (with ethane as main reaction product). The same reactor in a flow through configuration achieved removal rates up to 1.059 mg of TCE per gram of “bio-Pd” and day.

Feasibility of other organisms for reduction of Pd(II) to Pd(0) for organic catalysis has been also demonstrated by other studies. Bacterial strains *Rhodobacter capsulatus* and *Arthrobacter oxidans* were employed in “bioPd” formation for partial hydrogenation of 2-butyne-1,4-diol to 2-butene-1,4-diol³⁷. This “bioPd” was proven to be a highly selective catalyst for partial hydrogenation reactions. Bunge et al.²⁴ tested possibilities of three bacterial strains (*Cupriavidus necator*, *Pseudomonas putida*, *Paracoccus denitrificans*) on bioPd(0) catalysis of hydrogen production from hypophosphite and further discusses the hypothetical mechanism of bacterial reduction of Pd(II) to Pd(0). Remarkably, Pd(0)

catalysts fabricated by the organisms mentioned above were used also for catalysis of Suzuki–Miyaura and Mizoroki–Heck reactions (briefly C - C bond formation) by Søbberg et al.³⁸ and Gauthier et al.³⁹. The enormous importance of these reactions for organic synthesis was confirmed by the Nobel Prize in Chemistry 2010 for their discoverers – Richard F. Heck, Ei-ichi Negishi and Akira Suzuki. Moreover, aforementioned studies also contribute to the hot issue of metal waste management and waste recovery.

Interestingly, Jia et al.⁴⁰ published a bioreduction method – reduction of palladium chloride by crude water extract – with plant *Gardenia jasminoides* Ellis'. Abilities of this “bioPd(0)” nanocatalyst were tested and documented on hydrogenation reaction of p-nitrotoluene. The catalysts showed a conversion of 100% under conditions of 5 MPa, 150°C for 2 h. The selectivity of the product – p-methyl-cyclohexylamine – achieved 26.3%. The “bioPd(0)” catalyst was recycled five times keeping its activity and without any agglomeration. Wu et al. 2011 published an example of combination and utilization of biosynthesized Pd nanoparticles with artificial TiO₂ (Degussa P25)⁴¹. Pd NPs prepared with gardenia extract and loaded with TiO₂ were beneficial to enhance the photocatalytic activity for H₂ evolution from pure water. This is a promising avenue for the synthesis of novel photocatalytic materials.

It is also well known that bacterial species such as *Shewanella alga*, *Pseudomonas putida* or *Desulfovibrio vulgaris*⁴² may be used to biologically treat contaminated wastewaters by reduction of Cr(VI) – known as a carcinogen and mutagen – to Cr(III) – a relatively non-toxic and non-carcinogenic form. Some studies showed that “bio-Pd(0)” is more efficient at Cr(VI) reduction than live cells of *D. desulfuricans* or chemically reduced Pd(II), using hydrogen as the electron donor⁴³. Pd(0) mediates hemolytic bond cleavage of H₂, with the production of radical H*, which can then donate its electron to Cr(VI). Continuous-flow studies using *D. vulgaris* Bio-Pd(0) with agar as the immobilization matrix were investigated⁴⁴ showing the effect of Bio-Pd(0) loading, inlet Cr(VI) concentration, and flow rate on the efficiency of Cr(VI) reduction. Mabbett et al.⁴⁵ presents the possibility of mixed-metal-bioPd(O) catalysts employing *D. desulfuricans*, Pd(II) and Pt(IV) or industrial waste leachates (e.g. Rh, Cu, Fe, Al, Pt). Two flow-through reactor systems were also compared. Similar experiments were performed by Beauregard et al.⁴⁶ using *Serratia sp.* and formate as the electron donor. Remarkably, Cr species concentrations within the reactor were controlled by spatial mapping

using a magnetic resonance imaging technique ($\text{Cr(VI)}_{(\text{aq})}$ is non-paramagnetic while $\text{Cr(III)}_{(\text{aq})}$ is paramagnetic).

Chidambaram et al.⁴⁷ published experiments where the electron donor is substituted by fermentation process (fermentatively produce hydrogen in presence of glucose) in bacteria *Clostridium pasteurianum*. This organism also acted as reductant for Pd(II) reduction into form PdNPs “bio-Pd(0)” that primarily precipitated on the cell wall and in the cytoplasm. Finally, *Escherichia coli* (and its mutants), contribute to the “bioPd(0)” catalyst knowledge. Experiments with three types of hydrogenases encoded by its bacterial DNA were performed by Deplanche et al.⁴⁸, based on optimal catalytic activity in Cr(VI)/Cr(III) system.

3.2.2. “BioPd(0)” and “bioPt(0)” as a fuel cells electro-catalysts

A similar approach to the utilization of microorganisms with the ability to enzymatically reduce and absorb palladium, platinum and other precious metals was also used for the manufacturing of a bio-fuel cell for the electric power production. Since fuel cells have been identified as a possible future technology to power motor vehicles, generators and portable electronic device⁴⁹.

In work by Yong et al.⁵⁰ Pt(0) and Pd(0) bio-accumulated by *D. desulfuricans* was applied onto carbon paper and tested as anodes in a polymer electrolyte membrane (PEM) fuel cell for power production and compared to commercial fuel cell grade Pt catalyst. A similar strategy has also been suggested by using yeast-based biomass, immobilized in polyvinyl alcohol cryogels, for the manufacture of a Pt(0) fuel cell. This is then used to generate electrical energy from renewable sources such as glucose and ethanol⁵¹. Finally, the dried biomass-supported palladium (*Shewanella oneidensis*) was tested as an anode catalyst in a PEM fuel cell for power production. It was shown to have a maximum power generation comparable to the commercial catalyst⁵².

A study of fusion of waste biorefining and cheap nanocatalyst for fuel cells and power generation employing *D. desulfuricans*, *E. coli* and *C. metallidurans*, carbon paper and proton exchange membrane fuel cell was recently published⁵³. Using an *E. coli* MC4100 strain, a mixed metallic catalyst was manufactured from an industrial processing waste. This mixed-metal biocatalyst gave approximately 50% of the power output compared to

commercial or “bioPd” *D. desulfuricans* catalyst. Electrical energy production efficiency of biocatalyst fabricated by aforementioned *E. coli* (parent) strain and its derived mutant strain IC007 (as well as a comparison with *D. desulfuricans*) is further discussed by Orozco et al.⁵⁴

Another electrocatalysis application with modified electrodes is also mentioned in section 3.4.1.

Table 2. Catalysis applications

NP	Organism used	Application	Reference
Pd	<i>Desulfovibrio vulgaris</i> , <i>D. desulfuricans</i>	dehalogenation of CP and PCBs	Baxter-Plant et al. 2003 ²²
Pd	<i>D. desulfuricans</i>	dehalogenation of CP and PCBs	Baxter-Plant et al. 2004 ²³
Pd	<i>D. desulfuricans</i>	dehalogenation PCBs and polybrominated diphenyl ether	Harrad et al. 2007 ²⁵
Pd	<i>D. desulfuricans</i>	dehalogenation of flame retardant materials	Deplanche et al. 2009 ²⁶
Pd	<i>D. desulfuricans</i> , <i>Rhodobacter sphaeroides</i>	dehalogenation of (PCBs) and penta-CP	Redwood et al. 2007 ²⁷
Pd	<i>D. desulfuricans</i> , <i>Bacillus sphaericus</i>	hydrogenation of itaconic acid	Creamer et al. 2007 ²⁸
Pd	<i>D. desulfuricans</i> , <i>B. sphaericus</i>	hydrogenation, reduction and selective dehalogenation in non-aqueous solvents	Creamer et al. 2008 ²⁹
Pd	<i>R. capsulatas</i> , <i>Arthrobacter oxidans</i>	hydrogenation of 2-Butyne-1,4-diol	Wood et al. 2010 ³⁷
Pd	<i>Cupriavidus necator</i> , <i>Pseudomonas putida</i>	Suzuki–Miyaura and Mizoroki–Heck reactions	Søbberg et al. 2009 ³⁸
Pd	<i>C. necator</i>	catalysis of C - C bond formation	Gauthier et al. 2010 ³⁹
Pd	<i>C. necator</i> , <i>P. putida</i> , <i>Paracoccus Denitrificans</i>	hydrogen production from hypophosphite	Bunge et al. 2010 ²⁴

(continued)

Table 2. (continued)

NP	Organism used	Application	Reference
Pd	<i>Gardenia jasminoides</i> Ellis	hydrogenation of p-nitrotoluene	Jia et al. 2009 ⁴⁰
Pd	<i>Shewanella oneidensis</i>	dehalogenation of chlorophenol and PCBs	De Windt et al. 2005 ³⁰
Pd	<i>S. oneidensis</i>	dehalogenation of perchlorate and PCBs	De Windt et al. 2006 ³¹
Pd	<i>S. oneidensis</i>	dechlorination of lindane	Mertens et al. 2007 ³²
Pd	<i>S. oneidensis</i>	dechlorination of TCE, membrane reactor	Hennebel et al. 2008 ³⁵
Pd	<i>S. oneidensis</i>	dechlorination of TCE, fixed bed reactor	Hennebel et al. 2009 ³⁶
Pd	<i>S. oneidensis</i>	degradation process for diatrizoate, ICM	Hennebel et al. 2010 ³³
Pd, Mn	<i>Pseudomonas putida</i>	secondary effluents of sewage treatment plants removal	Forrez et al. 2011 ⁵⁵
Pd, Pt	<i>D. desulfuricans</i>	continuous reduction Cr(VI) to Cr(III)	Mabbett et al. 2006 ⁵⁶
Pd	<i>D. vulgaris</i> , <i>D. desulfuricans</i>	reduction of Cr(VI) to Cr(III)	Humphries et al. 2006 ⁴⁴
Pd	<i>Serratia sp.</i> (NCIMB)	reduction of Cr(VI) to Cr(III)	Beauregard et al. 2010 ⁴⁶
Pd	<i>E. coli</i> mutant strains	reduction of Cr(VI) to Cr(III)	Deplanche et al. 2010 ⁴⁸
Pd	<i>Clostridium pasteurianum</i>	reduction of Cr(VI) to Cr(III)	Chidambaram et al. 2010 ⁴⁷
Pt	waste yeast biomass	fuel cell; energy production	Dimitriadis et al. 2007 ⁵¹
Pd, Pt	<i>D. desulfuricans</i>	fuel cell; energy production	Yong et al. 2007 ⁵⁰
Pd	<i>D. desulfuricans</i> , <i>E. coli</i> , <i>C. metallidurans</i>	waste biorefining, fuel cells	Yong et al. 2010 ⁵³
Pd	<i>E. coli</i> MC4100 (parent), mutant (IC007)	fuel cell; energy production	Orozco et al. 2010 ⁵⁴
Pd	<i>S. oneidensis</i>	fuel cell; energy production	Ogi et al. 2011 ⁵²
Au	<i>Sesbania drummondii</i>	reduction of 4 - nitrophenol	Sharma et al. 2007 ⁵⁷

(continued)

Table 2. (continued)

NP	Organism used	Application	Reference
Au	<i>Cacumen platycladi</i>	reduction of 4 - nitrophenol	Huang et al. 2009 ⁵⁸
Ag	<i>Sepia esculenta</i> cuttle-bone organic matrix	reduction of 4 - nitrophenol	Jia et al. 2008 ⁵⁹
Ag, Au	<i>Breynia rhamnoides</i>	reduction of 4 – nitrophenol	Gangula et al. 2011 ⁶⁰
Pd/Au	<i>Cupriavidus necator</i>	reduction of 4 – nitrophenol	Hosseinkhani et al. 2012 ⁶¹
Au	<i>Cacumen platycladi</i>	propylene epoxidation	Du et al. 2011 ⁶²
Au	<i>Cacumen platycladi</i>	propylene epoxidation	Zhan et al. 2011 ⁶³
Au	<i>Camellia sinensis</i>	reduction of methylene blue	Gupta et al. 2010 ⁶⁴
Fe	<i>Camellia sinensis</i>	degradation of aqueous cationic and anionic dyes	Shahwan et al. 2011 ⁶⁵
Fe/Pd	<i>Camellia sinensis</i>	dechlorination of TCE	Smuleac et al. 2011 ⁶⁶
Pt	honey	preparation of organic dye	Venu et al. 2011 ⁶⁷
Pd	<i>Gardenia jasminoides</i>	H ₂ evolution from pure water	Wu et al. 2011 ⁴¹

3.2.3. 4-nitrophenol reduction catalysts

The presence of toxic pollutants such as nitro-aromatic compounds in soil and water is a result of incomplete combustion of fossil fuels and their usage as chemical feedstock for the synthesis of explosives, pesticides, herbicides, dyes, pharmaceuticals, etc. The headlong and reckless utilization of these pollutants in the past has resulted in wide-ranging environmental pollution. The usage of biosynthesized NPs capable to catalyze degradation of nitro-aromatics and other chemicals (and then together with microbial remediation), would be a great contribution to this particularly topical issue.

As the first report of a NP-bearing biomatrix directly reducing a toxic pollutant 4-nitrophenol (*p*-nitrophenol; 4-NP), Sharma et al.⁵⁷ published experiments on the growth of *Sesbania* seedlings in chloroaurate Au(III) solution. This procedure resulted in the accumulation of gold with the formation of stable AuNPs in plant tissues. The catalytic

effectiveness of the biomass with AuNPs was documented by the reduction of aqueous (4-NP).

Remarkably, extensive research was performed using twenty-one traditional Chinese medicinal plant and herb species⁵⁸. After classification into four categories including leaves, flowers, fruits, and grasses, effectiveness of the protocol in producing AuNPs was demonstrated usually after 30 minutes of incubation with aqueous HAuCl₄. Potential application of these biogenic AuNPs as catalysts was exhibited in *Cacumen platycladi* (which exhibited biosynthesis of very small and monodisperse NPs). Catalytic reduction of 4-NP showed excellent catalytic performance compared to the aforementioned study⁵⁷.

Jia et al.⁵⁹ reported the use of a cuttlebone-derived organic matrix (from *Sepia esculenta*) as scaffold and reducer for the formation of AgNPs. The resulting composite was applied to catalyze the reduction of 4-NP. Possibilities of separation from the liquid-phase reaction and reusability in more cycles have been also reported.

3.2.4. Other heterogeneous catalysis reactions

Membranes containing Fe and Fe/Pd nanoparticles biosynthesized with the tea extract (*Camellia sinensis*) immobilized in a polymer film were successfully used for the degradation of TCE⁶⁶. The addition of Pd to form bimetallic Fe/PdNPs increased the reaction rate constant. Although the value of the reaction rate constant of the chemically synthesized FeNPs (prepared by means of sodium borohydride as a reducing agent) is higher than the biosynthesized NPs, the reactivity is reduced rapidly – less than 20% within 4 cycles. The initial reactivity of the green tea extract NPs was preserved after 3 months of repeated use – probably thanks to a number of polyphenols that can act as capping agents. Moreover, the reactivity of TCE was verified with a “real” water system.

Other FeNPs biosynthesized by means of green tea extract were used as a Fenton-like catalyst for decolorization of aqueous solutions of methylene blue and methyl orange dyes⁶⁵. Compared with iron nanoparticles produced by borohydride reduction, biosynthesized iron NPs demonstrated more effective capability, both in terms of kinetics and percentage removal.

Gupta et al.⁶⁴ published another study dealing with green tea extract and dye. Biosynthesized AuNPs were used as a catalyst for the reduction of methylene blue dye in the presence of Sn(II) in aqueous and micellar media. The authors also proved that presence of a small quantity of gold nanoparticles decreases the activation energy, and thus accelerates the reduction of methylene blue. A complete discharge of the blue color is observed even at low temperature.

On the other hand, catalytic application of biosynthesized PtNPs for the preparation of organic dye (antipyrilquinoneimine) by the reaction of aniline with 4-aminoantipyrine in an acidic aqueous medium was reported.⁶⁷ These honey mediated platinum nanostructures were found to be stable in water for more than four months.

One of the previously mentioned studies³⁴ also introduced biogenic manganese oxides synthesized by means of *Pseudomonas putida*. Membrane reactor technique described in section 3.2.1 was used for the removal of micropollutants such as ibuprofen (>95%), diclofenac (86%), mecoprop (81%), triclosan (>78%) etc. Authors suggest that the removal mechanisms occurred as chemical oxidation by MnO_x and/or the biological removal by *P. putida* cells.

3.3. Medical applications

Applications of metallic NPs in the medical and biopharmaceutical fields are both numerous and promising. AgNPs can be utilized for protection against an infection (wound coatings, bone cements and implants) or for prophylactic environment (paints, disinfectants) due to their antibacterial effects. Other qualities of silver nanoparticles include regenerative properties (skin regeneration) and wound-healing ability (dressing for burns and ulcers)⁶⁸.

There are also recent review articles dealing with nanogold pharmaceutical applications. Alanazi et al.⁶⁹ describes properties such as surface plasmon absorption, surface plasmon light scattering, and biosensing, diagnostic and therapeutic applications of AuNPs. The second review by Patra et al.⁷⁰ concerns the specific application and fabrication of AuNPs for targeted therapy in pancreatic cancer.

Magnetic NPs appear as very promising for targeted drug delivery or hyperthermia applications. For further reading, see the prominent review by Pankhurst et al.⁷¹ and its continuance⁷² (see also section dedicated to biogenic magnetic nanoparticles 3.6).

As previously mentioned, the obvious drawback of biological methods is the need to purify the sample and extract the NPs. This is due to potential pathogens or poisons that might contaminate material and is particularly important for medical applications. One possible way to solve this problem is through the usage of extract from medically important herbs and plants⁷³ – their extracts are non-toxic for the human body and previously used (often for hundreds years).

3.3.1. Antimicrobial applications

Due to the outbreak of infectious diseases caused by different pathogenic bacteria and fungi and the development of antibiotic or metal resistant strains, there is increasing need to find new antibacterial products. Although different types of nanomaterials like titanium, copper, magnesium or alginate have promising antibacterial properties, Au and AgNPs have showed the best efficiency against bacteria, viruses and fungi⁷⁴. The broad-spectrum antimicrobial properties of metallic NPs (mostly silver and gold) encourage their use as disinfectants in purification processes (medicine, water and air), food production, cosmetics, clothing, and numerous household products.⁷⁵

This section illustrates the antibacterial, antiviral, antifungal and other effects of biosynthesized NPs (Table 3). These applications promise to be very beneficial for commercial and public healthcare.

3.3.1.1. Antibacterial activity

Bacterial properties and sensitivity may vary regarding their morphology, particularly the cell wall. Generally, we can classify them generally as Gram-negative (G-) or Gram-positive (G+). The key component of the membrane, peptidoglycan, is a decisive factor in the organization of the membrane. G- bacteria have only a thin peptidoglycan layer (~2–3 nm) between their two membranes, while G+ bacteria lack the outer membrane (is substituted by thick peptidoglycan layer).

Morones et al.⁷⁶ published a study regarding possible interactions between AgNPs and G-bacteria. Small NPs disturb the function of the membrane (such as permeability or respiration) by attaching to its surface and, which than penetrate the cell, release silver ions and cause further damage by interacting with the DNA.

A spectrum of organisms used for biosynthesis of NPs with antibacterial effect varies from bacteria, fungi and alga to leaf, root, bark and tuber extracts of higher plants and trees. As one of the first records, Ingle et al.⁷⁷ reported a mycosynthesis of silver antibacterial NPs with biological activity against different human pathogens including multidrug resistant and highly pathogenic bacteria such as *Staphylococcus aureus*, *Salmonella typhi*, *Staphylococcus epidermidis*, and *Escherichia coli*. Similarly, fungal strain *Aspergillus clavatus* was used for extracellular biosynthesis of stable AgNPs with antibacterial activity against methicillin (antibiotics) resistant *Staphylococcus aureus* and *Staphylococcus epidermidis*.⁷⁸ Antibacterial activity against *Staphylococcus aureus* KCCM 12256 was also observed in case of AgNPs biosynthesized by filamentous mold *Aspergillus oryzae*.⁷⁹ Bioreductive synthesis of nanosized Ag particles was performed using live and dead cell filtrates with size varying from 5 to 50 nm. Another phytopathogenic fungal species *Bipolaris nodulosa* can serve as reducing agent for silver nitrate reduction with the resulting Ag NPs active against *Bacillus subtilis*, *Bacillus cereus*, *Pseudomonas aeruginosa*, *Proteus vulgaris*, *Escherichia coli* and *Micrococcus luteus* pathogens.⁸⁰ AgNPs biosynthesized by gilled mushroom specie *Pleurotus sajor-caju*⁸¹ can serve against *Pseudomonas aeruginosa*, *Escherichia coli* (G-) and *Staphylococcus aureus* (G+). Identical bacterial species were used in a similar study⁸² employing the famous genus of ascomycetous fungi, *Penicillium sp*, with major importance in the natural environment as well as food and drug production.

Fungal plant pathogen *Phoma glomerata* was employed in the synthesis of AgNPs and, together with antibiotics, proved effective against *Escherichia coli*, *Staphylococcus aureus* and *Pseudomonas aeruginosa*.⁸³ Synthesized NPs showed comprehensive bactericidal activity against the aforementioned G- and G+ bacterial species and enhanced the antimicrobial activity of antibiotics (ampicillin, gentamycin, streptomycin and vancomycin). Interestingly by using gold, a mold species *Trichoderma viride* (widely used as bio-fungicide) was used to biosynthesize vancomycin bound NPs and exhibited activity against vancomycin resistant *Staphylococcus aureus*, vancomycin sensitive *S. aureus* and *E. coli*.⁸⁴

Additionally, all experiments were performed as a comparison between vancomycin bound AuNPs and vancomycin as such.

Streptomyces sp. bacterially derived AgNPs were reported⁸⁵ as biologically active against 7 species of both G+ and G- bacteria (*Staphylococcus aureus*, *S. epidermidis*, *E. coli*, *S. typhi*, *Pseudomonas aeruginosa*, *Klebsiella pneumonia*, *Proteus vulgaris*). Metal reducing G- bacteria *Shewanella oneidensis* was used for silver nanocrystallites biofabrication.⁸⁶ Bacterial toxicity assessments showed that prepared biogenic Ag NPs have a greater bactericidal activity on *E. coli*, *S. oneidensis*, and *B. subtilis* strains than chemically synthesized colloidal AgNPs. U'berg et al.⁸⁷ reported usage of four bacterial species leading to bio-AgNPs active against *E. coli*.

Photosynthetic organisms in antimicrobial biofabrication are represented by algae, plants and trees. Four species of marine microalgae (normal and microwave irradiated) were used in the comparison and assessment of antimicrobial properties of biosynthesized AgNPs against human pathogens *Escherichia coli*, *Klebsiella sp*, *Proteus vulgaris*, *Pseudomonas aeruginosa*.⁸⁸ Higher plants can also take a place in NP synthesis. Leaf extract of *Garcinia mangostana* (Mangosteen) was employed in AgNPs biofabrication. Antibacterial assays were performed on human pathogenic *E. coli* and *Staphylococcus aureus* by standard disc diffusion method with considerable results.⁸⁹ Krishnaraj et al.⁹⁰ investigated biosynthesis of AgNPs and its activity on waterborne bacterial pathogens (*E. coli* and *Vibrio cholerae*). During the antibacterial experiments, alteration in membrane permeability and respiration of the AgNP treated bacterial cells were recorded.

Gade et al.⁹¹ reported *Opuntia ficus-indica* mediated synthesis of colloidal AgNPs and their antimicrobial assessment in combination with commercially available antibiotics. The maximum activity was demonstrated by ampicillin followed by streptomycin and vancomycin. Similarly, the extracellular biosynthesis of AgNPs from silver nitrate solution by fungus *Trichoderma viride* was also reported.⁹² An increase antimicrobial activity with various antibiotics against gram-positive and gram-negative bacteria was described. Although antibacterial activities of ampicillin, kanamycin, erythromycin, and chloramphenicol were increased in the presence of AgNPs against test strains, ampicillin showed the highest enhancing effect.

Food-storage possibilities of biofabricated NPs were examined using the same organism.⁹³ Antibacterial activities of AgNP-incorporated sodium alginate films were tested against *E. coli* ATCC 8739 and *S. aureus* ATCC 6538 strains – the disk method exhibited antibacterial activity against both G+ and G- bacteria. Antimicrobial coatings were applied to carrot and pear surfaces and the conservation impact was compared to untreated samples.

Table 3. Antimicrobial applications

NP	Organism used	Application	Reference
Ag	<i>S. oneidensis</i>	activity vs. G+ and G- bacteria	Suresh et al. 2010 ⁸⁶
Ag	<i>Penicillium sp.</i>	activity vs. G+ and G- bacteria	Maliszewska and Puzio 2009 ⁸²
Ag	<i>Pleurotus sajor caju</i>	activity vs. G+ and G- bacteria	Nithya and Ragunathan 2009 ⁸¹
Ag	<i>Bipolaris nodulosa</i>	activity vs. G+ and G- bacteria	Saha et al. 2010 ⁸⁰
Ag	<i>Streptomyces sp</i>	activity vs. G+ and G- bacteria	Shirley et al. 2010 ⁸⁵
Ag	<i>Aspergillus oryzae</i> var. <i>viridis</i>	activity vs <i>S. aureus</i>	Binupriya et al. 2010 ⁷⁹
⁷⁹ Au	<i>Trichoderma viride</i>	activity vs VRSA	Fayaz et al. 2011 ⁸⁴
Ag	<i>T. viride</i>	vegetable and fruit preservation	Fayaz et al. 2009 ⁹³
Ag	<i>Aspergillus clavatus</i>	activity vs. MRSA, MRSE	Saravanan et al. 2010 ⁷⁸
Ag	<i>Garcinia mangostana</i> (Mangosteen) leaf	activity against <i>E. coli</i> , <i>S. aureus</i>	Veerasamy et al. 2011 ⁹⁴
Ag	<i>Candida albicans</i> , <i>E. coli</i> , <i>B. cereus</i> , <i>P. fluorescens</i>	activity against <i>E. coli</i>	Ul'berg et al. 2010 ⁹⁵
Ag	<i>Phoma glomerata</i>	synergy with antibiotics	Birla et al. 2009 ⁸³
Ag	<i>Opuntia ficus-indica</i>	effect in combination with antibiotics	Gade et al. 2010 ⁹¹
Ag	<i>T. viridae</i>	effect in combination with antibiotics	Fayaz et al. 2010 ⁹²
Ag	<i>Fusarium acuminatum</i>	activity vs. G+ and G- bacteria	Ingle et al. 2008 ⁷⁷
Ag	varied microalgae species	activity vs. G+ and G- bacteria	Merin et al. 2010 ⁸⁸
Ag	<i>Acalypha indica</i> leaf	activity vs <i>E. coli</i> , <i>Vibrio cholerae</i>	Krishnaraj et al. 2010 ⁹⁰
Ag	<i>Fusarium oxysporum</i>	cotton fabrics incorporated with AgNPs	Durán et al. 2007 ⁹⁶

(continued)

Table 3. (continued)

NP	Organism used	Application	Reference
Ag	<i>Fusarium solani</i>	cotton fabrics incorporated with AgNPs	El-Rafie et al. 2010 ⁹⁷
Ag	<i>Azadirachta indica</i> (Neem) leaf	bactericidal effect in cotton cloth against <i>E. coli</i>	Tripathi et al. 2009 ⁹⁸
Ag	<i>Cinnamom zeylanicum</i> bark	activity against <i>E. coli</i> BL-21	Sathishkumar et al. 2009 ⁹⁹
Ag	<i>Curcuma longa</i> tuber	immobilization on cotton cloth	Sathishkumar et al. 2010 ¹⁰⁰
Ag	<i>Eucalyptus citriodora</i> , <i>Ficus bengalensis</i>	antibacterial activity against <i>E. coli</i> , loaded on the cotton fibers	Ravindra et al. 2010 ¹⁰¹
Ce	<i>Leptothrix discophora</i> , <i>Pseudomonas putida</i>	activity against bacteriophage UZ1	De Gusseme et al. 2010 ¹⁰²
Ag	<i>Lactobacillus fermentum</i>	activity against bacteriophage UZ1	De Gusseme et al. 2010 ¹⁰³
Ag	<i>Amylomyces rouxii</i>	antifungal and antibacterial activity	Musarrat et al. 2010 ¹⁰⁴
Ag	<i>S. hygroscopicus</i>	antifungal and antibacterial activity	Sadhasivam et al. 2010 ¹⁰⁵
Ag	<i>A. niger</i>	antifungal and antibacterial activity	Jaidev et al. 2010 ¹⁰⁶
Ag	<i>Sesuvium portulacastrum</i> callus and leaf	antifungal and antibacterial activity	Nabikhan et al. 2010 ¹⁰⁷
Ag	<i>Alternaria alternate</i>	activity in combination with fluconazol	Gajbhyie et al. 2009 ¹⁰⁸
Au	genus <i>Musa</i> - banana peel	antifungal and antibacterial activity	Bankar et al. 2010 ¹⁰⁹
Au	<i>Rhizopus oryzae</i>	antifungal and antibacterial activity	Das et al. 2009 ¹¹⁰
Ag	<i>Aspergillus clavatus</i>	antifungal and antibacterial activity	Verma et al. 2010 ¹¹¹
Ag	<i>Solanum torvum</i>	antifungal and antibacterial activity	Govindaraju et al. 2010 ¹¹²

3.3.1.2. Antifungal and combined activity

Although there are reports of biosynthesized NPs with antifungal activity, they will only usually exhibit it in combination with antibacterial activity. It is in this context, that they will be mentioned in the following text.

Mycelia-free water extracts from *Amylomyces rouxii* facilitated the production of stable, monodispersed and spherical AgNPs (size range of 5–27 nm). Biosynthesized AgNPs

exhibited antimicrobial activity against bacterial (*Shigella dysenteriae* type I, *Staphylococcus aureus*, *Citrobacter* sp., *E. coli*, *Pseudomonas aeruginosa*, *Bacillus subtilis*) as well as fungal (*Candida albicans*, *Fusarium oxysporum*) species. Biological reduction of aqueous silver ions by extracellular components of *Streptomyces hygroscopicus*¹⁰⁵ resulted in AgNPs which significantly inhibited the growth of medically-important pathogenic gram-positive bacteria (*Bacillus subtilis*, *Enterococcus faecalis*), gram-negative bacteria (*Escherichia coli* and *Salmonella typhimurium*) and yeast (*Candida albicans*). The colloidal AgNPs biosynthesized with filtrate from *Aspergillus niger* inhibited the growth of the fungus seeded in the nutrient agar plate. Potential antifungal activity was due to inactivation of sulfhydryl groups in the fungal cell wall and disruption of membrane bound enzymes and lipids which causes cell lysis.¹⁰⁶ Antibacterial activity against both G+ (*Staphylococcus* sp., *Bacillus* sp.) and G- (*E. coli*) bacterial species was observed. Similar results were obtained employing *Aspergillus clavatus* against *Candida albicans*, *Pseudomonas fluorescens* and *Escherichia coli* by Verma et al.¹¹¹ Govindaraju et al.¹¹² published a study utilizing *Solanum torvum* as a mediator for biosynthesis of AgNPs eliciting antibacterial activity against pathogenic bacteria *Pseudomonas aeruginosa*, *Staphylococcus aureus* and pathogenic fungi *Aspergillus flavus* and *Aspergillus niger*.

Interestingly, extracts from tissue culture-derived callus and leaf of the saltmarsh plant *Sesuvium portulacastrum* were used for AgNP growth¹⁰⁷. The antibacterial activity against *Pseudomonas aeruginosa*, *Staphylococcus aureus*, *Listeria monocytogenes*, *Micrococcus luteus*, and *Klebsiella pneumoniae* was more distinct compared to antifungal activity against *Alternaria alternata*, *Penicillium italicum*, *Fusarium equisetii*, *Candida albicans*. Moreover, antimicrobial activity was enhanced when polyvinyl alcohol was added as a stabilizing agent in comparison with samples prepared with distilled water.

Study of antifungal properties against large group of fungal species (*Phoma glomerata*, *Phoma herbarum*, *Fusarium semitectum*, *Trichoderma* sp., *Candida albicans*) in combination with triazole antifungal drug fluconazol was published by Gajbhyie et al.¹⁰⁸. AgNPs biosynthesized by the phyto-pathogenic fungus *Alternaria alternata* enhanced antifungal activity of fluconazole against the test fungi showing maximum inhibition against *C. albicans*, followed by *P. glomerata* and *Trichoderma* sp. However, no significant enhancement was found against *P. herbarum* and *F. semitectum*.

Last but not least, the formation of AuNPs with antifungal activity was also described. As a contribution to the water hygiene and treatment management, Das et al.¹¹⁰ describes a simple procedure to obtain potable water free of pathogens and pesticides. AuNPs (10 nm average) were produced on the surface of fungus *Rhizopus oryzae* and showed antimicrobial activity against several G- and G+ pathogenic bacteria as well as the yeasts *Saccharomyces cerevisiae* and *Candida albicans*. Simulated contaminated water containing organophosphate pesticides (malathion, parathion, chlorpyrifos, and dimethoate) along with *E. coli* was treated with gold bionanoconjugate. Successful removal of contaminants was monitored by means standard disk method (*E. coli*) and gas chromatography analysis (pesticides). AuNPs with antibacterial activity against *Citrobacter kosari*, *Escherichia coli*, *Proteus vulgaris*, *Pseudomonas aeruginosa*, *Enterobacter aerogenes* and *Klebsiella sp.* and antifungal activity against (*Candida albicans*) were also obtained employing banana peel extract.¹⁰⁹

3.3.1.3. Antiviral activity

Although humankind is waging an ongoing war against viruses in such wide ranging fields as medicine and agriculture, there have been only few recorded studies about antiviral activity of biosynthesized NPs. Although not of the biosynthesized nature, the post-infected anti-HIV-1(BaL) activities of AgNPs (prepared chemically, 10 nm) toward Hut/CCR5 cells (cells derived from a human T cell line, which express the chemokine receptor CCR5) were evaluated by Sun et al.¹¹³. When compared to the control sample, AgNPs showed dose-dependent anti-retrovirus activities and showed high activity (at 50 mM - 98%) in inhibiting HIV-1 replication. For comparison, the AuNPs exhibited relatively low anti-HIV-1 activities 6–20%. This is an interesting example of the use of strictly chemically fabricated NPs. De Gusseme et al.¹⁰² published a study of virus removal by biogenic rare earth element cerium, produced by the addition of aqueous Ce(III) to actively growing cultures of either freshwater manganese-oxidizing bacteria *Leptothrix discophora* or *Pseudomonas putida*. A model organism for the antiviral assay was bacteriophage UZ1 (bacteriophage specific for common pathogenic bacterium *Enterobacter aerogenes*).

In a study by the same research group¹⁰³, *Lactobacillus fermentum* served as a reducing agent and carrier matrix for AgNPs. The antiviral qualities of biogenic AgNPs was confirmed in water containing aforementioned bacteriophage UZ1 and murine norovirus 1 (a model

organism for human noroviruses). For continuous disinfection capability in a water environment, the biogenic material was applied to an electropositive filter (NanoCeram) and exhibited higher antiviral activity in comparison with the results obtained from the original filter.

3.3.1.4. Antibacterial fabrics and cloth

Another interesting utilization for biosynthesized NPs is immobilization on cotton cloth or cotton fibers. This approach demonstrates the possible use of such cloth in disinfection or sterilization.

As the first record, Durán et al.⁹⁶ reported the extracellular production of AgNPs by fungus *Fusarium oxysporum* and antimicrobial effect of the NPs incorporated in cotton fabrics against *Staphylococcus aureus*. Moreover, effluent from impregnated fabrics (after several washing cycles) was treated with the suspension of *Chromobacterium violaceum*, metal binding bacteria, to reabsorb released NPs. Using a similar procedure and organism, fungi *Fusarium solani*, El-Rafie et al.⁹⁷ prepared AgNPs and applied them to cotton fabrics with and without binder. The bleached cotton fabrics were padded through silver colloidal baths and squeezed with a laboratory padder. Following the incorporation of a binder, after 20 washing cycles the material still exhibited effectiveness in antibacterial activity against *Staphylococcus aureus* and *E. coli*.

Azadirachta indica (Neem) is a genus from mahogany family *Meliaceae*. Tripathi et al.⁹⁸ studied the biosynthetic production of AgNPs by aqueous extract of Neem leaves and their immobilization on cotton cloth. Subsequently, utilizing a standard disk method (including the effect of consecutive washing in distilled water), their bactericidal effect against *E. coli* was observed. NP incorporation into cotton disks was performed by three approaches: (a) centrifuging the disks with liquid extract containing biosynthesized NPs; (b) *in-situ* coating process during synthesis, and (c) coating with dried and purified NPs. Antibacterial effect against *E. coli* BL-21 strain was also tested with AgNPs prepared by means of phyto-reductive extract and powder of *Cinnamom zeylanicum*⁹⁹ and *Curcuma longa* tuber.¹⁰⁰ The second work presents immobilization of AgNPs on cotton cloth. NPs were resuspended in water or polyvinylidene fluoride (PVDF) and sprayed over the pre-sterilized white cotton cloth in aseptic condition. PVDF immobilized cloth exhibited less antibacterial activity.

However, consecutive washing drastically reduced antibacterial effectiveness of AgNPs immobilized in sterile water.

Table 4. Medical applications

NP	Organism used	Application	Reference
Au	<i>Cymbopogon citratus</i> - lemon grass	NIR tunable absorption; coating technology and hyperthermia of cancer cells	Shankar et al. 2005 ¹¹⁴
Au	<i>Psidium guajava</i> leaf	antidiabetic study, inhibition of PTP1B	Basha et al. 2010 ¹¹⁵
Ag	<i>Camellia sinensis</i>	biocompatible	Moulton et al. 2010 ¹¹⁶
Fe ₃ O ₄	<i>Magnetospirillum gryphiswaldense</i>	drug carrier	Sun et al. 2008 ¹¹⁷
Ag	<i>Aspergillus niger</i>	wound healing activity	Sundaramoorthi et al. 2009 ¹¹⁸
Au	egg shell	blood serum glucose sensor	Zheng et al. 2011 ¹¹⁹
Au, Ag	guava	anti-cancer efficiency	Raghunandan et al. 2011 ¹²⁰
Au, Ag	Cloves (<i>Syzygium aromaticum</i>)	anti-cancer efficiency	Raghunandan et al. 2011 ¹²¹
Ag	<i>Citrullus colocynthis</i> (L.) Schrad	anti-cancer efficiency	Satyavani et al. 2011 ¹²²
Ag	<i>Piper longum</i>	cytotoxic activity against Hep-2 cells	Jacob et al. 2011 ¹²³
Au	<i>Vites vinefera</i>	cytotoxic activity against HBL-100 cells	Amarnath et al. 2011 ¹²⁴
Cu	<i>Euphorbia nivulia</i>	anti-cancer efficiency	Valodkar et al. 2011 ¹²⁵
Au	<i>Zingiber officinale</i>	blood compatibility	Kumar et al. 2011 ⁷³
Au	<i>Porphyra vietnamensis</i>	carrier for delivery of anticancer drug	Venkatpurwar et al. 2011 ¹²⁶

3.3.1. Cancer treatment and drug delivery applications

As we can see from previous chapter, some metallic NPs are showing increased toxicity to certain organisms. For instance, NPs can interact with proteins and enzymes within mammalian cells and can interfere with the antioxidant defense mechanism leading to reactive oxygen species generation, destruction of the mitochondria and cell apoptosis.¹¹⁴ The impact of metal nanoparticles also strongly depends on the capping agent. The very same

AgNP has been reported both to exhibit cytotoxicity¹¹⁴ and be non-cytotoxic¹¹⁵ (see section 3.3.2). Due to the difference in capping agents, the cytotoxic activity of metallic NPs can be utilized therefore to the target tumor cells as will be shown in this chapter (Table 4).

The shape of NPs can also critically influence their properties, especially optical ones. Gold nanotriangles with tunable size were biofabricated by involving the reduction of aqueous gold ions with an extract of the lemongrass plant.¹¹⁴ Absorption in the near-infrared region of the electromagnetic spectrum is “expected to have possible application” in hyperthermia of cancer cells and in infra-red (IR) – absorbing optical coatings.

Cytotoxicology studies against different cancer cell lines can be also mentioned. Amarnath et al.¹²⁴ published experiments with phytochemicals present in grapes (*Vitis vinefera*). The grape-fabricated AuNPs have exhibited remarkable affinity towards HBL-100 (human breast cancer cells), causing their apoptosis. Guava and clove extracts were used to reduce gold and silver salts in a study by Raghunandan et al.¹²⁰ Although biosynthesized AuNPs showed a satisfactory anti-cancer effect on HEK-293, HeLa, and HT-29 cancer cell lines, AgNPs did not show any anti-cancer activity. The study revealed that the anti-cancer effect is caused by free radicals generated by AuNPs.

Biosynthesis of AgNPs by means of *Piper longum* leaf as a reducing and capping agent was also reported by Jacob et al.¹²³ These NPs showed excellent cytotoxic effect on HEp-2 cancer cell lines. Similarly, callus extract of *Citrullus colocynthis* was used to form AgNPs with an effect against HEp-2 cell line.¹²⁷

Extracellular synthesis of copper nanoparticles (CuNPs) was performed using stem latex of *Euphorbia nivulia*.¹²⁵ This complex study led to the conclusion that copper nanoparticles are toxic to A549 (human lung carcinoma) cells in a dose dependent manner.

As an elegant application of bacterial magnetosomes (BM), Sun et al.¹¹⁷ presented experiments leading to the employment of BM from *Magnetospirillum gryphiswaldense* as a chemotherapy drug carrier (for more detail information about biosynthesized magnetic NPs and magnetosomes see section 3.6). Doxorubicin (DOX) was loaded into the isolated and cleaned BMs using a bifunctional crosslinker. As drug efficiency and toxicity may be significantly altered by structural modification, evaluation of the drug effect (drug coupled with BM) was performed. The antitumor effects of DOX loaded BMs were evaluated by HL60 and EMT-6 carcinoma cells. They were cytotoxic to the cancer cells, inhibited cancer

cell proliferation and suppressed the mRNA levels of the significant oncogene *c-myc*. The drug releasing process from BMs was also monitored. The assets of this approach compared to artificial magnetic particles may be the ability to carry larger amounts of drug, ease of preparation and dispersion, high stability and more uniformity. Being surrounded with a membrane that consists of lipids and proteins, purified and sterilized magnetosomes were not toxic to mouse fibroblasts *in vitro*.¹²⁸ This indicates the advantage of biocompatibility.

Another drug delivery study¹²⁶ employed porphyrin from marine algae *Porphyrin vietnamensis* as a reducing and capping agent for biosynthesis of AuNPs. These NPs were further used again as a carrier for the delivery of DOX and demonstrated higher cytotoxicity on LN-229 (human glioma) cell line compared with the native DOX solution. Moreover, with regard to spectroscopic examination hydrogen bonds are involved in the DOX – AuNPs conjugating process.

3.3.2. Biocompatibility

Biocompatibility is a very important property for all material possibly dealing with medical usage in living organisms. Moulton et al.¹¹⁶ reported biosynthesis experiments with tea leaf extract as a reducing and capping agent for AgNP fabrication. Evaluation of mitochondrial function to assess cell viability and membrane integrity in human keratinocytes showed that these AgNPs were nontoxic. This may be attributed to the tea antioxidants on the NP surface. Although this method of synthesis appears to be promising based on the initial *in vitro* studies, they need to be followed up by future *in vivo* tests to accurately evaluate the biocompatibility (Table 4).

A previously mentioned paper by Kumar et al.⁷³ described *Zingiber officinale* extract, in particular blood compatibility of AuNPs synthesized by means of this extract. These AuNPs were non-platelet activating and non-complement activating on contact with the human blood. They also did not show any aggregation of other blood cells. Moreover, they were highly stable at normal physiological conditions compared to chemically prepared NPs (citrate capped), which aggregated.

3.3.3. Other medical applications

Wound healing activity of AgNPs, synthesized extracellularly using *Aspergillus niger*, was evaluated on a rat model for the case of an excision and thermal wound.¹¹⁸ Researchers illustrated the efficient antimicrobial property of AgNPs and also confirmed the ability of nanosilver to modulate the cytokines involved in wound healing.

Another medical application deals with diabetes, particularly with the inhibition of the enzyme protein tyrosine phosphatase (PTP), type PTP1B. Disturbance of the normal balance of PTP function has been implicated as the source of several human diseases, including diabetes, cancer, and inflammation.¹²⁹ The rapid formation of AuNPs with guavanoic acid from the leaf extract of *Psidium guajava* was reported by Basha et al.¹¹⁵ These were used in an antidiabetic PTP 1B inhibitory assay and showed significant inhibitory effect with an IC₅₀ of 1.14 $\mu\text{g.mL}^{-1}$.

Zheng et al. reported biofabrication of AuNPs (by means of egg shell membrane) and their application in the glucose biosensor for blood glucose determination (further information in section 3.4.1 and Zheng et al.¹³⁰). The biosensor has been also applied to measure the glucose content in human blood serum samples (showing agreement with a standard routine medical spectrophotometric test method).

Another study demonstrates green process for the production of Au- and AgNPs synthesized and stabilized using *Brevibacterium casei*.¹³¹ These NPs showed an anti-coagulate activity by the inhibition of formation of blood clots in the samples that received blood along with Ag and AuNPs. The stability of gold and silver nanoparticles function in the blood was also proved by the exposure of the blood plasma to the particles for 24h which did not show any significant reduction in the activity.

3.4. Electrochemical and sensing applications

Metallic NPs are at the center of intense research because an understanding of their surface chemistry might play a key role in effective utilization of technologies such as nanosensor, biosensor, electrocatalysis, nanodevice and nanoelectrochemistry.¹³² From the view of electro analytical chemistry, more attention has been paid to AuNPs because of their

good biological compatibility, excellent conducting capability and high surface-to-volume ratio. Usage of AuNPs in electrochemical interfaces has contributed to new vigor in electrochemistry. Development of new techniques and different electrode modified strategies may potentially enhance analytical selectivity and sensitivity of commonly used facilities.¹³³

While not yet containing any direct applications, there are several studies which are potentially remarkable for their discussion of electrochemical properties (Table 5). Biosynthesis of ferroelectric BaTiO₃ NPs in assistance of *Lactobacillus sp.* was reported by Jha and Prasad¹³⁴. After modification with PVDF, resulting nanocomposite exhibited enhancement in dielectric properties. AuNPs biosynthesized by alkalothermophilic actinomycetes *Thermomonospora curvata*, *Thermomonospora fusca*, and *Thermomonospora chromogena* and stabilized by cross-linker glutaraldehyde have potential usage as biosensor enhancer.¹³⁵ Shilov et al.¹³⁶ investigated electro-physical characteristics (cell ζ -potential, surface conductivity, electrophoretic mobility, dispersion of cell conductivity) of yeast cell with silver precipitate.

3.4.1. Sensors

Zheng et al.¹³⁷ reported biosynthesis of Au–Ag alloy NPs by yeast cells and their application to electrochemical vanillin sensing. Sensitive vanillin sensor based on glassy carbon electrode (GCE), modified by Au–Ag alloy NPs, was able to enhance the electrochemical response of vanillin. Electrochemical investigations confirmed a linear increase of the vanillin oxidation peak current at the sensor with its concentration in the range of 0.2–50 μ M (detection limit 40 nM). Constructed sensor was successfully applied to the determination of vanillin in samples of vanilla bean and vanilla tea. This approach suggests possible replacement of commonly used methods in vanillin monitoring system (chromatography, capillary electrophoresis etc.).

Interestingly, Zheng et al.¹³⁰ also published green biosynthesis method for AuNPs based on usage of natural biomaterial, eggshell membrane (“fresh eggs were bought from a local supermarket in Hong Kong”). AuNPs on the eggshell surface were used to immobilize glucose oxidase (by cross-linking method with glutaraldehyde) on the GCE for detection of glucose in solution. Enzyme activity of glucose oxidase was enhanced by the presence of

highly conductive AuNPs. Constructed biosensor showed linear response to glucose concentration ranged from 20 μM to 0.8 mM (with a detection limit of 17 μM) and has been successfully applied to detect the glucose level in glucose injections. Glucose sensor used for blood serum based on eggshell membrane and AuNPs¹³⁹ is mentioned in medicinal applications in medical section 3.3.

AuNPs biosynthesis by silica-encapsulated micro-algae *Klebsormidium flaccidum* leads to formation of a “living” bio-hybrid material¹⁴⁰. Researchers have used Raman spectroscopy for *in situ* imaging of entrapped cells – investigation of the influence of the AuNPs on the photosynthetic system of the algae. Coupling of Raman imaging and sol–gel encapsulation might allow the development of photosynthesis-based biosensors.

Even though it pertains to semi-metals, we will also mention a study dealing with synthesis of semiconductor selenium NPs employing cells of bacteria *Bacillus subtilis*. Two kinds (spherical, 1D-trigonal) of Se nanomaterial crystals with good adhesive ability and biocompatibility were employed as enhancing materials for hydrogen peroxide (H_2O_2) horseradish peroxidase biosensor, with the detection limit 8×10^{-8} M (for H_2O_2 concentration). Different types of Se crystals had no significant difference in sensor usage. Due to the obtained results, selenium nanomaterials GCE can be a promising instrument for applications dealing with the detection of H_2O_2 in food, pharmaceutical, clinical, industrial and environmental analyses¹⁴¹.

3.4.2. Electrochemical applications and properties

Du et al.¹⁴² demonstrated in communication the bioreduction of aqueous Au(III) ions by *E. coli* DH5 α bacterial strain. AuNPs bound to the surface of the bacteria were used for application in direct electron transfer of protein hemoglobin (glass carbon electrode (GCE) coated by protein layer as well as the AuNPs biocomposite). Cyclic voltametry experiments were reported for different electrodes at scan rates of 0.1 V/s in pH 7.0 phosphate buffer solution. Although there are no obvious redox peaks at the blank electrodes (GCE, *E. coli*-GCE, hemoglobin-*E. coli*-GCE and AuNPs-*E. coli*-GCE), a pair of redox peaks (with formal potential of -0.325 V vs. Ag/AgCl reference electrode) was observed at AuNPs-hemoglobin-

E. coli-GCE. These results proved the electron transfer between hemoglobin and GCE provided by means of the AuNPs modified electrode.

Table 5. Electrochemical and sensing applications

NP	Organism used	Application	Reference
Ag	<i>Trichoderma viride</i>	blue orange emission - photoluminescence	Fayaz et al. 2010 ¹⁴³
Ag	<i>Parthenium hysterophorus</i>	photoluminescence	Sarkar et al. 2010 ¹⁴⁴
Ag	<i>Coriandrum sativum</i> leaf	reverse sat. absorption, optical limiting	Sathyavathi et al. 2010 ¹⁴⁵
Te	<i>Bacillus selenitireducens</i>	optical limiting	Liao et al. 2010 ¹⁴⁶
Au	<i>Maduca longifolia</i>	efficient in absorbing IR radiation	Fayaz et al. 2011 ¹⁴⁷
CdTe	<i>Saccharomyces cerevisiae</i>	CdTe QDs for biolabeling and biosensing	Bao et al. 2010a ¹⁴⁸
CdTe	<i>Escherichia coli</i>	CdTe QDs for biolabeling and biosensing	Bao et al. 2010b ¹⁴⁹
Au- Ag	<i>Saccharomyces cerevisiae</i>	vanillin sensor	Zheng et al. 2010 ¹³⁷
Au	eggshell	glucose sensor	Zheng et al. 2010 ¹³⁰
Se	<i>Bacillus subtilis</i>	H ₂ O ₂ sensor	Wang et al. 2010 ¹⁴¹
Au	<i>Klebsormidium flaccidum</i>	photosynthesis-based environmental biosensor	Sicard et al. 2010 ¹⁴⁰
CdS	<i>Schizosaccharomyces pombe</i>	construction of ideal diode	Kowshik et al. 2002 ¹⁵⁰
CdS	<i>Brevibacterium casei</i>	fluorescence emission	Pandian et al. 2011 ¹⁵¹
Au	<i>Escherichi coli</i>	direct electrochemistry of hemoglobin	Du et al. 2007 ¹⁴²
Au	<i>Scutellaria barbata</i>	direct electrochemistry of 4-NP	Wang et al. 2009 ¹⁵²
Ag, Au	<i>Rosa damascena</i>	modified glassy carbon electrode	Ghoreishi et al. 201 ¹⁵³
Au	<i>Streptomyces hygroscopicus</i>	modified Cu ₂ O–Pt electrode	Sadhasivam et al. 2011 ¹⁵⁴

Similarly, extracellular synthesis of AuNPs using plant *Scutellaria barbata* as the reducing agent was observed.¹⁵² The obtained AuNPs were modified on the GCE and enhanced the electronic transmission rate between the electrode and the 4-NP.

Utilization of modified GCE with AuNPs prepared by means of the flower extract of *Rosa damascena* as a reducing and stabilizing agent was investigated.¹⁵³ Results of cyclic

voltammetry in a solution of 0.1 M KCl and 5.0 mM $[\text{Fe}(\text{CN})_6]^{3-/4-}$ show that electronic transmission rate between the modified electrode and $[\text{Fe}(\text{CN})_6]^{3-/4-}$ increased.

Cyclic voltammetry studies with three-electrode configuration modified with AuNPs biosynthesized by *Streptomyces hygroscopicus* were conducted in study by Sadhasivam et al.¹⁵⁴ Platinum (Pt) and Ag/AgCl electrodes were used as counter and reference electrode. Electrochemically-coated Cu_2O on Pt substrate (Cu_2O -Pt) with AuNPs-methylene blue monolayer was employed as the working electrode.

Remarkably, biosynthesized CdSNPs were also used for construction of an ideal diode.¹⁵⁰ Semiconducting NPs were biofabricated by *Schizosaccharomyces pombe* and were confirmed to have a Wurtzite ($\text{Cd}_{16}\text{S}_{20}$)-type structure. Diode was fabricated by means of tin-doped indium oxide coated glass substrate. This structure was spin coated by thin film of poly-phenylene vinylene (p-type material) and with washed *S. pombe* CdSNPs (n-type material) respectively. Silver contacts were also added. Obtained diode operated at low voltage and had forward current value, which makes the structure suitable for use as an ideal diode.

3.5. Optical, bio-imaging, bio-labeling applications

The metallic nanocrystals are held at the center due to their photo-induced nonlinear optical properties. In particular, the unique optical properties associated with NPs and their composite materials include a high- or low-refractive index, high transparency, novel photoluminescence properties, photonic crystal, and plasmon resonance.¹⁵⁵ In nanoregime (hundreds to thousands of atoms) optical and electro-optical properties of materials can be tuned by varying the physical size of the crystal, leading to new phenomena, such as surface plasmon resonance (SPR) in Au and AgNPs and the size dependent band gap of semiconductor.¹⁵⁶ Scientists are therefore able to tailor the electronic structure and properties without introducing any changes in the sample chemical composition. Methods for NP synthesis that allow control of NP characteristics, including size distribution, morphology, crystallinity, purity, and composition are of particular note.¹⁵⁵ Several methods for the synthesis of NPs and their composite materials have been reported previously. However, to be feasible for utilization in industrial scale, the process needs to be simple, low-cost, and

able to operate continuously with a high production rate. Therefore, utilization of the biosynthesis approach may be beneficial.

Non-pathogenic, fast-growing fungus *Trichoderma viride* (habited in dead organic materials) was used to biosynthesis small (2-4 nm), highly dispersed AgNPs¹⁴³. Interestingly, photoluminescence measurements showed an emission in the range of 320–520 nm (fall in blue-orange region). This fact indicates such a method of AgNPs preparation as suitable for future bioimaging and labeling application. Sarkar et al.¹⁴⁴ published a similar study utilizing the flowering plant species *Parthenium hysterophorus* and AgNPs.

A simple, fast, and economical biological procedure using *Coriandrum sativum* leaf extract to synthesize AgNPs was reported by Sathyavathi et al.¹⁴⁵. These NPs have an important application in nonlinear optics. Nonlinear refraction and absorption coefficients were measured using Z-scan technique with laser pulses. AgNPs were found to exhibit strong reverse saturable absorption, which has been identified as the main mechanism responsible for optical limiting. Similarly, microbiologically-formed nanorods (*Bacillus selenitireducens*) composed of elemental tellurium Te(0) were described¹⁴⁶. These TeNPs form unusual nanocomposites when combined with organic chemical host and exhibit excellent broadband optical limiting at 532 and 1064 nm. In this regard, they significantly exceeded the best commercial optical limiters currently available. Their relative biomanufacturing ease combined with their unique properties makes these Te-based nanocomposites particularly attractive for their immediate employment as coatings (e.g. protecting worker eyesight from damage caused by exposure to focused beams and lasers).

Fayaz et al.¹⁴⁷ performed experiments with *Maduca longifolia* extract. The NIR absorption of biosynthesized AuNPs has possible important application as IR blocker in optical coating in building windows (see the section 3.3 for similar application promising for cancer hyperthermia coatings¹¹⁴).

Extracellular synthesis cadmium telluride CdTe quantum dots (QDs) with tunable fluorescence emission employing *Saccharomyces cerevisiae* cells was published by Bao et al.¹⁴⁸. Fabricated CdTe QDs with uniform size (2–3.6 nm) were protein-capped, which makes them highly soluble in water. A similar approach¹⁴⁹ was used for CdTe QDs by means of *E. coli*. Size-tunable optical properties were confirmed in both cases by ultraviolet–visible, photoluminescence, X-ray diffraction and transmission electron microscopy, with

fluorescence emission from 488 to 551 nm. Moreover, QDs functionalized with folic acid were used to image cultured cervical cancer cells *in vitro*.¹⁴⁹ The biosynthesized QDs may therefore have potential in broad bio-imaging and bio-labeling applications.

Similarly, another study introduced *Brevibacterium casei* SRKP2 as a potential producer for the biosynthesis of CdSNPs¹⁵¹. These biologically synthesized NPs exhibits fluorescent emission which remained unaffected even after immobilization within polyhydroxybutyrate matrix.

3.6. Magnetic applications

Area of biogenic magnetic nano- and microparticles is well known for a decades.¹⁵⁷ However, only some of these particles are synthesized spontaneously and naturally by magnetotactic bacteria. Biologically synthesized magnetically responsive NPs have been already employed in various biotechnological, medicinal and environmental applications.¹⁵⁷ This chapter shows therefore several selected important biotechnological applications and gives an update to already existing reviews.^{157,158}

Natural ability of magnetotactic bacteria to synthesize magnetite nanoparticles (MNPs) can be used for their production and subsequent utilization (Table 6). Interestingly, Kundu et al.¹⁵⁹ performed experiments leading to changes in magnetosome formation (size, number, alignment) in the presence of Zn and Ni salts. This approach can be employed to influence and enhance the yield and quality of the desired magnetic products.

One of possible applications uses ability of MNPs to reduce Cr(VI) which leads to its potential bioremediation¹⁶⁰ (see also similar applications in section 3.2.1). Biologically synthesized MNPs (*Geobacter sulfurreducens*) were studied using X-ray absorption and X-ray magnetic circular dichroism following exposure to Cr(VI) solution. Study of the same research team examined also influence of Fe(III) starting material on the ability of magnetically recoverable biogenic magnetites produced by *G. sulfurreducens* to retain metal contaminants from water.¹⁶¹ MNPs produced by the bacterial reduction of schwertmannite (iron-oxyhydroxysulfate mineral) powder were more efficient at reducing Cr(VI) than either ferrihydrite (oxyhydroxide mineral) “gel”-derived biomagnetite or commercial nanoscale Fe₃O₄.

Strong advantage of magnetic materials is their ability to be simply collected or recovered. Therefore, MNPs synthesized by *G. sulfurreducens* were also used as a carrier for PdNPs creating magnetically recoverable palladium nanocatalyst¹⁶² (sodium tetrachloropalladate was added to shaken magnetite suspension). The Pd-MNPs were tested for catalytic activity in the Heck reaction (see section 3.2.1) coupling iodobenzene to ethyl acrylate or styrene. Moreover, the biomagnetite support keeps the PdNPs dispersed and prevents it from agglomerating and losing effective surface area.

Table 6. Magnetic applications

NP	Organism used	Application	Reference
Fe ₃ O ₄	<i>Geobacter sulfurreducens</i>	magnetically recoverable Pd nanocatalyst	Coker et al. 2010 ¹⁶²
Fe ₃ O ₄	<i>Geobacter sulfurreducens</i>	Cr(VI) and Tc(VII) remediation	Cutting et al. 2010 ¹⁶¹
Fe ₃ O ₄	<i>Geobacter sulfurreducens</i>	Cr(VI) remediation	Telling et al. 2009 ¹⁶⁰
Fe ₃ O ₄	<i>Thermoanaerobacter sp. TOR-39</i>	magnetite substituted with Co, Ni, Cr, Mn, Zn and rare earth metals	Moon et al. 2010 ¹⁶³
Fe ₃ O ₄	<i>Theroanaerobacter ethanolicus</i> and <i>Shewanella sp</i>	magnetite substituted with Co, Ni, Cr, Mn	Roh et al. 2006 ¹⁶⁴
Fe ₃ O ₄	<i>Magnetospirillum</i>	cobalt doping of magnetosomes	Staniland et al. 2008 ¹⁶⁵
Fe ₃ O ₄	<i>Gluconacetobacter xylinum</i>	adsorption of Pb ²⁺ , Mn ²⁺ , and Cr ³⁺	Zhu et al. 2011 ¹⁶⁶

Coker et al.¹⁶⁷ published improvement of magnetic properties of biosynthesized magnetic NPs. As a starting material, FeCo-oxyhydroxides were created by adding CoCl₂·6H₂O to FeCl₃ precursor and then treated with *G. sulfurreducens* culture. Resulting cobalt ferrite (CoFe₂O₄) nanoparticles exhibited dramatic enhancement in the magnetic properties in comparison to simultaneously produced MNPs. This introduction of cobalt into magnetic structures therefore represents an advance over other biomineralization studies using magnetotactic bacteria. Similarly, controlled cobalt doping of magnetosomes *in vivo* was published.¹⁶⁵ Study shows increase of the coercive field of the bacterial magnetosomes by 36–45% in presence of cobalt with estimated cobalt content between 0.2 to 1.4%.

Substitution of iron by other metals in MNPs synthesized by other microorganisms has been also reported. Roh et al.¹⁶⁴ reported Co, Cr, Mn and Ni doping of magnetite biosynthesized by means of Fe(III)-reducing thermophilic bacteria *Thermoanaerobacter ethanolicus* and psychrotolerant *Shewanella sp.* Moreover, biofabrication of doped MNPs were performed in large-scale using bacterial fermentation¹⁶⁸, leading to large quantities achievement at low cost. Also *Thermoanaerobacter*, strain TOR-39 was involved in biosynthesis of zinc-ferrite NPs.¹⁶⁹

3.7. Further applications and properties

Throughout this study, were encountered various works that, while relevant, did not fit neatly in to any of aforementioned sections. Therefore, we chose several studies and publications with interesting applications or properties of biofabricated NPs for additional consideration (Table 7).

Fabrication of otherwise difficult-to-synthesize NPs is undoubtedly an asset of bio methods. Ahmad et al.¹⁷⁰ reported such a synthesis - multifunctional CuAlO₂ NPs based on fungus *Humicola sp.*

Table 7. Further applications and properties

NP	Organism used	Application	Reference
CuAlO ₂	<i>Humicola sp.</i>	difficult-to-synthesize nanoparticles	Ahmad et al. 2007 ¹⁷⁰
Au, Ag	<i>Emblica Officinalis</i>	phase transfer, transmetallation	Ankamwar et al. 2005a ¹⁷¹
Au	<i>Tamarindus indica</i> leaf	nanotriangles, vapor sensing	Ankamwar et al. 2005b ¹⁷²
Au-Ag-Cu	<i>Brassica juncea</i> seed	alloys	Haverkamp et al. 2007 ¹⁷³
PbS, ZnS	different <i>cocci</i> and <i>bacilli</i> cells	hollow nanostructures; light harvesting and photocatalytic properties	Zhou et al. 2009 ¹⁷⁴

Phase transfer of biosynthesizes Au and AgNPs was published in a paper by Ankamwar et al.¹⁷¹ NPs were fabricated using *Emblica officinalis* (amla, Indian Gooseberry) fruit extract. The experiments contained also their subsequent phase transfer to an organic solution

(methanol) and the transmetallation reaction of hydrophobized AgNPs with hydrophobized chloroaurate ions (resulted in AuNPs).

Different shapes of resulting NPs also play a role in determining their properties. Tamarind leaf extract served as the reducing agent for the synthesis of gold nanotriangles ranged from 20 to 40 nm in thickness.¹⁷² The effect of different organic solvent vapors like methanol, benzene and acetone on the conductivity of AuNPs triangles was investigated. Current-voltage characteristics were determined in presence of aforementioned organic solvent vapors and observation suggests possible application as chemical sensors. Biofabrication of anisotropic gold nanotriangles was also reported by Verma et al.¹¹¹ On the other hand, Xie et al.¹⁷⁵ performed experiments resulting in silver nanoplates employing green algal species *Chlorella vulgaris*.

Fabrication of alloys without sophisticated equipment or appropriately high temperature¹⁷³ demonstrated the ability to synthesis the Au–Ag–Cu class of alloy by means of the *Brassica juncea* seed. Similarly, studies dealing with bimetallic Au–Ag alloy biosynthesis processes employing fungi were also published.^{176,177}

Morph-biotemplates, hollowed, former-bacterial cells, coated by chalcogenide NPs also represent an innovative approach to material science. Moreover, these PbS and ZnS structures, prepared by the sonochemical method in presence of different *cocci* and *bacillus* (rod) templates, exhibited light harvesting and photocatalytic properties. Hollow structures possess superior photocatalytic activity to their solid counterparts during photocatalytic degradation of acid fuchsine and can be used as electromagnetic wave absorbers, ultraviolet shielding materials, photocatalysts or solar cells.¹⁷⁴

4. Diatoms

Diatoms are unicellular photosynthesizing microorganisms belonging into the group of brown algae (division Chromophyta, class Bacillariophyceae) encased in siliceous cell walls—frustules. Frustule of a diatom is always formed by two valves (epitheca and hypotheca) connected together by circular pieces of silica called girdle bands. The construction material of a frustule is mainly nanostructured amorphous polymerized silicic acid.¹⁷⁸ Surface of the frustule is finely structured with extensions, perforations, thickenings,

or thin areas in the wall, and the final pattern together with a frustule shape is characteristic for each species. The ability of reproduction of such precise forms results from unique mechanism of silica acquirement and processing, which has been previously described in detail.^{179,180} New valves are produced after cell division and cytokinesis of the mother protoplast. The final silica polymerization and its deposition onto the forming diatom wall occur in flattened vesicles called silica deposit vesicles (SDVs). It is likely, that the precise formation of the valve pattern is facilitated by organic macromolecules of the vesicle matrix. When the siliceous wall is completely formed, exocytosis occurs and two daughter cells each containing maternal epitheca and newly formed hypotheca are separated. The inner membrane of the SDVs becomes the new plasmalemma, whereas the outer membrane now forms primary coatings around the silica.¹⁸¹ The proteins associated with the mature diatom cell wall contain highly conserved repeated building block and have been denoted as frustulins.^{182,183} The mechanism of diatom frustule formation is further investigated as a model for biomimetic synthesis of silica nanostructures.^{184,185}

Although biosynthesis of nanoparticles through phototrophic organisms such as cyanobacteria, algae^{13,14} or higher plants¹⁸⁶ was noted previously, this study describes the very first detailed experiments carried out using diatoms, or generally organisms with silica based shells. Formation of nanoparticles in presence of siliceous frustules likely provides occasions for novel bionanocomposite use.

C) EXPERIMENTAL PART

1. *Materials and Methods*

1.1. **Diatom strains and cultures**

Diatom cultures (*Navicula atomus* CCALA 383 – NA; *Diadesmis gallica* CCALA 766 – DG) were obtained from the Culture Collection of the Centre of Algology in Třebon, Biology Centre of the AS CR, Institute of Hydrobiology, Czech Republic. Strains were kept in 1 L Erlenmayer flasks with cotton plugs containing WC Medium.¹⁸⁷ Sodium metasilicate pentahydrate ($\text{Na}_2\text{SiO}_3 \cdot 5\text{H}_2\text{O}$) was added to obtain final concentration of 500 mg of silica per liter of media, ensuring no silica limitation for the diatom growth. The conditions of the growth chamber (KBW-240, Binder, Germany) were at 21°C and 16h/8h light/dark cycle (5 x 36 W/m² Osram Lumilux Cool Daylight fluorescent lamp). Prior to the beginning of the experiment, the cultures were transferred into fresh medium (20% (v/v) of inoculum) and were grown for approximately four weeks to reach a stationary growth phase.

Biosynthesis experiments with Au salt were performed with DG and NA cultures. Subsequently, DG strain was selected for experiments with AgNO_3 .

1.2. **Diatoms Biosynthesis Experiments**

Experiments were conducted to examine the role of diatoms in the synthesis of AuNPs and AgNPs from aqueous solutions of Au and Ag salts respectively. To initiate the experiments, tetrachloroaurate solution (Sigma-Aldrich) and sodium nitrate solution (Sigma-Aldrich) were added to 100 mL of 4-weeks old diatom culture sediment in liquid WC Medium (≈ 400 mg dry weight) in culture flasks (EasYFlasks, Nunc, USA; 225 cm² culture area) to form final 1 mM concentration of the metal salt.

The solutions in flasks were incubated in laboratory conditions (moderate light and 23°C) for 24 hours. Experiments were organized as triplicates. Abiotic control was performed in the same conditions using liquid WC Medium without the diatom cultures.

Suspensions of incubated bionanocomposites (BNC) and control diatom frustules were divided into 15 mL polypropylene centrifuge Falcon tubes and washed three times with distilled water and once with methanol. Suspensions were centrifuged after each washing step (20 minutes, 8000 x g, Rotina 320, Hettich, Germany). List of all samples in this study is given in Table 8.

Table 8. List of samples and their content

Sample code	Organism used	Noble metal used	Magnetically modified
NA	<i>Navicula atomus</i>	x	NO
NA_Au	<i>Navicula atomus</i>	Au	NO
DG	<i>Diadesmis gallica</i>	x	NO
DG_Au	<i>Diadesmis gallica</i>	Au	NO
DG_Ag	<i>Diadesmis gallica</i>	Ag	NO
DG_Au_FF	<i>Diadesmis gallica</i>	Au	YES
DG_Ag_FF	<i>Diadesmis gallica</i>	Ag	YES
DG_FF	<i>Diadesmis gallica</i>	x	YES

1.3. UV-VIS Analyses and Light Microscopy (LM)

Noble metal nanoparticles exhibit a strong UV-visible (UV-VIS) absorption band that is not present in the spectrum of the bulk metal due to SPR phenomenon.¹⁸⁸ An amount of 1.5 mL of each sample suspension was centrifuged for 2 minutes (8.000 x g, EBA 21, Hettich, Germany). The optical absorption spectra of the samples were measured by UV-VIS spectrophotometer Cintra 303 (GBC Scientific Equipment, Illinois, USA).

Due to very strong adsorption of gold nanoparticles to diatoms frustules, golden based samples were sonicated for 10 minutes in Ultrasonic Bath Sonicator (PCI Analytics Pvt. Ltd., India). The diatom cultures alone (reference control) as well as their suspension with tetrachloroaurate were examined using an OLYMPUS BX 51 brightfield microscope with high resolution Nomarski DIC optics, equipped with a DC 71 digital camera, under an immersion oil lens at 1000x magnification.

1.4. Elemental analysis

The content of samples were investigated by an atomic emission spectrometer with inductively coupled plasma (ICP-AES; Spectro Vision EOP, Spectro, Germany) and an atomic absorption spectrometer with flame atomization (AAS; UNICAM 969, Pye Unicam Ltd., UK). Samples were dissociated with concentrated hydrofluoric acid (HF) and metal concentrations were measured using ICP-AES (total gold, silver, and iron) and AAS (total iron) with reference to appropriate standards.

1.5. Transmission Electron Microscopy (TEM) and Scanning Electron Microscopy (SEM)

Unstained whole sample mounts of diatoms and metallic NPs from the experiments were examined with a Jeol 1200 EX TEM microscope (JEOL Ltd., Japan) operating at 120 kV and a field emission SEM microscope JSM-7401F (JEOL Ltd., Japan) with a cryo system for high-resolution SEM Gatan ALTO 2500 (Gatan Inc., USA). The mounts were prepared by floating carbon-coated grids on a drop of culture for several minutes to allow the cells and any fine-grained particles to attach. Nature of observed crystalline structures was confirmed by the Selected Area Electron Diffraction (SAED) method.

1.6. Image analysis

The image analysis tool (JMicrovision: Image Analysis Toolbox, www.jmicrovision.com) was used for size distribution analysis of the nanoparticles in the experimental samples. At least 400 NPs from TEM micrographs underwent the image analysis per sample.

1.7. X-ray diffraction (XRD)

X-ray diffraction patterns were obtained using a Multipurpose Powder Diffractometer X'PERT PRO MPD (PANalytical B.V., Netherlands) working with the Bragg-Brentano geometry, fixed slits, X'CELERATOR detector. The measurement parameters were: 40 kV, 30 mA. The samples were scanned from 3° to 75° 2 θ with interpolated step size 0.02°.

Diffraction patterns were taken from dried specimens and were interpreted by means of ICSD crystallographic databases.

1.8. Magnetic modification

The following optimal procedure was used for the magnetic modification of diatom cells or gold and silver based BNCs. Water-based ionic magnetic fluid (ferrofluid, pH 1.63) stabilized with perchloric acid and prepared using a standard procedure was employed in the modification process.^{189,190} The relative magnetic fluid concentration (17.3 mg.mL^{-1}) was given as the maghemite content determined by a colorimetric method.

The bionanocomposite sediments (2 mL) were suspended in 10.0 mL of methanol and 600 μL of ferrofluid. The suspensions were mixed on a rotary mixer (Dynal, Norway) for 1 h at laboratory temperature. Magnetically modified diatoms were washed several times in methanol in order to remove non-magnetic frustules and residual ferrofluid until the supernatant was clear and stored in methanol at 4 °C.

A vibrating sample magnetometer (VSM) EV9 (Microsense, LLC, USA) was used for measurements of magnetization curves (M vs. H) at RT. The longitudinal magnetization components, i.e. component parallel with applied magnetic field H, were also measured.

1.9. Catalytic Study

To test the efficacy of AuNPs and AgNPs for their catalytic activity, reduction of 4-NP was monitored as follows: Distilled water, 4-NP (Sigma Aldrich – final concentration 0.1 mM), and NaBH_4 (Sigma Aldrich – final concentration 100 mM) were mixed to form a total volume of 25 mL in a 100 mL glass distillation flask. To this reaction mixture, 0.1 mL (approximately 4.5 g.L^{-1}) of bionanocomposite was added.

A whole reaction mixture was stirred using a mechanical stirrer RZR 2041 (Heidolph, Germany). Samples were taken every 2 minutes and analyzed immediately in a quartz cuvette by UV-VIS spectrometer Cintra 20 (GBC Scientific Equipment Ltd., Australia). Control experiments were performed with the same conditions with the clean and magnetically modified diatom frustules. All the experiments were performed as triplicates.

To confirm the reaction products, reaction solution was analyzed by means of HPLC. Analysis of samples containing 4-NP and its metabolic intermediates were conducted by HPLC System DeltaChrom (Watrex Prague Ltd., Czech Republic) using a 250 mm × 4 mm Nucleosil, 120-5 C18 column (Watrex Prague Ltd., Czech Republic). A mobile phase of methanol/water (50:50) with 0.1% (vol.) H₃PO₄ was used at a flow rate of 1.0 mL.min⁻¹. Peaks were detected by measuring the absorbance at 215, 230, and 265 nm (4-NP and 4-AP quantified at 265 nm) with a diode array detector Model UV 6000 LP (Thermo Separation Products, Inc., USA). Reaction conditions were slightly different (1 mM 4-NP, 53 mM NaBH₄) due to higher time demands of used methods. Experiments were performed as duplicates (DG_Au) with a corresponding control (DG).

1.10. Antimicrobial Study

The minimum inhibitory concentration (MIC) assessment and selective diffusion (SD) test were performed to describe the antimicrobial properties of prepared BNC. Samples were completely dried (37°C) and the obtained powder was used for antimicrobial study.

SD test was performed as follows: Bacterial cultures were inoculated onto agar plates (Luria agar, Blood agar) as a uniform lawn. The bionanocomposite powder was then spread onto the agar plates, which were incubated for 24 hours in 37°C. Obtained growth inhibition was qualitatively compared with control agar plates without the bionanocomposite powder. All experiments were performed as duplicates.

MIC was determined as the lowest concentration that completely inhibits bacterial growth.¹⁹¹ Samples were suspended in PBS buffer within 2 mL Eppendorf tubes at 10% (w), 3.33% (w) and 1.12% (w) concentrations. Bacterial cultures of *Staphylococcus aureus* (CCM 299), *Streptococcus agalactiae* (CCM 6187), *Escherichia coli* (CCM 3954), and *Pseudomonas aeruginosa* (CCM 1960) were provided by Czech collection of microorganisms (Brno, Czech Republic). The *Bacillus anthracis* spores were originated from the Antraxen vaccine (Bioveta a.s., Czech Republic). Bacterial cultures were inoculated into each tube ($\approx 10^5$ cells per mL). Samples were divided for cultivation in RT and 37°C for intervals of 6 hours, 1, 2, and 3 days. Samples taken in select intervals were inoculated in agar plates (Luria agar, Blood agar) followed by incubation for 48 – 72 hours at 37°C.¹⁹²

2. Results and Discussion

2.1. Nanoparticle biosynthesis – bionanocomposite formation

2.1.1. Gold based bionanocomposite formation

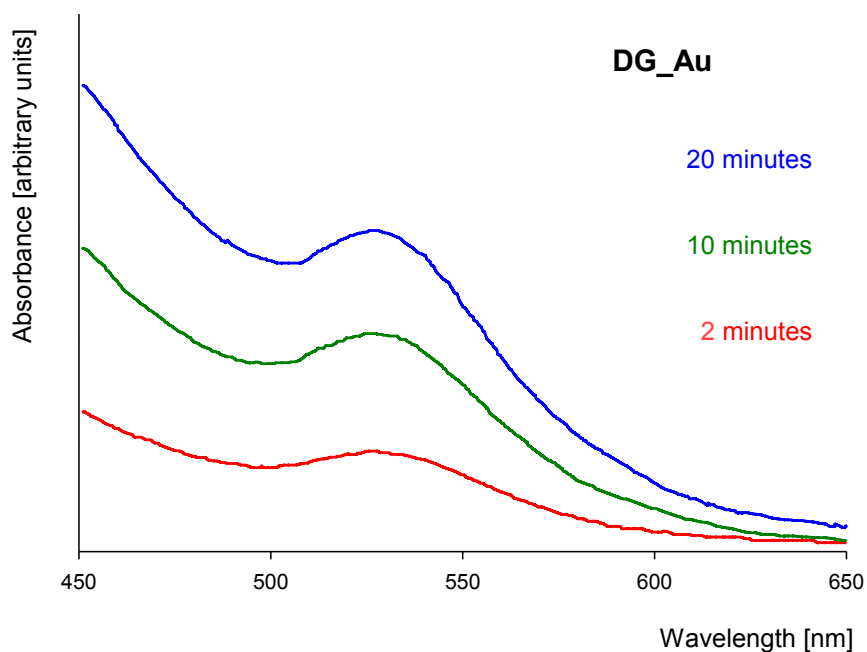
Approximately 2 hours after experiment initiation, the color of the experimental suspensions began to turn dark red. The samples were left to incubate for 24 hours and subsequently centrifuged. Although the color of the suspension was still red, measurement of UV-VIS spectra did not prove any characteristic AuNPs SPR peak. This indicated the presence of AuNPs solely in the pellet of the cells, tightly adsorbed to diatom frustules. However, a portion of AuNPs was released after the sonication. UV-VIS spectrum of gold colloid obtained from DG_Au sample is given in Figure 1 a). The material remained purple after all the washing steps without any significant color loss or washing out.

2.1.2. Silver based bionanocomposite formation

Similarly, suspension DG cells treated with AgNO_3 exhibited a color change after 4-6 hours. The color changed from orange to orange-brown. Unlike the formation of gold nanoparticles, silver nanoparticles were present on the diatom biomass and in the solution. UV-VIS spectra during the biosynthesis experiments are given in Figure 1 b). During the washing (mainly the methanol step), BNC color changed to brownish green (probably due to extraction of chlorophyll).

Concerning the speed of diatom nanoparticle biosynthesis, the duration of the bioreduction of gold tested was in the order of hours. Such time is shorter when compared to studies of NPs biosynthesis in cyanobacteria, where the bioreduction took place in order of days^{193,194, 177,178} but it was longer than studies performed on bacteria or fungi^{195,196}. However, all of the experiments indeed strongly depend on the weight of biomass used, pH of bioreduction, salt concentration, etc.^{197,198}

a)



b)

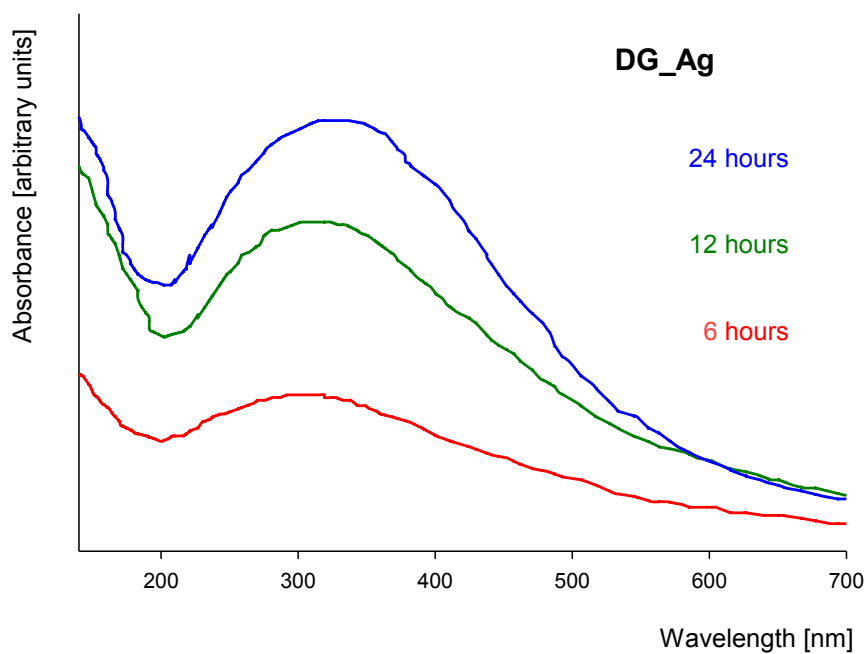


Figure 1. UV-VIS spectra of a) solution of biosynthesized gold nanoparticles after 2, 10 and 20 minutes of sonication; b) biogenic silver nanoparticle solution 6, 12 and 24 hours after start of the experiments. Both spectra represent maximum characteristic for Au, and Ag nanoparticles resp.

2.2. Elemental Analysis and XRD Study

Due to the fact that NPs are attached to diatom frustules, ICP-AES and AAS can only provide quantitative information about selected elements, not data about particle size.¹⁹⁹ Elemental content of all samples is given in Table 9. ICP-AES and AAS analysis confirms significant presence of gold and silver in all samples. These measurements also proved high content of iron in samples treated with ferrofluid. Regarding the ICP-AES results, gold content is higher. These results were also confirmed by TEM and SEM observations, which showed a higher concentration of gold nanoparticles in the micrographs. It can also assume that both noble metals are present predominantly in nano form (see section 2.4).

Table 9. Elemental analysis of BNC

Sample code	Au [% (w)]	Ag [% (w)]	Fe [% (w)]
DG_Au	11.31 ± 1,20	x	x
DG_Au_FF	6,63 ± 0,67	x	4,42 ± 0,22
DG_Ag	x	0,73 ± 0,08	x
DG_Ag_FF	x	1,19 ± 0,12	18 ± 1
DG_FF	x	x	26 ± 2

More specific qualitative information about sample content was given by XRD studies. X-ray diffraction explicitly confirmed presence of crystalline gold in all of the experimental suspensions containing diatoms treated with tetrachloroaurate (diffractograms of DG_Au and DG_Au_FF are shown in Figure 2). Peaks of the diffractogram are in agreement with theoretical presumptions for cubical gold patterns (indexed [1,1,1], [2,0,0] and [2,2,0]). A similar diffractogram was observed in the case of the NA strain (not shown), which differed in additional peaks indicating minute presence of other ingredients originating from the WC medium salt precipitates or unexpended tetrachloroaurate.

Similarly, presence of cubic silver ([1,1,1], [2,0,0] and [2,4,1]) was confirmed in the case of the DG_Ag and DG_Ag_FF samples (Figure 3). With regard to previous measurements (data not shown), certain amounts of silver oxides can be found in these samples, probably due to the lower stability of silver in comparison to gold.²⁰⁰

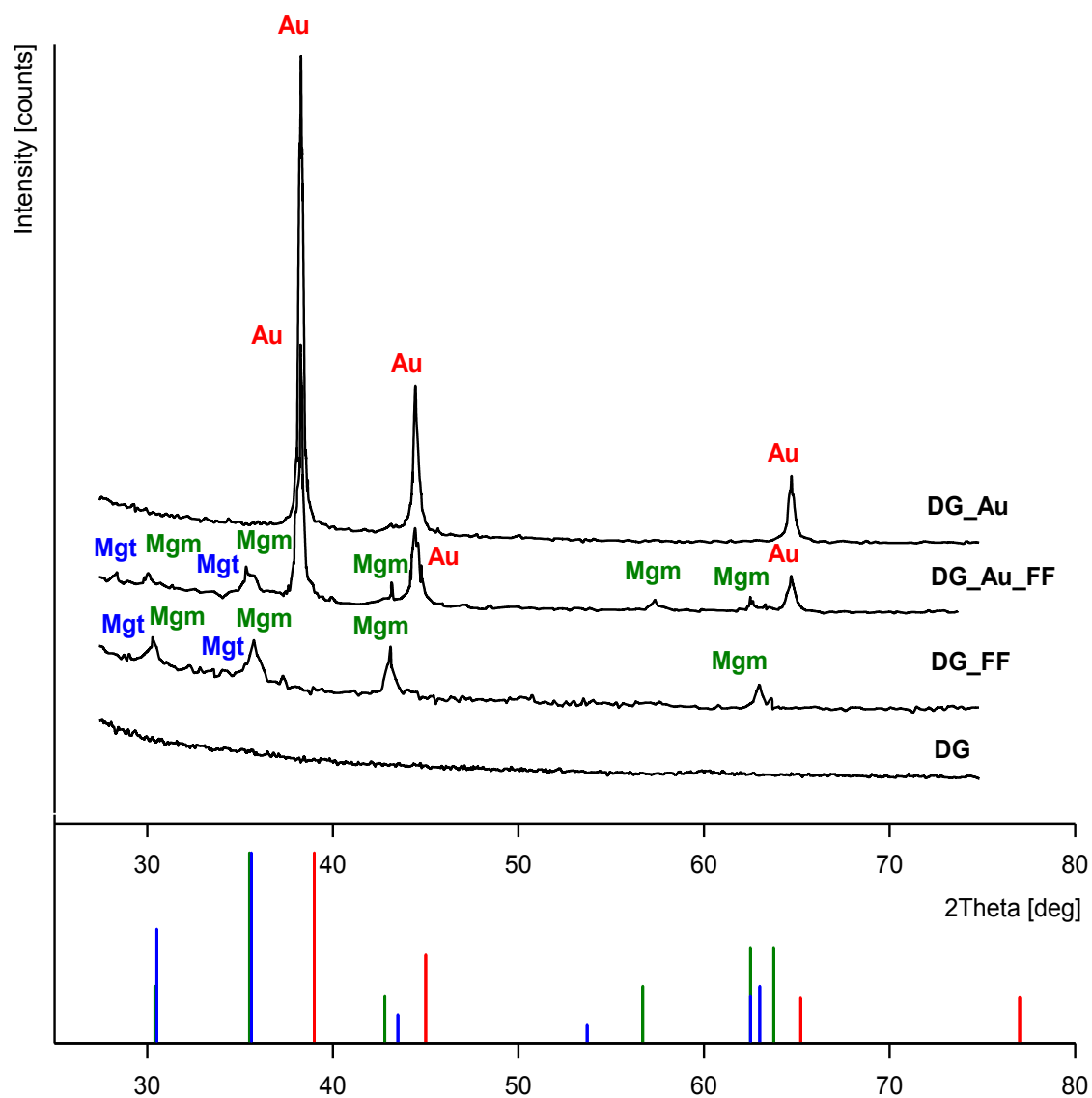


Figure 2. XRD diffractogram of BNC samples containing gold nanoparticles (Au) and ferrofluid. The lower graph represents theoretical diffraction patterns for cubic gold (red), maghemite (dark green – Mgm) and magnetite (blue – Mgt).

Water-based ionic magnetic fluid was prepared using the standard Massart procedure.¹⁸⁹ Regarding the Mössbauer spectroscopy measurements in a similar study,²⁰¹ ferrofluid

contained mostly maghemite ($\gamma\text{-Fe}_2\text{O}_3$). XRD measurements proved these expectations (Figures 2 and 3) and showed presence of certain amounts of magnetite (Fe_3O_4).

However, due to similar positions of maghemite and magnetite peaks in the XRD pattern, it is difficult to differentiate their content in the samples.²⁰²

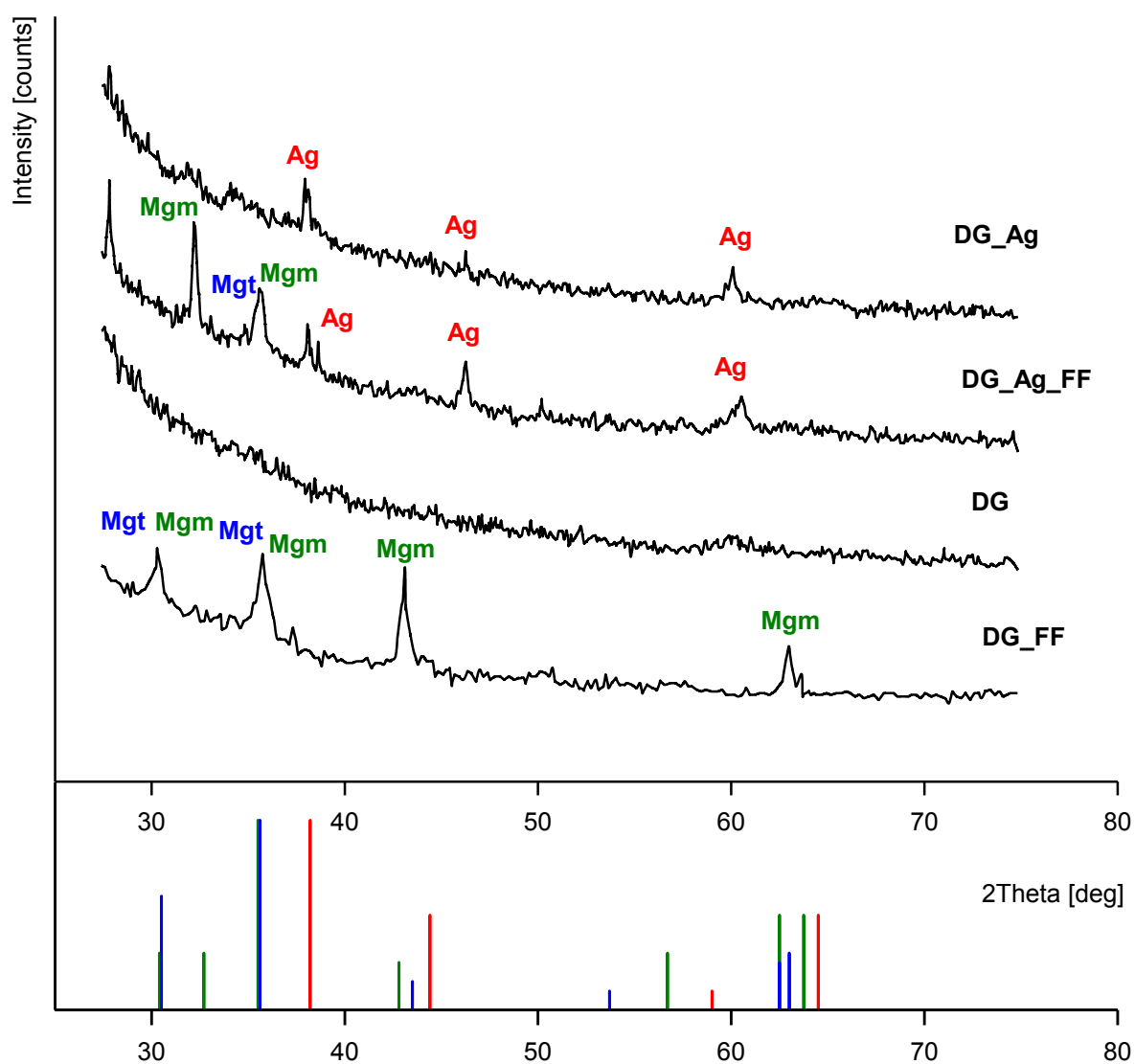


Figure 3. XRD diffractogram of BNC samples containing silver nanoparticles (Ag) and ferrofluid. The lower graph represents theoretical diffraction patterns for cubic silver (red), maghemite (dark green – Mgm) and magnetite (blue – Mgt).

2.3. Light Microscopy

LM observations were conducted with Au based BNC due to their favorable optical properties (see Figure 4²⁰³). LM micrographs provide overall morphologies of the samples. Compared to the reference control (Figure 4 a), b)), diatom cells in the experimental samples and their proximate surroundings changed their color to purple, signaling the presence of AuNPs fixed to the living substance (Figure 4 c), d)). LM micrograph also showed substances from disrupted cells, indicating that some diatom cells have died during the biosynthesis process²⁰³.

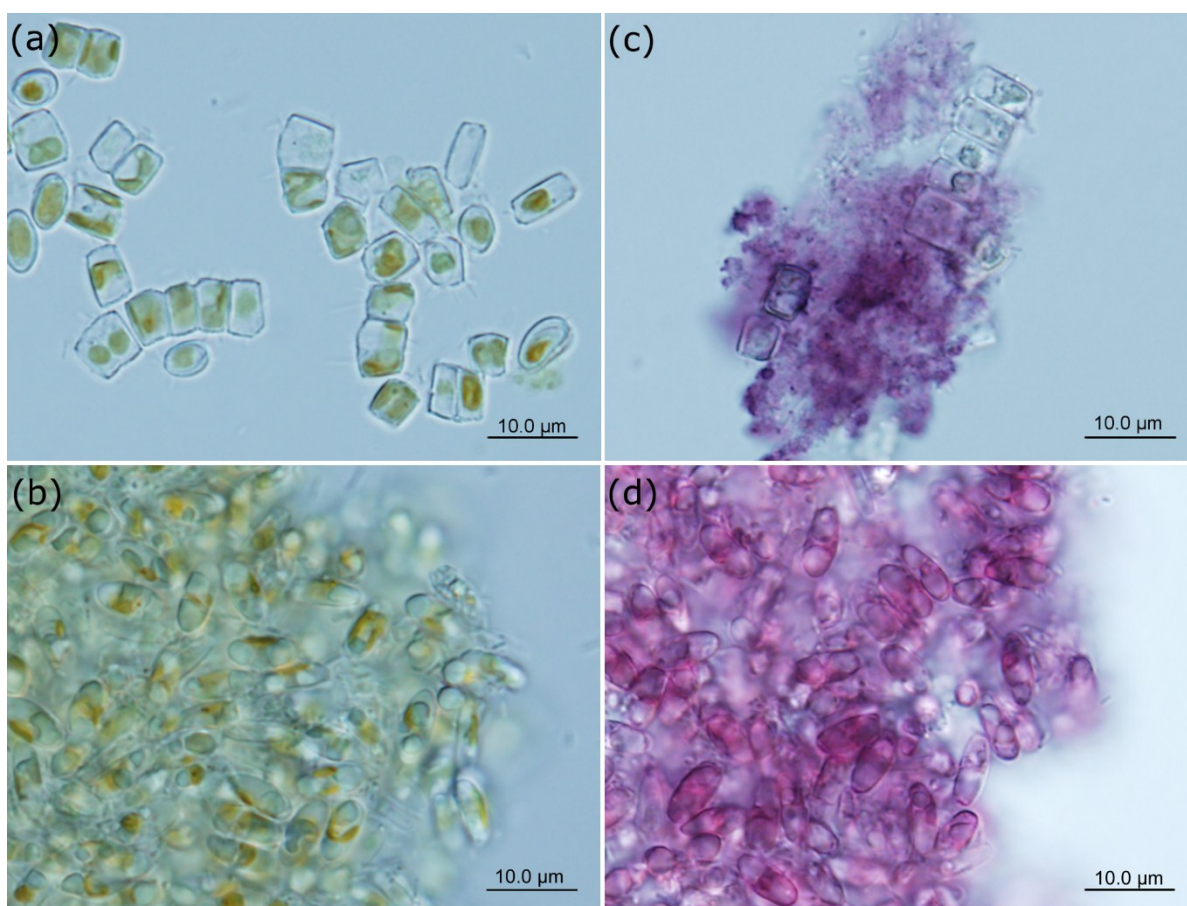


Figure 4. Light microscope photographs of the diatom cells before (left) and 24 hours after (right) tetrachloroaurate addition for (a,c) *Diadlesmis gallica*, and (b,d) *Navicula atomus*.

Although no viability studies were performed during the biosynthesis process, LM showed remarkable changes in the cells. Based on this fact and previous studies^{197,204} we can assume that reduction of HAuCl_4 occurs in the presence of both living and lifeless biomass. However, it is difficult to distinguish the contributions of vital and dead diatom cells to the bioreduction process.

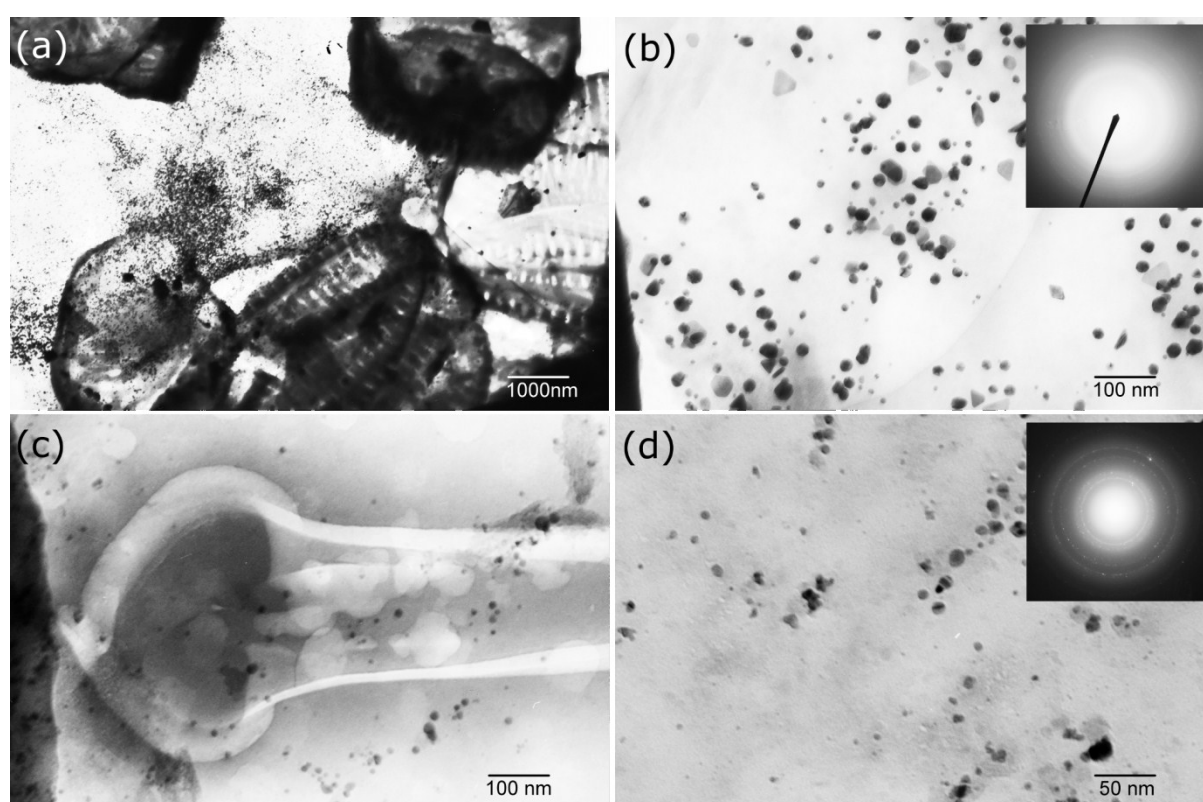


Figure 5. TEM micrographs of (a,c) *Diadesmis gallica*, and (b,d) *Navicula atomus* cells after tetrachloroaurate addition. Gold nanoparticles captured in the EPS net of the intercellular space of DG (a). Detail of association of gold nanoparticles with the frustule surface in the raphe region of NA (c). Detail micrographs of AuNPs and SAED patterns for DG (b), and NA strains (d).

2.4. TEM

Photographs from the TEM clearly show the presence of spherical AuNPs in experimental samples for both diatom strains (see Figure 5²⁰³). The Au nature of these crystalline nanoparticles was confirmed by SAED patterns (Figure 5 b), d)). It was observed that the AuNPs remain captured in EPS net in the extracellular space (Figure 5 a)), or are directly associated with the diatom frustule structures (Figure 5 c)).

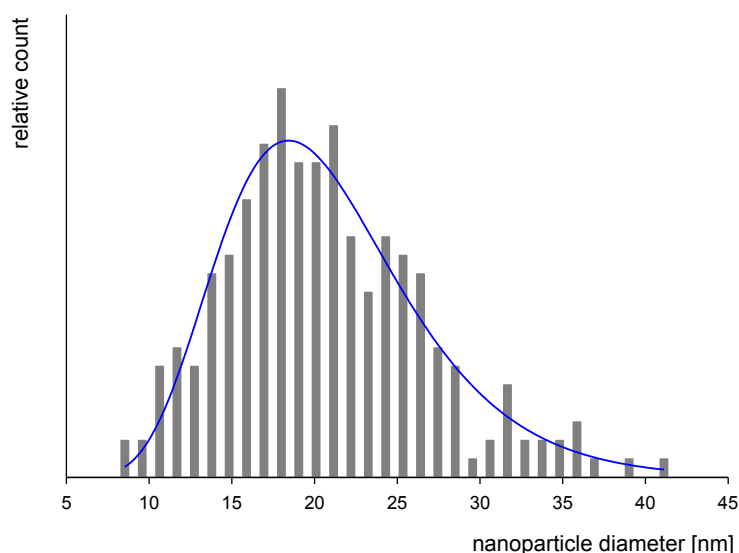


Figure 6. Histogram of size distribution of gold nanoparticles synthesized by *Diadesmis gallica* after tetrachloroaurate addition

Both detailed TEM pictures (Figure 5 b), d)) and image analysis (JMicrovision programme) confirmed mostly spherical shape of the nanoparticles. Size of the biosynthesized nanoparticles differed in each strain. Whereas DG samples showed larger mean particle size (around 18 nm) and wider range of the size distribution (Figure 6), AuNPs synthesized by the NA strain had a smaller mean particle size (9 nm) and higher homogeneity in size (Figure 7).

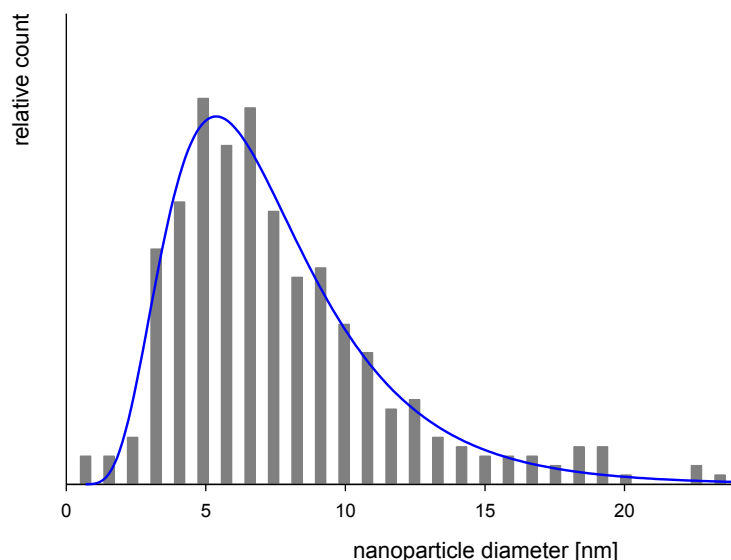


Figure 7. Histogram of size distribution of gold nanoparticles synthesized by *Navicula atomus* after tetrachloroaurate addition

Moreover, JMicrovision image analysis revealed notable differences between the size of the AuNPs embedded in the EPS structures and the AuNPs adsorbed to frustule surface. When compared, particles in the EPS are roughly 50% smaller than the ones on the silica surface. This phenomenon is likely caused either by the nature of the microstructure of the silica surface or by the constitution of the EPS net. Yet, for the potential practical application of the nanoparticles synthesized by diatoms, the possibility of certain regulation of the size and the size distribution by using alternative tetrachloroaurate concentration, temperature or other parameters is expected.¹⁹⁸

DG strain has been subsequently employed in magnetic modification and also in biosynthesis experiments with silver nitrate. Figure 8 shows a series of samples containing AgNPs (DG_Ag), ferrofluid particles used for magnetic modification (DG_FF) and both AgNPs and ferrofluid NPs (DG_Ag_FF). Similarly, golden based BNC (DG_Au and DG_Au_FF) TEM micrographs are presented in Figure 9. These TEM micrographs allow determination of dimensional distribution of these nanoparticles. AgNPs, and ferrofluid nanoparticle size distribution histograms are given in Figures 10 and 11. The size histograms are satisfactorily described by a log-normal distribution of the particle diameters with a mean

particle diameter of AgNPS and ferrofluid NPs to be 23 nm, and 12.5 nm respectively. Nature of these crystalline nanoparticles has been confirmed by SAED patterns (Figures 8, 9).

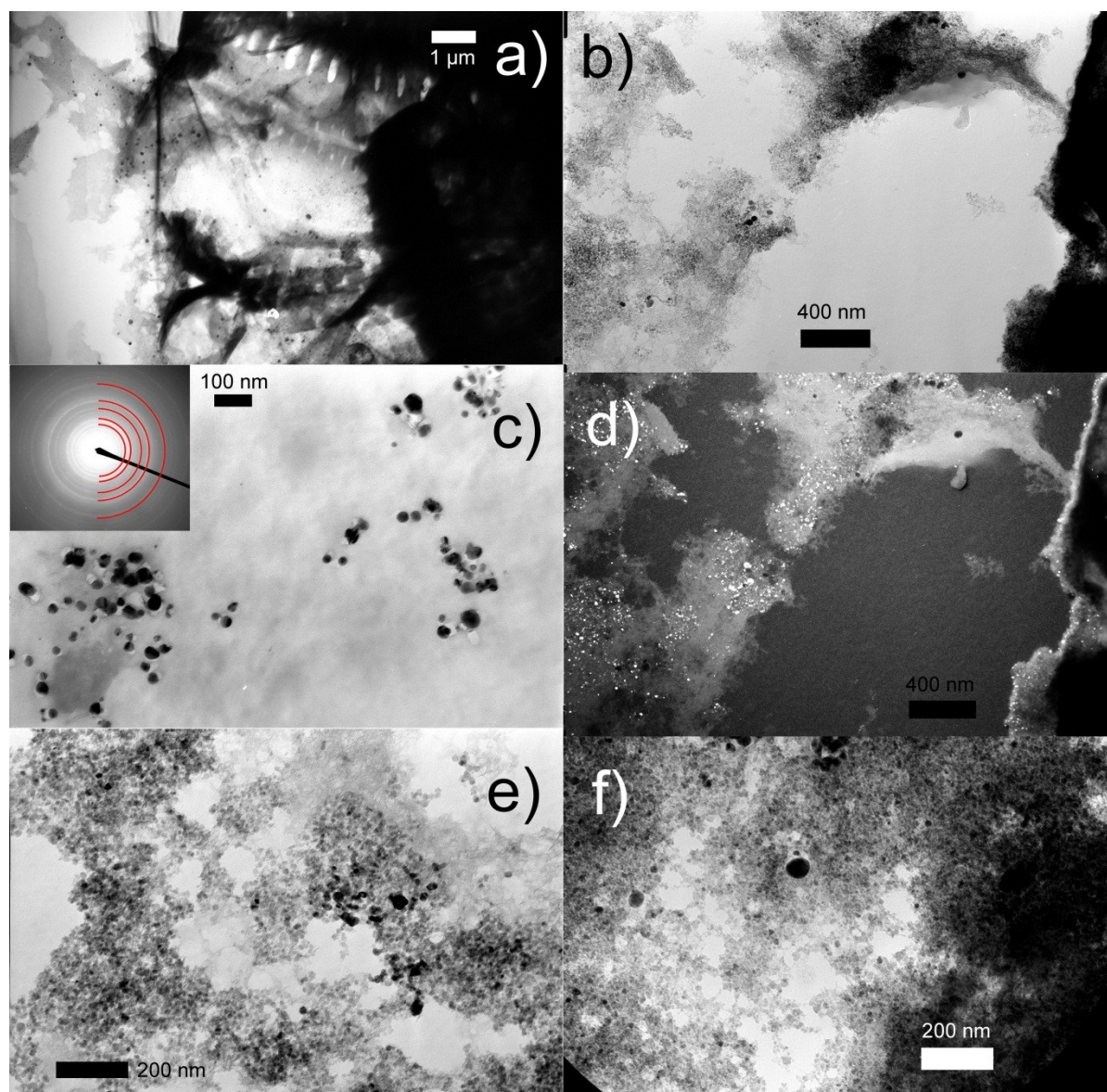


Figure 8. TEM micrographs of samples DG_Ag (a, c), DG_Ag_FF (b, d, f) and DG_FF (e). Silver nanoparticles associated with the diatom frustule (a), detailed micrographs and SAED pattern of silver nanoparticles (c). Ferrofluid and silver nanoparticles – pictures were taken in bright field (d) and dark field regime (f) respectively.

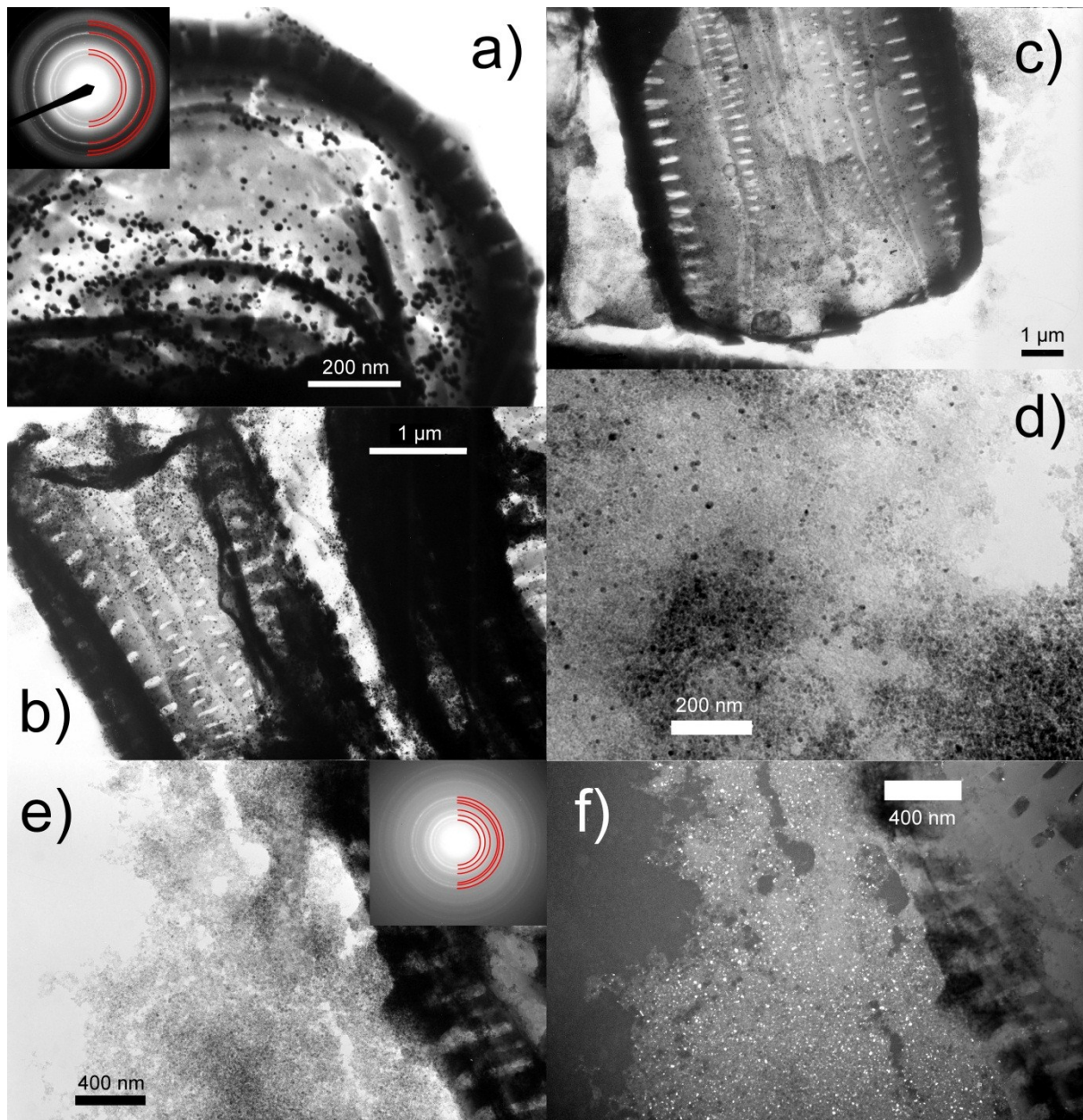


Figure 9. TEM micrographs of samples DG_Au (a, b), DG_Au_FF (c, d) and DG_FF (e, f). Detail of gold nanoparticles associated with the diatom frustule, SAED pattern corresponding with cubic gold (a). Larger part of diatom frustule with gold nanoparticles (b). Gray ferrofluid veil together with gold nanoparticles (dark dots) on the frustule surface (c) and in the detail (d). Ferrofluid nanoparticles by the diatom surface in bright (e) and dark (f) field, SAED pattern of maghemite (e).

TEM micrographs have well-documented the sizes and shapes of the investigated NPs. They have also proved the coexistence of Ag or Au NPs with the ferrofluid nanoparticles in the case of magnetically modified samples.

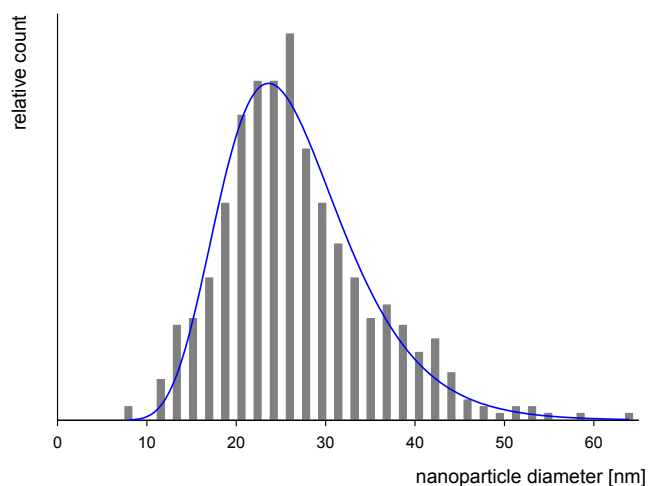


Figure 10. Histogram of size distribution of silver nanoparticles synthesized by *Diadlesmis gallica* after silver nitrate addition

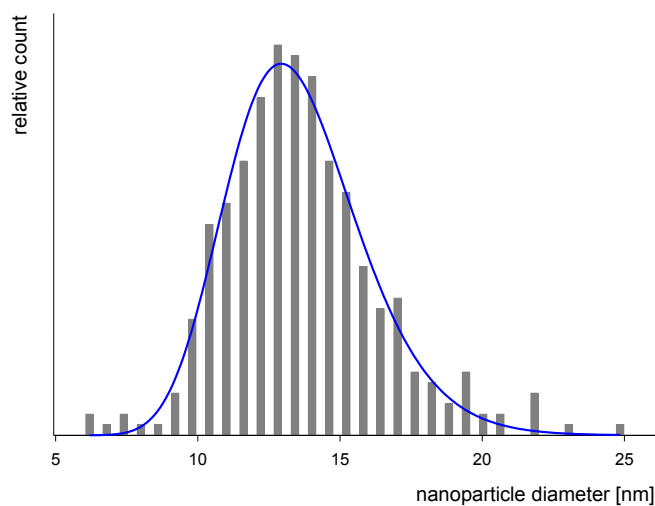


Figure 11. Histogram of size distribution of ferrofluid nanoparticles after magnetic modification of diatom cells

2.5. SEM

The spatial distribution of the nanoparticles in all samples was examined using SEM with a cryochamber, which allowed us to avoid structural changes caused by dehydration procedures in standard SEM preparation methods. Using the backscatter secondary electron detector (for the better differentiation of elements based on their atomic weight), the attachment of the nanoparticles to the diatom frustules was observed.

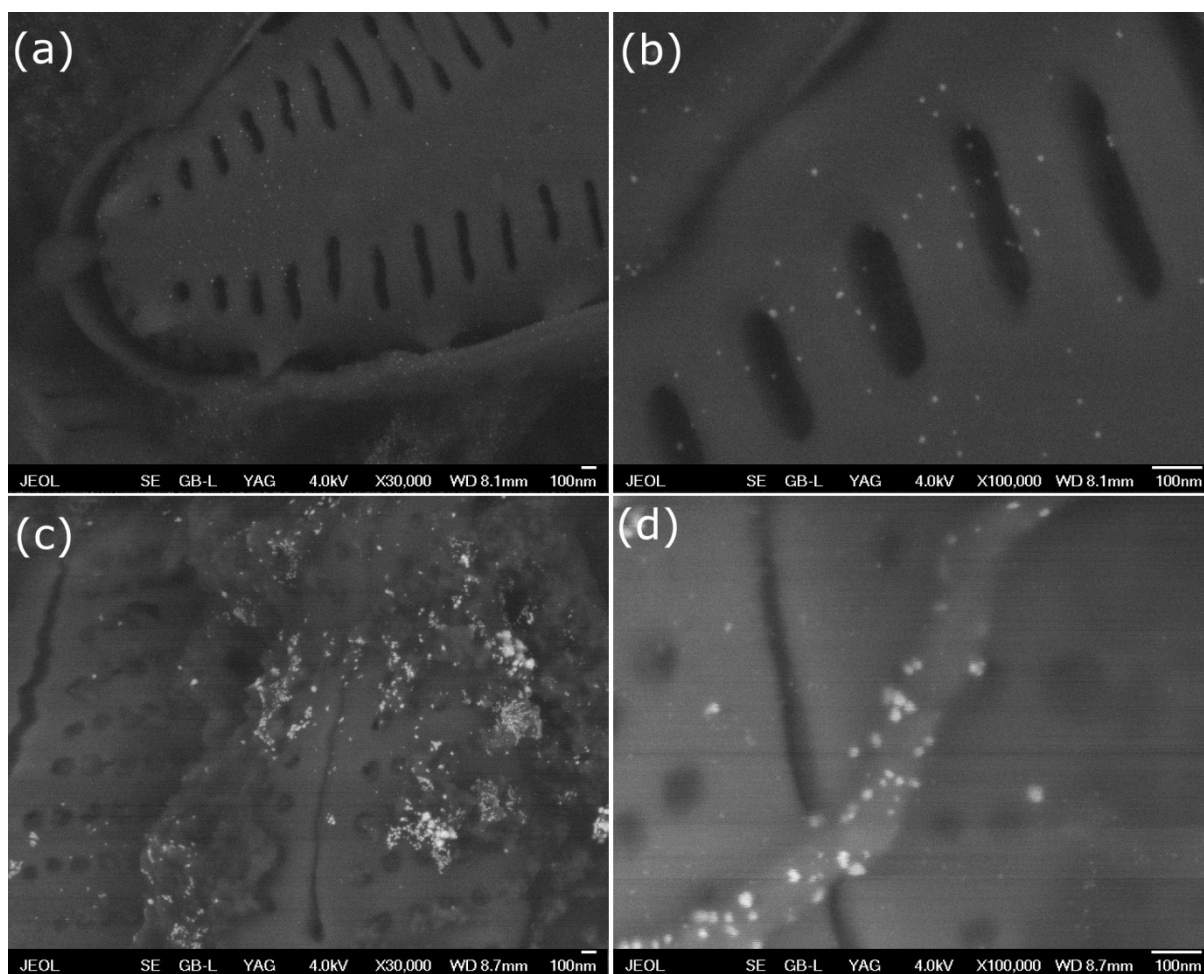


Figure 12. SEM micrographs of (a,c) *Diadlesmis gallica*, and (b,d) *Navicula atomus* cells after tetrachloroaurate addition. Detail of gold nanoparticles deposition on the silica frustule surface of the DG cells (b). Association of gold nanoparticles with the EPS structures of the NA cell (c). Detail micrograph of gold nanoparticles embedded into the EPS chain of the NA cell (d).

2.5.1. SEM analysis of NA_Au and DG_Au

The SEM micrographs (Figure 12²⁰³) clearly show the shape of the diatom frustules, as well as the structures of the intercellular matter (EPS) with attached nanoparticles. In accordance with the light microscopy observations, SEM depicted the nanoparticles distributed in the more loosened and thicker layer of the EPS structures around the cells and directly on the frustule surface of the DG strain, whereas a dense fibrous net of the EPS close to the frustule surface with entrapped nanoparticles can be seen in pictures of the NA strain (Figure 12).

On the other hand, abiotic control experiments without diatom cultures did not prove the presence of AuNPs in the solution neither by the color change nor by means of any microscopy technique (data not shown).

The observations from the LM and EM suggest slightly different ways of the AuNPs deposition in each diatom strain.²⁰³ DG cells were strongly surrounded by a veil of EPS in which the AuNPs were captured and distributed (Figure 12 c, d)), whereas in DG cells the AuNPs were attached to a thin layer of the EPS in direct proximity to the frustule (Figure 12 a, b)). Besides, both strains had nanoparticles directly adhered to the surface of the siliceous frustule.²⁰³ Yet, the conclusions on the EPS abundance and extent are uncertain, as it was also noticed remarkable disintegration of the living matter due to the unfavorable growth conditions caused by the tetrachloroaurate added into the medium (especially in the DG strain). The cell content discharged off some of the frustules might have mixed with the EPS. On the other hand, observed embedding of the nanoparticles in the organic matter seemed to be very stable; the very same picture was obtained more than 30 days after the experiment was performed.²⁰³

Significance of the EPS structures for the NPs stabilization was previously discussed in the case of cyanobacteria¹⁹⁷. The function of the EPS is basically the same for both cyanobacteria and diatoms. Primarily, they form a mechanical and chemical protective biofilm around the cells; other functions are formation of interspecies communication network in symbioses etc.²⁰⁵⁻²⁰⁹ EPS are negatively charged and possess metal-binding capabilities^{210,211}, so that after intracellular synthesis, gold nanoparticles are released to the culture medium (as observed in cyanobacteria e.g. by Bhattacharia and Gupta²¹²) and can be

directly attached to the EPS. Embedding of released nanoparticles into a polysaccharide network of the diatom EPS is clearly visible in both TEM and SEM micrographs attained in this study. Moreover, these observations indicate a stabilization function of the diatom EPS against NPs aggregation²⁰³.

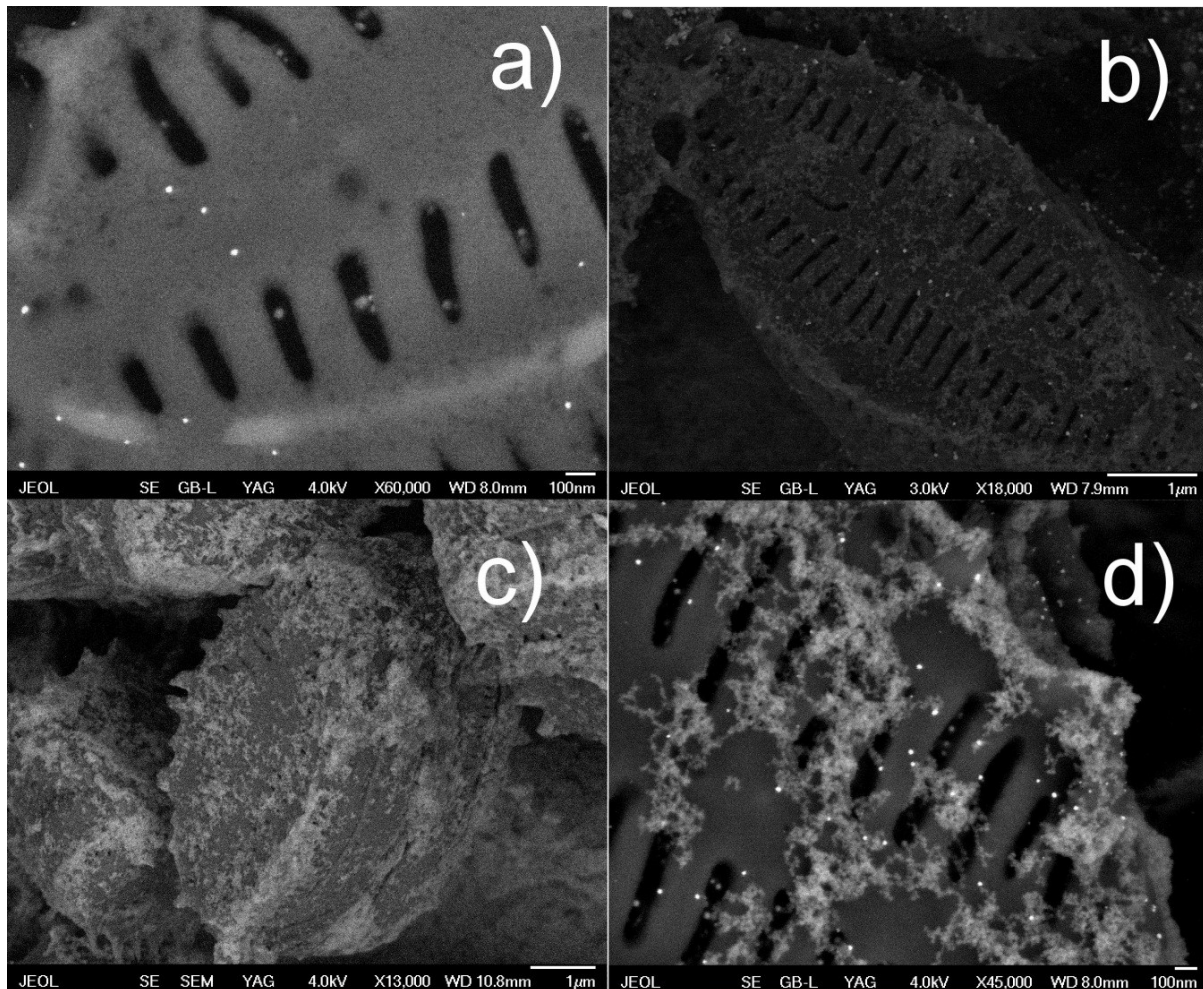


Figure 13. SEM micrographs of samples DG_Au (a), DG_Au_FF (b,d) and DG_FF (c). Gold nanoparticles are attached on the surface of diatom cells, but can be often also inside the pore (a). Diatom frustules veiled into the ferrofluid (b, c). Detail of gold nanoparticles mixed with ferrofluid (d).

2.5.2. SEM analysis of magnetically modified BNC

SEM analysis of series of magnetically modified samples of silver and gold based bionanocomposites is given in Figures 13 and 14. Figures show comparison of sample containing only AuNPs and AgNPs (DG_Au, DG_Ag resp.), both noble metals and ferrofluid (DG_Au_FF, DG_Ag_FF) and only ferrofluid (DG_FF). Intensity of particular object in micrographs differs with regards to relative atomic weights of their atoms. Therefore, both silver and gold nanoparticles are more intensive than iron based ferrofluid nanoparticles and can be easily recognized.

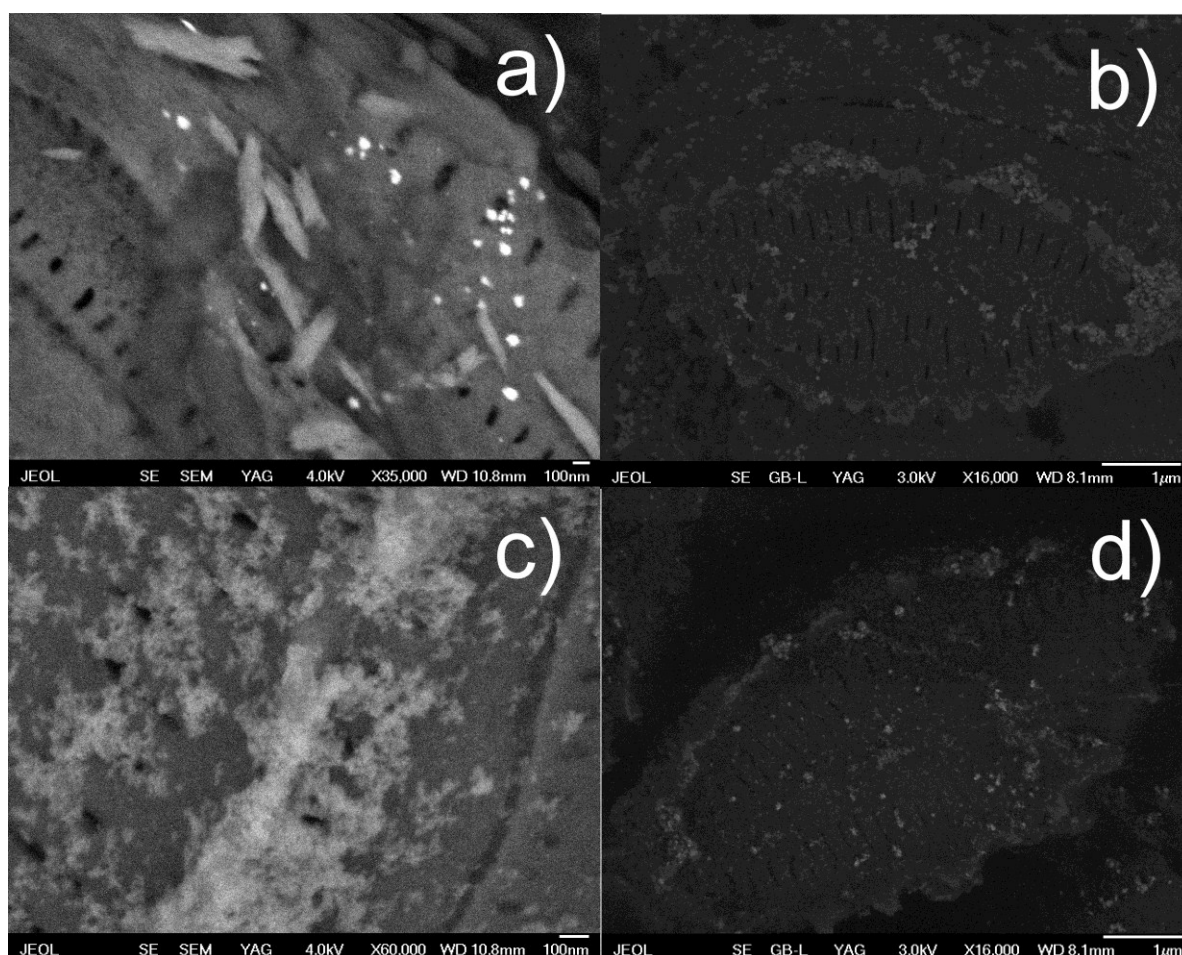


Figure 14. SEM micrographs of samples DG_Ag (a), DG_Ag_FF (b,d) and DG_FF (c). Amount of silver nanoparticles is lower when compare to gold NPs and they are usually aggregated in certain areas (a). Magnetically modified cells of diatoms with biosynthesized silver nanoparticles (b, d). Ferrofluid detail (c).

Pictures show that diatom frustules with attached noble metal nanoparticles are veiled to ferrofluid nanoparticles. These nanoparticles are mostly aggregated forming thin net around the cell surface. Amount of silver nanoparticles is significantly lower and they are concentrated in certain areas. In contrary, gold nanoparticles are spread randomly on the surface of frustule.

2.6. Possible mechanism of nanoparticle biosynthesis

It is likely that important role in AuNPs biosynthesis and transport off the cell in diatoms is played by the SDVs, as the formations of corresponding proportions were frequently seen on the TEM micrographs of the experimental samples. However, the mechanism of nanoparticles formation by the living cells (or with their contribution) is still largely unclear, despite increasing number of new studies concerned with this question. According to the accessible sources, reduction in phototrophic organisms occurs through interaction of the metallic salt with cellular organic compounds such as carbohydrates or proteins. Previous studies with heavy metal recovery in brown algae¹³ indicated that reduction of Au^{3+} to Au^0 occurred through oxidation of hydroxyl groups (abundant in polysaccharides of the algal cell wall) to carbonyl groups. Also algal pigments rich in hydroxyl groups (e.g. fucoxanthins²¹³), or other highly reactive functional groups such as sulfhydryl present in the polysaccharides of the cell wall (responsible for its brown color – fucoidans²¹³), could be involved in the reduction processes. Greene et al.²¹⁴ determined the importance of these groups in experiments with the green alga *Chlorella vulgaris* (their chemical modification reduced the gold uptake).

Last but not least, the role of silaffin polypeptides in the nanoparticles formation should be mentioned. Silaffins are a class of heavily posttranslationally modified proteins responsible for mediating silica deposition at ambient temperature and pressure^{215,216}. Within the native peptides, lysine residues are modified to long-chain polyamines and serine residues phosphorylated.^{181,217} Native silaffin polypeptides isolated from a diatom *Cylindrotheca fusiformis* can catalyze the silica precipitation in vitro from a silica precursor under slightly acidic conditions²¹⁸). This process is caused by a self-assembly of the silica due to the silaffins activity resulting into the silica nanoparticle formation.²¹⁹ I expect that the silaffins

might play role also in synthesis of other types of nanoparticles such as AuNPs; however additional research beyond the scope of this study would be necessary to verify this hypothesis.

2.7. Magnetization Measurements

Ferrofluid modification of silver and gold based diatom composites has been performed as mentioned in section 1.8. The response of magnetic nanoparticles (maghemite, magnetite) in ferrofluid to external magnetic fields reflects characteristically different spin dynamical



Figure 15. Illustration of ferrofluid modified BNC behavior in external magnetic field.

processes compared to those of their bulk counterparts.²²⁰ In order to test if the obtained ferrofluid-modified BNC could be used in the magnetic separation procedures, simple test with magnet and also magnetization measurements as a function of applied magnetic field was performed. Figure 15 shows response of magnetically modified BNC to applied magnetic field from dipole magnet.

At the RT, the field dependent magnetization curves of all prepared magnetic materials show the superparamagnetic behavior indicated by the absence of hysteresis (see Figure 16). Coercive field (H_c) values were also relatively small (Figure 16). Regarding saturation curves, samples have been already saturated in applied external magnetic field (15.000 Oe). All the curves have similar shapes – that assume similar magnetic behavior of all samples. The main differences are the saturation magnetization values M_s (Figure 16). These values are approximately 10x higher than in similar study by Mosiniewicz-Szablewska et al.²⁰¹

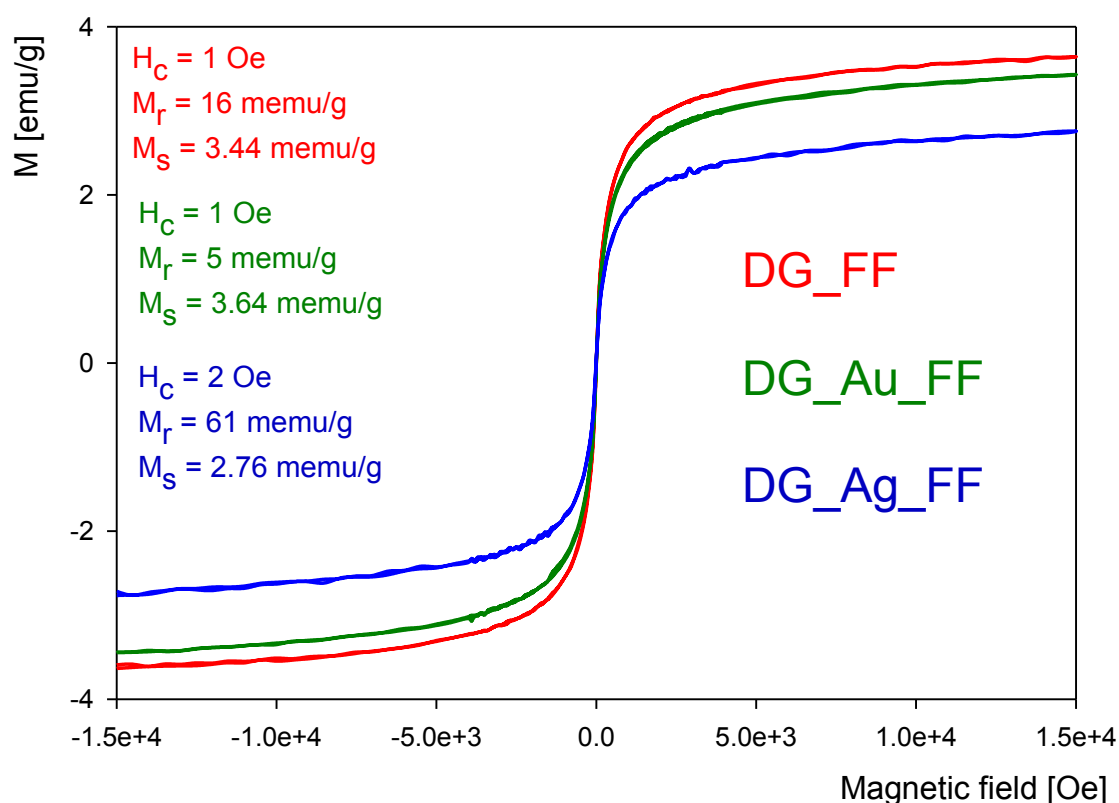


Figure 16. Magnetic saturation curves of magnetically modified BNCs in external magnetic field (15.000 Oe)

When comparing magnetically modified BNC DG_Au_FF, DG_Ag_FF and DG_FF, difference in M_s can be related to higher content of iron in sample DG_FF (see ICP-AES analysis in section 2.2). Lower saturation magnetization of DG_Au_FF can be also caused by presence of gold or silver nanoparticles and their possible interaction with ferrofluid

nanoparticles. Magnetic properties also depend in mutual orientation of ferrofluid nanoparticles.²⁰¹ Last but not least, magnetic properties of the samples can vary due to the preparation process and resulting $\text{Fe}_2\text{O}_3/\text{Fe}_3\text{O}_4$ ratio.²²¹

2.8. Catalysis – 4-NP reduction

The step involving reduction of nitro compounds to amino compounds is environmentally and industrially important.²²² Due to its characteristics (well defined – no byproduct formation, easy and fast UV-VIS monitoring), conversion of 4-NP to 4-aminophenol (4-AP) using aqueous NaBH_4 as a reducing agent has been identified as a model reaction.²²³ Although thermodynamically favorable, the presence of the kinetic barrier due to the large potential difference between donor and acceptor molecules prevents the reaction from proceeding.⁶⁰ Therefore, a catalyst causing decrease of activation energy is necessary for this reaction. The conversion to 4-AP occurs via an intermediate 4-nitrophenolate ion (formation is caused by the presence of alkaline NaBH_4). All the aromatic compound forms – 4-NP, 4-AP and 4-nitrophenolate ion – can be detected by means of UV-VIS spectrometry. The concentration of the reducing agent that was used significantly exceeds the concentration of 4-NP. Therefore, we can assume the reaction rate to be independent of reductant concentration and the reaction has pseudo-first order kinetics (regarding 4-NP concentration).²²⁴

Reduction of 4-nitrophenol with NaBH_4 in the presence of small amounts of silver and gold based bionanocomposites in aqueous medium was reported. The reduction was visualized by the disappearance of the 400 nm peak (4-nitrophenolate ion) with the subsequent appearance of a new peak at 290 nm (4-AP).

The catalytic activity of AuNPs present in two different types of composites – DG_Au, and DG_Au_FF - was studied. Figure 17 shows time dependent decrease of 4-NP in the presence of NaBH_4 and nanocatalyst. For the comparison of tested materials, the relationship between $\ln A$ and time t [min] was used. Apparent rate constants (k_{app}) can be estimated from the slopes of the linear sections of these rows (Figure 18). DG_Au exhibits the highest catalytic rate, regarding the highest content of AuNPs (see ICP/MS section 2.2). 4NP is almost completely removed (>4%) in 10 minutes. However, catalytic rate of magnetically responsive DG_Au_FF sample is not significantly lower. Diminished catalytic rate constant

of DG_Au_FF in comparison to DG_Au can be caused by ferrofluid shading of AuNPs catalytically active surface.

Similarly, samples DG_Ag and DG_Ag_FF undertake catalytic measurements. Results are presented in Figures 17 and 18. Generally, catalytic efficiency of these nanocomposites is lower when compared to the gold based samples (3% of initial 4-NP concentration in 20 minutes). When comparing both magnetically modified bionanocomposites, conversion of 4-NP catalyzed by DG_Au_FF is faster and also more efficient (6% vs. 23% with DG_Ag_FF).

Control measurements (Figure 17 e), f) with cleaned diatom cells (DG) and magnetically modified diatom cells (DG_FF) clearly illustrated that neither the cells with silica frustules nor ferrofluid nanoparticles are catalytically active. However, experiments showed possible adsorption of 4-paranitrofenol on the biomass. This adsorption was slightly higher in the case of DG_FF, most likely due to the presence of ferrofluid nanoparticles with high surface to volume ratio.

HPLC analysis proved the formation of 4-AP as the only reaction product. Chromatographs from monitoring the initial state, progress and final phases of the reaction are given in Figure 19.

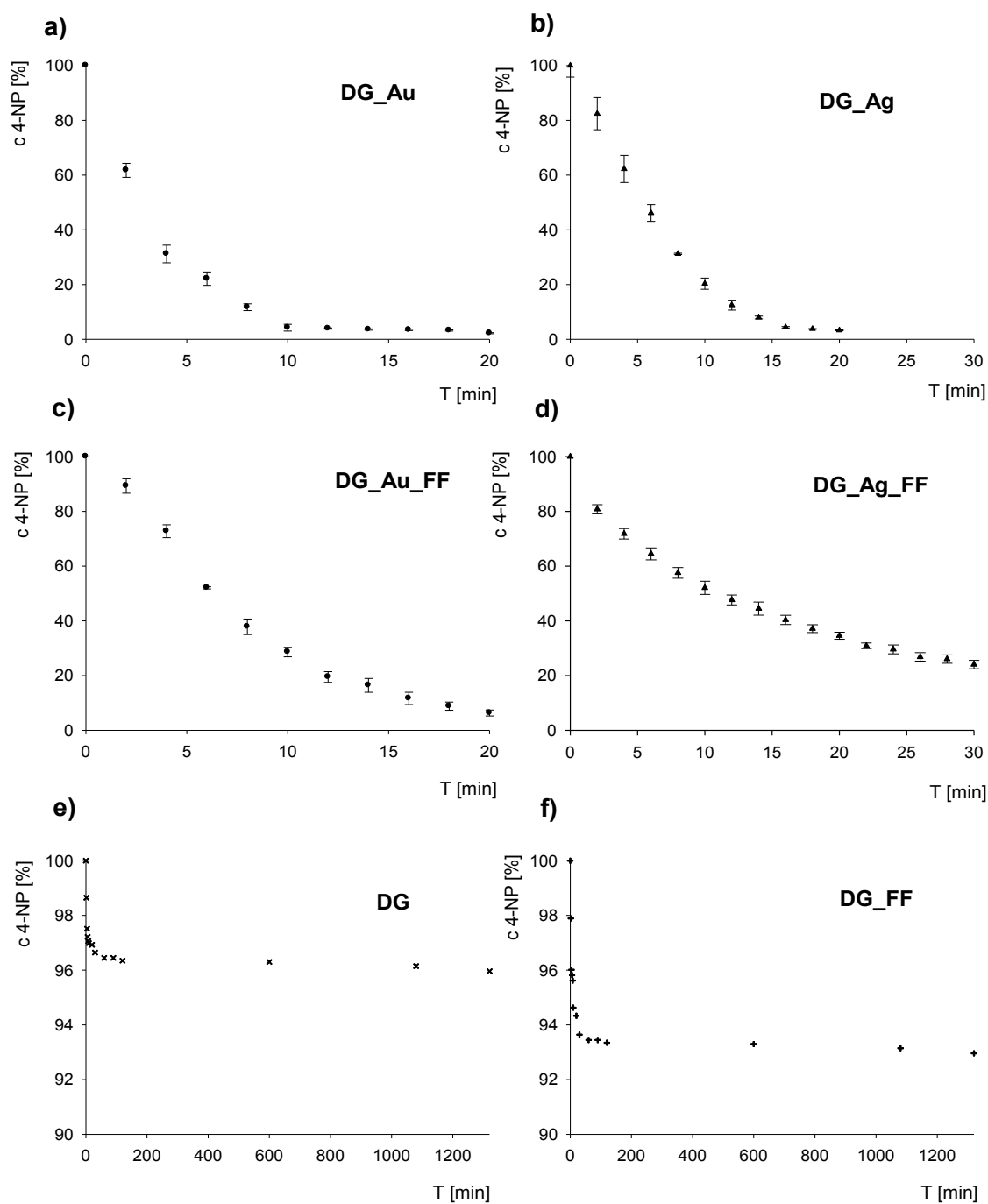


Figure 17. Catalytic conversion of 4-NP by NaBH₄ in presence of noble metal catalysts. Reaction condition: total volume 25 ml; 0.1 mM 4-NP; 100 mM NaBH₄, 0.45 mg of catalyst (DG_Au, DG_Ag, DG_Au_FF, DG_Ag_FF) or control (DG, DG_FF)

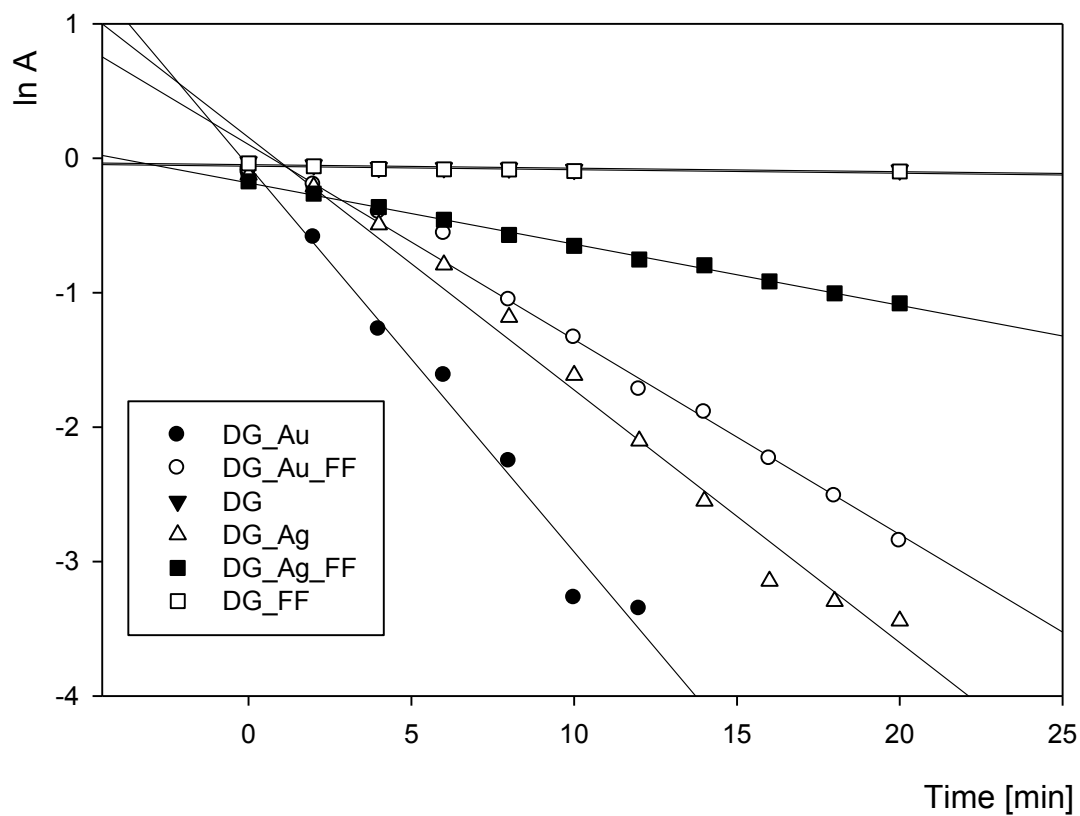


Figure 18. Plot of $\ln[A]$ against time for the reduction of 4-NP. Reaction condition: total volume 25 ml; 0.1 mM 4-NP; 100 mM NaBH_4 , 0.45 mg of catalyst (DG_Au, DG_Ag, DG_Au_FF, DG_Ag_FF) or control (DG, DG_FF)

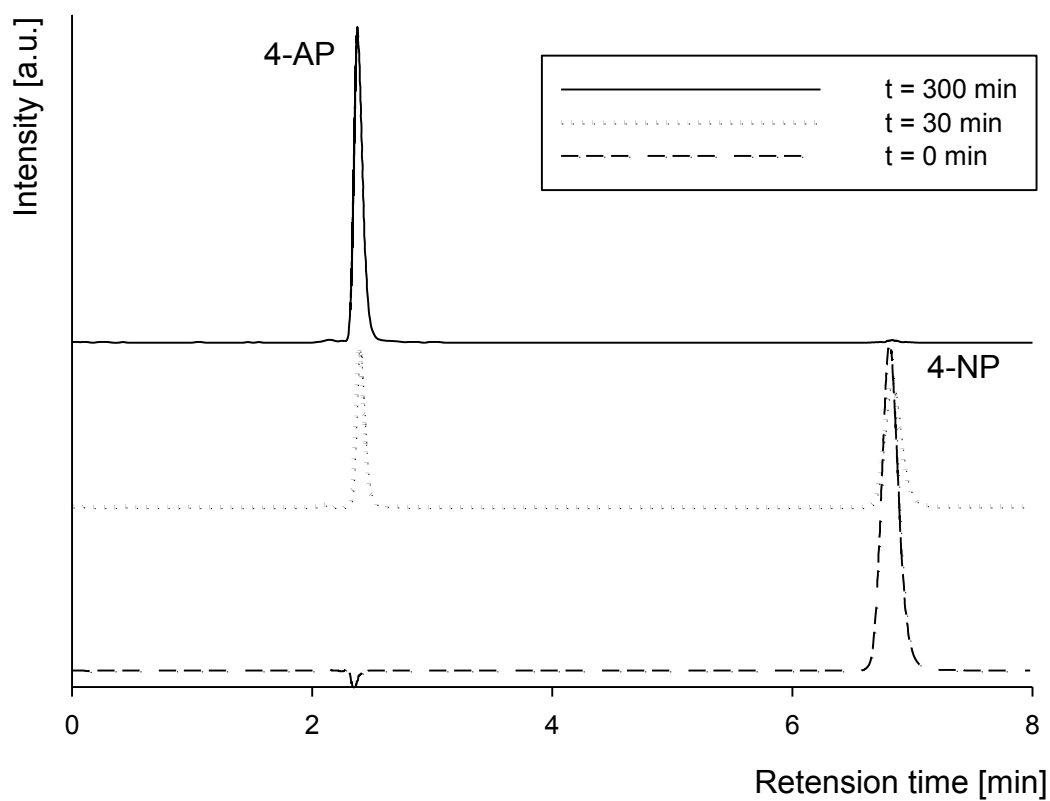


Figure 19. HPLC chromatogram – conversion of 4-NP (0.1 mM) to 4-AP in presence of NaBH_4 (8mM) and DG_Au (4.5 g.L^{-1}). Plot of $\ln[A]$ against time for the reduction of 4-NP. Reaction condition: total volume 25 ml; 0.1 mM 4-NP; 100 mM NaBH_4 , 0.45 mg of catalyst (DG_Au, DG_Ag, DG_Au_FF, DG_Ag_FF) or control (DG, DG_FF)

2.9. Antimicrobial assessment

A selective diffusion test was performed to obtain overall information about bionanocomposite behavior in porous media (agar). Therefore, data from this type of test are only qualitative. Effectiveness of bacterial inhibition to all strains has been proven in silver based binanocomposite samples. On the other hand, gold based samples did not show any antimicrobial activity. These results are most likely caused by the ability of silver nanoparticles to release Ag^+ ions which can penetrate and diffuse through the agar ²²⁵.

Tables 10 and 11 represent the MIC results of all tested BNC in RT and 37°C respectively. Responses of bacterial cultures were observed and divided to three classes – inhibition (100% killed), slowing down (some bacteria survive) and no effect (no significant inhibition). Results show antimicrobial efficiency of DG_Ag samples against all tested bacterial strains except *B. anthracis* (spores). Tested bacterial strains did not show any significant sensitivity to DG_Au sample. Generally, increase of the temperature (from RT to 37°C) during the incubation caused better antimicrobial efficiency of the BNC used. Regarding the specific effectiveness of BNC, *S. aureus*, *S. agalactiae* and *E. coli* strain were most sensitive to Ag BNC treatment.

Table 10. Minimum inhibitory concentration assessment, DG_Ag, RT

	1 day			2 days			3 days		
Bacterial cult.	10%	3.33%	1.12%	10%	3.33%	1.12%	10%	3.33%	1.12%
<i>B. anthracis</i> *									
<i>S. aureus</i>									
<i>S. agalactiae</i>									
<i>E. coli</i>									
<i>P. aeruginosa</i>									

* bacterial spores

Slowing down



Inhibition



No effect



Table 11. Minimum inhibitory concentration assessment, DG_Ag, 37°C

	1 day			2 days			3 days		
Bacterial cult.	10%	3.33%	1.12%	10%	3.33%	1.12%	10%	3.33%	1.12%
<i>B. anthracis</i> *									
<i>S. aureus</i>									
<i>S. agalactiae</i>									
<i>E. coli</i>									
<i>P. aeruginosa</i>									

* bacterial spores

Slowing down Inhibition No effect

It is necessary to mention that higher MICs are caused by the silica matrix of BNC. Regarding ICP/AES data (section 2.2), the amount of silver as an active compound is lower than 1% (w), resulting in much higher specific antimicrobial efficiency. Also, the mobility of AgNPs embedded on the diatom frustules is obviously smaller in comparison to free colloidal solutions.^{104,106} This can therefore result in fewer NP-cell interactions and lower antimicrobial efficiency.²²⁵ On the other hand, material can be easily dried and stored, either in the freezer at or RT. This important fact, together with a stable frustule matrix, enables a much wider spectrum of applications in comparison with a colloidal system.

The microbial inhibition assessment performed in this study contains two types of tests. Although the diffusion test is suitable only for preliminary assessment, it has become widely used in numerous studies concerning nanoparticle biosynthesis.⁸⁸ It is fast and easy to perform, but provides only qualitative results which are difficult to analyze. However, the MIC test delivers more reliable and quantitative data about antimicrobial efficiency. Additionally, in these experiments it has been shown that although all the SD tests were positive, further investigation by means of the MIC test showed obvious limitations of this method.

D) CONCLUSIONS

- write a review of recent literature in field of metallic nanoparticle biosynthesis

Results of this specific aim are contained in this dissertation and have been published as a book chapter from esteemed publisher.²²⁶ In this review, recent advances in the application of biosynthesized metallic NPs have been addressed. Applications have been categorized into a wide spectrum of sections such as catalysis, medicine, disinfection, sensors, etc. When possible, comparison with the common chemical and physical synthesis approaches was investigated and discussed. The introduction of relatively novel biosynthesized metallic NPs into medicine, electrochemistry, optics and material science can reinforce their unique functions and properties, resulting in new methods and strategies for applied research and industrial utilization.

Based on this study, further development of biosynthesis methods and their utilization in many pertinent and advantageous real-world applications is anticipated. In combination with other NP preparation methods, further investigation of processes and an expansion of potential applications will result in the deeper development of bionanotechnology.

- develop protocol for biosynthesis of noble metal nanoparticles employing algae

Biosynthesis of gold and silver nanoparticles has been successfully conducted using two strains of diatoms mixed with aqueous HAuCl_4 and AgNO_3 at laboratory conditions. The interaction of diatoms with aqueous salt promoted the precipitation of metallic nanoparticles.

Presented method of tetrachloroaurate reduction by diatoms appears to be an effective and low-cost method of binanocomposites preparation. Additionally, performance of the described method is very simple (uses organisms commonly living in streams and ponds worldwide, can be performed at room temperature and in physiologic pH) and environmentally friendly compared to other chemical methods that use toxic reagents.

- produce and characterize functional silica based bionanocomposite containing noble metal nanoparticles and diatom frustules

Biosynthesis experiments led to development of fully functional bionanocomposites. Reduction, capping and immobilization of metallic nanoparticles are performed in one single and fast step. As far as we know, this is the first record of similar technique for preparation of biomaterials.

Resulting material can be further stored either in solution or dried in the form of a powder. Nanoparticles are stable for weeks due to support from the silica matrix and biomolecular capping agents. Due to its accessibility, simplicity, and effectiveness, this method of bionanocomposites preparation has great importance for possible usage.

Shapes, sizes, chemical composition, and interaction with siliceous frustules and EPS of the diatoms were described by the methods of light microscopy, electron microscopy, and X-ray diffraction techniques.

- adjust and modify the material for further usage

Bionanocomposite was successfully modified to obtain magnetically responsive material. The resulting material is easily recoverable with a magnet. Therefore, it is suitable for applications in which it is necessary to recollect the reagent (catalyst, antimicrobial material). Magnetic properties of magnetically modified bionanocomposite were characterized by means of vibrating sample magnetometer.

Due to its unique properties, bionanocomposite can be used in different conditions. Diatom frustules are very chemically stable, but their porous morphology offers a large surface for nanoparticles to attach. Unlike the commonly used polymers (such as polyvinyl alcohol), silica frustules are expected to resist high temperatures. This fact can be of concern due to possible catalytic applications. Material can be used in dry or wet conditions, stored as a powder, frozen or in methanol.

- prove the material efficiency and functionality in appropriate applications

Biosynthesized composite material was used as catalyst and antimicrobial agent. Reduction of 4-NP in presence of sodium borohydrate was successfully conducted using both silver and gold based bionanocomposites. These preliminary results are promising for other possible reactions and applications (nitroaromates removal from contaminated wastewater, degradation of halogen derivates etc.). Due to its physical properties, bionanocomposite can be used as magnetically recoverable nanocatalyst, chromatography column filling, or for usage in dry filters.

Silver bionanocomposite have been proven to effectively inhibit bacterial growth of four different bacterial strains. Disk diffusion tests and minimal inhibition concentration assessments were performed for more detailed descriptions of biocomposite antibacterial properties and showed promising results for further investigation. Material can be possibly used in water purification (disinfection) system, membranes, or wastewater treatment plants.

E) LIST OF FIGURES

Figure 1. UV-VIS spectra of a) solution of biosynthesized gold nanoparticles after 2, 10 and 20 minutes of sonication; b) biogenic silver nanoparticle solution 6, 12 and 24 hours after start of the experiments. Both spectra represent maximum characteristic for Au, and Ag nanoparticles resp.

Figure 2. XRD diffractogram of BNC samples containing gold nanoparticles (Au) and ferrofluid. The lower graph represents theoretical diffraction patterns for cubic gold (red), maghemite (dark green – Mgm) and magnetite (blue – Mgt).

Figure 3. XRD diffractogram of BNC samples containing silver nanoparticles (Ag) and ferrofluid. The lower graph represents theoretical diffraction patterns for cubic silver (red), maghemite (dark green – Mgm) and magnetite (blue – Mgt).

Figure 4. Light microscope photographs of the diatom cells before (left) and 24 hours after (right) tetrachloroaurate addition for (a,c) *Diadesmis gallica*, and (b,d) *Navicula atomus*.

Figure 5. TEM micrographs of (a,c) *Diadesmis gallica*, and (b,d) *Navicula atomus* cells after tetrachloroaurate addition. Gold nanoparticles captured in the EPS net of the intercellular space of DG (a). Detail of association of gold nanoparticles with the frustule surface in the raphe region of NA (c). Detail micrographs of AuNPs and SAED patterns for DG (b), and NA strains (d).

Figure 6. Histogram of size distribution of gold nanoparticles synthesized by *Diadesmis gallica* after tetrachloroaurate addition

Figure 7. Histogram of size distribution of gold nanoparticles synthesized by *Navicula atomus* after tetrachloroaurate addition

Figure 8. TEM micrographs of samples DG_Ag (a, c), DG_Ag_FF (b, d, f) and DG_FF (e). Silver nanoparticles associated with the diatom frustule (a), detailed micrographs and SAED pattern of silver nanoparticles (c). Ferrofluid and silver nanoparticles – pictures were taken in bright field (d) and dark field regime (f) respectively.

Figure 9. TEM micrographs of samples DG_Au (a, b), DG_Au_FF (c, d) and DG_FF (e, f). Detail of gold nanoparticles associated with the diatom frustule, SAED pattern corresponding with cubic gold (a). Larger part of diatom frustule with gold nanoparticles (b). Gray ferrofluid veil together with gold nanoparticles (dark dots) on the frustule surface (c) and in the detail (d). Ferrofluid nanoparticles by the diatom surface in bright (e) and dark (f) field, SAED pattern of maghemite (e).

Figure 10. Histogram of size distribution of silver nanoparticles synthesized by *Diadlesmis gallica* after silver nitrate addition

Figure 11. Histogram of size distribution of ferrofluid nanoparticles after magnetic modification of diatom cells

Figure 12. SEM micrographs of (a,c) *Diadlesmis gallica*, and (b,d) *Navicula atomus* cells after tetrachloroaurate addition. Detail of gold nanoparticles deposition on the silica frustule surface of the DG cells (b). Association of gold nanoparticles with the EPS structures of the NA cell (c). Detail micrograph of gold nanoparticles embedded into the EPS chain of the NA cell (d).

Figure 13. SEM micrographs of samples DG_Au (a), DG_Au_FF (b,d) and DG_FF (c). Gold nanoparticles are attached on the surface of diatom cells, but can be often also inside the pore (a). Diatom frustules veiled into the ferrofluid (b, c). Detail of gold nanoparticles mixed with ferrofluid (d).

Figure 14. SEM micrographs of samples DG_Ag (a), DG_Ag_FF (b,d) and DG_FF (c). Amount of silver nanoparticles is lower when compare to gold NPs and they are usually aggregated in certain areas (a). Magnetically modified cells of diatoms with biosynthesized silver nanoparticles (b, d). Ferrofluid detail (c).

Figure 15. Illustration of ferrofluid modified BNC behavior in external magnetic field.

Figure 16. Magnetic saturation curves of magnetically modified BNCs in external magnetic field (15.000 Oe)

Figure 17. Catalytic conversion of 4-NP by NaBH_4 in presence of noble metal catalysts. Reaction condition: total volume 25 ml; 0.1 mM 4-NP; 100 mM NaBH_4 , 0.45 mg of catalyst (DG_Au, DG_Ag, DG_Au_FF, DG_Ag_FF) or control (DG, DG_FF)

Figure 18. Plot of $\ln[A]$ against time for the reduction of 4-NP. Reaction condition: total volume 25 ml; 0.1 mM 4-NP; 100 mM NaBH_4 , 0.45 mg of catalyst (DG_Au, DG_Ag, DG_Au_FF, DG_Ag_FF) or control (DG, DG_FF)

Figure 19. HPLC chromatogram – conversion of 4-NP (0.1 mM) to 4-AP in presence of NaBH_4 (8mM) and DG_Au (4.5 g.L^{-1}). Plot of $\ln[A]$ against time for the reduction of 4-NP. Reaction condition: total volume 25 ml; 0.1 mM 4-NP; 100 mM NaBH_4 , 0.45 mg of catalyst (DG_Au, DG_Ag, DG_Au_FF, DG_Ag_FF) or control (DG, DG_FF)

F) LIST OF TABLES

Table 1. Biosorption applications

Table 2. Catalysis applications

Table 3. Antimicrobial applications

Table 4. Medical applications

Table 5. Electrochemical and sensing applications

Table 6. Magnetic applications

Table 7. Further applications and properties

Table 8. List of samples and their content

Table 9. Elemental analysis of BNC

Table 10. Minimum inhibitory concentration assessment, DG_Ag, RT

Table 11. Minimum inhibitory concentration assessment, DG_Ag, 37°C

G) LIST OF ABBREVIATIONS

AAS	atomic absorption spectrometry
AgNPs	silver nanoparticles
AuNPs	gold nanoparticles
BM	bacterial magnetosomes
BNC	bionanocomposite
CP	chlorophenol
CuNPs	copper nanoparticles
DG	<i>Diademsis gallica</i>
DOX	Doxorubicin
EPS	extracellular polymeric substances
FF	ferrofluid
GCE	glassy carbon electrode
ICM	iodinated contrast media
ICP	inductively coupled plasma
ICSD	Inorganic Crystal Structure Database
LM	light microscopy
MIC	minimum inhibitory concentration
MNPs	magnetite nanoparticles
NA	<i>Navicula atomus</i>
NP	nanoparticle
NPs	nanoparticles
PBDE	polybrominated diphenyl ether
PCB	olychlorinated biphenyl
PEI	polyethyleneimine
PEM	polymer electrolyte membrane
PVDF	polyvinylidene fluoride
QD	quantum dot
RT	room temperature
SAED	Selected Area Electron Diffraction

SDV	silica deposit vesicle
SEM	scanning electron microscopy
SPR	surface plasmon resonance
TCE	trichlorethylene
TCPP	tris(chloroisopropyl)phosphate
TEM	transmission electron microscopy
UV-VIS	UV-visible
VSM	vibrating sample magnetometer
XRD	X-ray diffraction
γ -HCH	γ -hexachlorocyclohexane

H) REFERENCES

- 1 Wilbur, K. M. & Simkiss, K. in *Studies in Environmental Science* Vol. Volume 3 (eds P. A. Trudinger & D. J. Swaine) 69-106 (Elsevier, 1979). 0166-1116
- 2 Pérez-de-Mora, A. *et al.* Microbial community structure and function in a soil contaminated by heavy metals: effects of plant growth and different amendments. *Soil Biology and Biochemistry* **38**, 327-341 (2006). 0038-0717
- 3 Ahmad, A. *et al.* Extracellular biosynthesis of silver nanoparticles using the fungus *Fusarium oxysporum*. *Colloids and Surfaces B: Biointerfaces* **28**, 313-318 (2003). 0927-7765
- 4 Thakkar, K. N., Mhatre, S. S. & Parikh, R. Y. Biological synthesis of metallic nanoparticles. *Nanomedicine-Nanotechnology Biology and Medicine* **6**, 257-262 (2010). 1549-9634
- 5 Lynch, I. & Dawson, K. A. Protein-nanoparticle interactions. *Nano Today* **3**, 40-47 (2008). 1748-0132
- 6 Das, N. Recovery of precious metals through biosorption - A review. *Hydrometallurgy* **103**, 180-189 (2010). 0304-386X
- 7 Gadd, G. M. Metals, minerals and microbes: geomicrobiology and bioremediation. *Microbiology-Sgm* **156**, 609-643 (2010). 1350-0872
- 8 Hennebel, T., De Gusseme, B., Boon, N. & Verstraete, W. Biogenic metals in advanced water treatment. *Trends in Biotechnology* **27**, 90-98 (2009). 0167-7799
- 9 Lesmana, S. O., Febriana, N., Soetaredjo, F. E., Sunarso, J. & Ismadji, S. Studies on potential applications of biomass for the separation of heavy metals from water and wastewater. *Biochemical Engineering Journal* **44**, 19-41 (2009). 1369-703X
- 10 Volesky, B. Biosorption and me. *Water Research* **41**, 4017-4029 (2007). 0043-1354
- 11 Chakraborty, N., Pal, R., Ramaswami, A., Nayak, D. & Lahiri, S. Diatom: A potential bio-accumulator of gold. *Journal of Radioanalytical and Nuclear Chemistry* **270**, 645-649 (2006). 0236-5731
- 12 Chakraborty, N. *et al.* Biorecovery of gold using cyanobacteria and an eukaryotic alga with special reference to nanogold formation - a novel phenomenon. *Journal of Applied Phycology* **21**, 145-152 (2009). 0921-8971

- 13 Mata, Y. N. *et al.* Gold(III) biosorption and bioreduction with the brown alga *Fucus vesiculosus*. *J. Hazard. Mater.* **166**, 612-618 (2009). 0304-3894
- 14 Chakraborty, N. *et al.* Biorecovery of gold using cyanobacteria and an eukaryotic alga with special reference to nanogold formation – a novel phenomenon. *Journal of Applied Phycology* **21**, 145-152 (2009). 0921-8971
- 15 Das, D., Das, N. & Mathew, L. Kinetics, equilibrium and thermodynamic studies on biosorption of Ag(I) from aqueous solution by macrofungus *Pleurotus platypus*. *J. Hazard. Mater.* **184**, 765-774 (2010). 0304-3894
- 16 Won, S. W., Mao, J., Kwak, I.-S., Sathishkumar, M. & Yun, Y.-S. Platinum recovery from ICP wastewater by a combined method of biosorption and incineration. *Bioresource Technology* **101**, 1135-1140 (2010). 0960-8524
- 17 Sathishkumar, M., Mahadevan, A., Vijayaraghavan, K., Pavagadhi, S. & Balasubramanian, R. Green Recovery of Gold through Biosorption, Biocrystallization, and Pyro-Crystallization. *Industrial & Engineering Chemistry Research* **49**, 7129-7135 (2010). 0888-5885
- 18 Selvakumar, R. *et al.* As(V) removal using carbonized yeast cells containing silver nanoparticles. *Water Research* **45**, 583-592 (2011). 0043-1354
- 19 Zhang, H. *et al.* Accumulation of Silver(I) Ion and Diamine Silver Complex by *Aeromonas* SH10 biomass. *Applied Biochemistry and Biotechnology* **143**, 54-62 (2007). 0273-2289
- 20 Sinha, A., Singh, V. N., Mehta, B. R. & Khare, S. K. Synthesis and characterization of monodispersed orthorhombic manganese oxide nanoparticles produced by *Bacillus* sp. cells simultaneous to its bioremediation. *J. Hazard. Mater.* **192**, 620-627 (2011). 0304-3894
- 21 De Corte, S., Hennebel, T., De Gusseme, B., Verstraete, W. & Boon, N. Bio-palladium: from metal recovery to catalytic applications. *Microbial Biotechnology* **5**, 5-17 (2012). 1751-7915
- 22 Baxter-Plant, V. S., Mikheenko, I. P. & Macaskie, L. E. Sulphate-reducing bacteria, palladium and the reductive dehalogenation of chlorinated aromatic compounds. *Biodegradation* **14**, 83-90 (2003). 0923-9820

- 23 Baxter-Plant, V. S., Mikheenko, I. P., Robson, M., Harrad, S. J. & Macaskie, L. E. Dehalogenation of chlorinated aromatic compounds using a hybrid bioinorganic catalyst on cells of *Desulfovibrio desulfuricans*. *Biotechnology Letters* **26**, 1885-1890 (2004). 0141-5492
- 24 Bunge, M. *et al.* Formation of palladium(0) nanoparticles at microbial surfaces. *Biotechnology and Bioengineering* **107**, 206-215 (2010). 1097-0290
- 25 Harrad, S. *et al.* Dehalogenation of polychlorinated biphenyls and polybrominated diphenyl ethers using a hybrid bioinorganic catalyst. *Journal of Environmental Monitoring* **9**, 314-318 (2007). 1464-0325
- 26 Deplanche, K., Snape, T. J., Hazrati, S., Harrad, S. & Macaskie, L. E. Versatility of a new bioinorganic catalyst: Palladized cells of *Desulfovibrio desulfuricans* and application to dehalogenation of flame retardant materials. *Environmental Technology* **30**, 681 - 692 (2009). 0959-3330
- 27 Redwood, M. D., Deplanche, K., Baxter-Plant, V. S. & Macaskie, L. E. Biomass-supported palladium catalysts on *Desulfovibrio desulfuricans* and *Rhodobacter sphaeroides*. *Biotechnology and Bioengineering* **99**, 1045-1054 (2008). 1097-0290
- 28 Creamer, N. J. *et al.* Novel supported Pd hydrogenation bionanocatalyst for hybrid homogeneous/heterogeneous catalysis. *Catalysis Today* **128**, 80-87 (2007). 0920-5861
- 29 Creamer, N. J. *et al.* A biogenic catalyst for hydrogenation, reduction and selective dehalogenation in non-aqueous solvents. *Hydrometallurgy* **94**, 138-143 (2008). 0304-386X
- 30 De Windt, W., Aelterman, P. & Verstraete, W. Bioreductive deposition of palladium (0) nanoparticles on *Shewanella oneidensis* with catalytic activity towards reductive dechlorination of polychlorinated biphenyls. *Environmental Microbiology* **7**, 314-325 (2005). 1462-2920
- 31 De Windt, W. *et al.* Biological control of the size and reactivity of catalytic Pd(0) produced by *Shewanella oneidensis*. *Antonie van Leeuwenhoek* **90**, 377-389 (2006). 0003-6072
- 32 Mertens, B., Blothe, C., Windey, K., De Windt, W. & Verstraete, W. Biocatalytic dechlorination of lindane by nano-scale particles of Pd(0) deposited on *Shewanella oneidensis*. *Chemosphere* **66**, 99-105 (2007). 0045-6535

- 33 Hennebel, T. *et al.* Removal of diatrizoate with catalytically active membranes incorporating microbially produced palladium nanoparticles. *Water Research* **44**, 1498-1506 (2010). 0043-1354
- 34 Forrez, I. *et al.* Biogenic metals for the oxidative and reductive removal of pharmaceuticals, biocides and iodinated contrast media in a polishing membrane bioreactor. *Water Research* **45**, 1763-1773 (2011). 0043-1354
- 35 Hennebel, T. *et al.* Biocatalytic dechlorination of trichloroethylene with bio-palladium in a pilot-scale membrane reactor. *Biotechnology and Bioengineering* **102**, 995-1002 (2009). 1097-0290
- 36 Hennebel, T. *et al.* Remediation of trichloroethylene by bio-precipitated and encapsulated palladium nanoparticles in a fixed bed reactor. *Chemosphere* **76**, 1221-1225 (2009). 0045-6535
- 37 Wood, J., Bodenes, L., Bennett, J., Deplanche, K. & Macaskie, L. E. Hydrogenation of 2-Butyne-1,4-diol Using Novel Bio-Palladium Catalysts. *Industrial & Engineering Chemistry Research* **49**, 980-988 (2009). 0888-5885
- 38 Sobjerg, L. S. *et al.* Bio-supported palladium nanoparticles as a catalyst for Suzuki-Miyaura and Mizoroki-Heck reactions. *Green Chemistry* **11**, 2041-2046 (2009). 1463-9262
- 39 Gauthier, D. *et al.* Environmentally Benign Recovery and Reactivation of Palladium from Industrial Waste by Using Gram-Negative Bacteria. *ChemSusChem* **3**, 1036-1039 (2010). 1864-564X
- 40 Jia, L., Zhang, Q., Li, Q. & Song, H. The biosynthesis of palladium nanoparticles by antioxidants in *Gardenia jasminoides* Ellis : long lifetime nanocatalysts for p - nitrotoluene hydrogenation. *Nanotechnology* **20**, 385601 (2009). 0957-4484
- 41 Wu, X. *et al.* Pd-Gardenia-TiO₂ as a photocatalyst for H₂ evolution from pure water. *International Journal of Hydrogen Energy* (2011). 0360-3199
- 42 Mabbett, A. N., Lloyd, J. R. & Macaskie, L. E. Effect of complexing agents on reduction of Cr(VI) by *Desulfovibrio vulgaris* ATCC 29579. *Biotechnology and Bioengineering* **79**, 389-397 (2002). 1097-0290

- 43 Mabbett, A. N. & Macaskie, L. E. A new bioinorganic process for the remediation of Cr(VI). *Journal of Chemical Technology & Biotechnology* **77**, 1169-1175 (2002). 1097-4660
- 44 Humphries, A. C., Mikheenko, I. P. & Macaskie, L. E. Chromate reduction by immobilized palladized sulfate-reducing bacteria. *Biotechnology and Bioengineering* **94**, 81-90 (2006). 1097-0290
- 45 Mabbett, A. N., Sanyahumbi, D., Yong, P. & Macaskie, L. E. Biorecovered Precious Metals from Industrial Wastes: Single-Step Conversion of a Mixed Metal Liquid Waste to a Bioinorganic Catalyst with Environmental Application. *Environmental Science & Technology* **40**, 1015-1021 (2005). 0013-936X
- 46 Beauregard, D. A., Yong, P., Macaskie, L. E. & Johns, M. L. Using non-invasive magnetic resonance imaging (MRI) to assess the reduction of Cr(VI) using a biofilm–palladium catalyst. *Biotechnology and Bioengineering* **107**, 11-20 (2010). 1097-0290
- 47 Chidambaram, D. *et al.* Concomitant Microbial Generation of Palladium Nanoparticles and Hydrogen To Immobilize Chromate. *Environmental Science & Technology* **44**, 7635-7640 (2010). 0013-936X
- 48 Deplanche, K., Caldelari, I., Mikheenko, I. P., Sargent, F. & Macaskie, L. E. Involvement of hydrogenases in the formation of highly catalytic Pd(0) nanoparticles by bioreduction of Pd(II) using *Escherichia coli* mutant strains. *Microbiology* **156**, 2630-2640 (2010)
- 49 Winter, M. & Brodd, R. J. What Are Batteries, Fuel Cells, and Supercapacitors? (Chem. Rev. 2003, 104, 4245–4269. Published on the Web 09/28/2004.). *Chemical Reviews* **105**, 1021-1021 (2005). 0009-2665
- 50 Yong, P., Paterson-Beedle, M., Mikheenko, I. P. & Macaskie, L. E. From biomineralisation to fuel cells: biomanufacture of Pt and Pd nanocrystals for fuel cell electrode catalyst. *Biotechnology Letters* **29**, 539-544 (2007). 0141-5492
- 51 Dimitriadis, S., Nomikou, N. & McHale, A. P. Pt-based electro-catalytic materials derived from biosorption processes and their exploitation in fuel cell technology. *Biotechnology Letters* **29**, 545-551 (2007). 0141-5492

- 52 Ogi, T., Honda, R., Tamaoki, K., Saitoh, N. & Konishi, Y. Direct room-temperature synthesis of a highly dispersed Pd nanoparticle catalyst and its electrical properties in a fuel cell. *Powder Technology* **205**, 143-148 (2011). 0032-5910
- 53 Yong, P., Mikheenko, I., Deplanche, K., Redwood, M. & Macaskie, L. Biorefining of precious metals from wastes: an answer to manufacturing of cheap nanocatalysts for fuel cells and power generation via an integrated biorefinery? *Biotechnology Letters* **32**, 1821-1828 (2010). 0141-5492
- 54 Orozco, R. *et al.* Towards an integrated system for bio-energy: hydrogen production by *Escherichia coli* and use of palladium-coated waste cells for electricity generation in a fuel cell. *Biotechnology Letters* **32**, 1837-1845 (2010). 0141-5492
- 55 Forrez, I. *et al.* Biogenic metals for the oxidative and reductive removal of pharmaceuticals, biocides and iodinated contrast media in a polishing membrane bioreactor. *Water Research* **45**, 1763-1773 (2011). 0043-1354
- 56 Mabbett, A. N., Yong, P., Farr, J. P. G. & Macaskie, L. E. Reduction of Cr(VI) by "Palladized" - Biomass of *Desulfovibrio desulfuricans* ATCC 29577. *Biotechnology and Bioengineering* **87**, 104-109 (2004). 0006-3592
- 57 Sharma, N. C. *et al.* Synthesis of plant-mediated gold nanoparticles and catalytic role of biomatrix-embedded nanomaterials. *Environmental Science & Technology* **41**, 5137-5142 (2007). 0013-936X
- 58 Huang, J. L. *et al.* A General Strategy for the Biosynthesis of Gold Nanoparticles by Traditional Chinese Medicines and Their Potential Application as Catalysts. *Chemistry-an Asian Journal* **4**, 1050-1054 (2009). 1861-4728
- 59 Jia, X. P., Ma, X. Y., Wei, D. W., Dong, J. & Qian, W. P. Direct formation of silver nanoparticles in cuttlebone-derived organic matrix for catalytic applications. *Colloids and Surfaces a-Physicochemical and Engineering Aspects* **330**, 234-240 (2008). 0927-7757
- 60 Gangula, A. *et al.* Catalytic Reduction of 4-Nitrophenol using Biogenic Gold and Silver Nanoparticles Derived from *Breynia rhamnoides*. *Langmuir* (2011). 0743-7463
- 61 Hosseinkhani, B. *et al.* Microbially supported synthesis of catalytically active bimetallic Pd-Au nanoparticles. *Biotechnology and Bioengineering* **109**, 45-52 (2012). 1097-0290

- 62 Du, M. *et al.* Ionic liquid-enhanced immobilization of biosynthesized Au nanoparticles on TS-1 toward efficient catalysts for propylene epoxidation. *Journal of Catalysis* **283**, 192-201 (2011). 0021-9517
- 63 Zhan, G. *et al.* Vapor-Phase Propylene Epoxidation with H₂/O₂ over Bioreduction Au/TS-1 Catalysts: Synthesis, Characterization, and Optimization. *Industrial & Engineering Chemistry Research* **50**, 9019-9026 (2011). 0888-5885
- 64 Gupta, N., Singh, H. P. & Sharma, R. K. Single-pot synthesis: Plant mediated gold nanoparticles catalyzed reduction of methylene blue in presence of stannous chloride. *Colloids and Surfaces A: Physicochemical and Engineering Aspects* **367**, 102-107 (2010). 0927-7757
- 65 Shahwan, T. *et al.* Green synthesis of iron nanoparticles and their application as a Fenton-like catalyst for the degradation of aqueous cationic and anionic dyes. *Chemical Engineering Journal* **172**, 258-266 (2011). 1385-8947
- 66 Smuleac, V., Varma, R., Sikdar, S. & Bhattacharyya, D. Green synthesis of Fe and Fe/Pd bimetallic nanoparticles in membranes for reductive degradation of chlorinated organics. *Journal of Membrane Science* **379**, 131-137 (2011). 0376-7388
- 67 Venu, R., Ramulu, T. S., Anandakumar, S., Rani, V. S. & Kim, C. G. Bio-directed synthesis of platinum nanoparticles using aqueous honey solutions and their catalytic applications. *Colloids and Surfaces A: Physicochemical and Engineering Aspects* **384**, 733-738 (2011). 0927-7757
- 68 Chaloupka, K., Malam, Y. & Seifalian, A. M. Nanosilver as a new generation of nanoparticle in biomedical applications. *Trends in Biotechnology* **28**, 580-588 (2010). 0167-7799
- 69 Alanazi, F. K., Radwan, A. A. & Alsarra, I. A. Biopharmaceutical applications of nanogold. *Saudi Pharmaceutical Journal* **18**, 179-193 (2010). 1319-0164
- 70 Patra, C. R., Bhattacharya, R., Mukhopadhyay, D. & Mukherjee, P. Fabrication of gold nanoparticles for targeted therapy in pancreatic cancer. *Advanced Drug Delivery Reviews* **62**, 346-361 (2010). 0169-409X
- 71 Pankhurst, Q. A. & *et al.* Applications of magnetic nanoparticles in biomedicine. *Journal of Physics D: Applied Physics* **36**, R167 (2003). 0022-3727

- 72 Pankhurst, Q. A. & et al. Progress in applications of magnetic nanoparticles in biomedicine. *Journal of Physics D: Applied Physics* **42**, 224001 (2009). 0022-3727
- 73 Kumar, K. P., Paul, W. & Sharma, C. P. Green synthesis of gold nanoparticles with *Zingiber officinale* extract: Characterization and blood compatibility. *Process Biochemistry* **46**, 2007-2013 (2011). 1359-5113
- 74 Rai, M., Yadav, A. & Gade, A. Silver nanoparticles as a new generation of antimicrobials. *Biotechnology Advances* **27**, 76-83 (2009). 0734-9750
- 75 Marambio-Jones, C. & Hoek, E. M. V. A review of the antibacterial effects of silver nanomaterials and potential implications for human health and the environment. *Journal of Nanoparticle Research* **12**, 1531-1551 (2010). 1388-0764
- 76 Morones, J. R. *et al.* The bactericidal effect of silver nanoparticles. *Nanotechnology* **16**, 2346 (2005). 0957-4484
- 77 Ingle, A., Gade, A., Pierrat, S., Sönnichsen, C. & Rai, M. Mycosynthesis of Silver Nanoparticles Using the Fungus *Fusarium acuminatum* and its Activity Against Some Human Pathogenic Bacteria. *Current Nanoscience* **4**, 141-144 (2008)
- 78 Saravanan, M. & Nanda, A. Extracellular synthesis of silver bionanoparticles from *Aspergillus clavatus* and its antimicrobial activity against MRSA and MRSE. *Colloids and Surfaces B: Biointerfaces* **77**, 214-218 (2010). 0927-7765
- 79 Binupriya, A. R., Sathishkumar, M. & Yun, S.-I. Myco-crystallization of Silver Ions to Nanosized Particles by Live and Dead Cell Filtrates of *Aspergillus oryzae* var. *viridis* and Its Bactericidal Activity toward *Staphylococcus aureus* KCCM 12256. *Industrial & Engineering Chemistry Research* **49**, 852-858 (2009). 0888-5885
- 80 Saha, S. *et al.* Production of silver nanoparticles by a phytopathogenic fungus *Bipolaris nodulosa* and its antimicrobial activity. *Digest Journal of Nanomaterials and Biostructures* **5**, 887 - 895 (2010). 1842 - 3582
- 81 Nithya, R. & Ragunathan, R. Synthesis of silver nanoparticles using *Pleurotus sajor caju* and its microbial study. *Digest Journal of Nanomaterials and Biostructures* **4**, 623-629 (2009). 1842-3582
- 82 Maliszewska, I. & Puzio, M. Extracellular biosynthesis and antimicrobial activity of silver nanoparticles. *Acta Physica Polonica A* **116**, S160-S162 (2009). 1898-794X

- 83 Birla, S. S. *et al.* Fabrication of silver nanoparticles by *Phoma glomerata* and its combined effect against *Escherichia coli*, *Pseudomonas aeruginosa* and *Staphylococcus aureus*. *Letters in Applied Microbiology* **48**, 173-179 (2009). 1472-765X
- 84 Fayaz, A. M. *et al.* Vancomycin bound biogenic gold nanoparticles: A different perspective for development of anti VRSA agents. *Process Biochemistry* **46**, 636-641 (2011). 13595113
- 85 Shirley, A. D., Dayanand, A., Sreedhar, B. & Dastager, S. G. Antimicrobial activity of silver nanoparticles synthesized from novel *Streptomyces* species. *Digest Journal of Nanomaterials and Biostructures* **5**, 447-451 (2010)
- 86 Suresh, A. K. *et al.* Silver Nanocrystallites: Biofabrication using *Shewanella oneidensis*, and an Evaluation of Their Comparative Toxicity on Gram-negative and Gram-positive Bacteria. *Environmental Science & Technology* **44**, 5210-5215 (2010). 0013-936X
- 87 Ul'berg, Z., Podol'skaya, V., Voitenko, E., Grishchenko, N. & Yakubenko, L. Formation and biological activity of preparations based on microorganisms and colloidal silver. *Colloid Journal* **72**, 66-73 (2010). 1061-933X
- 88 Merin, D. D., Prakash, S. & Bhimba, B. V. Antibacterial screening of silver nanoparticles synthesized by marine micro algae. *Asian Pacific Journal of Tropical Medicine* **3**, 797-799 (2010). 1995-7645
- 89 Veerasamy, R. *et al.* Biosynthesis of silver nanoparticles using mangosteen leaf extract and evaluation of their antimicrobial activities. *Journal of Saudi Chemical Society* **In Press, Corrected Proof** (in press). 1319-6103
- 90 Krishnaraj, C. *et al.* Synthesis of silver nanoparticles using *Acalypha indica* leaf extracts and its antibacterial activity against water borne pathogens. *Colloids and Surfaces B: Biointerfaces* **76**, 50-56 (2010). 0927-7765
- 91 Gade, A. *et al.* Biofabrication of Silver Nanoparticles by *Opuntia ficus-indica*: In vitro Antibacterial Activity and Study of the Mechanism Involved in the Synthesis. *Current Nanoscience* **6**, 370-375 (2010). 1573-4137

- 92 Fayaz, A. M. *et al.* Biogenic synthesis of silver nanoparticles and their synergistic effect with antibiotics: a study against gram-positive and gram-negative bacteria. *Nanomedicine: Nanotechnology, Biology and Medicine* **6**, 103-109 (2010)
- 93 Fayaz, A. M., Balaji, K., Girilal, M., Kalaichelvan, P. T. & Venkatesan, R. Mycobased Synthesis of Silver Nanoparticles and Their Incorporation into Sodium Alginate Films for Vegetable and Fruit Preservation. *Journal of Agricultural and Food Chemistry* **57**, 6246-6252 (2009). 0021-8561
- 94 Veerasamy, R. *et al.* Biosynthesis of silver nanoparticles using mangosteen leaf extract and evaluation of their antimicrobial activities. *Journal of Saudi Chemical Society* **15**, 113-120 (2011). 1319-6103
- 95 Ul'berg, Z. R., Podol'skaya, V. I., Voitenko, E. Y., Grishchenko, N. I. & Yakubenko, L. N. Formation and Biological Activity of Preparations Based on Microorganisms and Colloidal Silver. *Colloid Journal* **72**, 66-73 (2010). 1061-933X
- 96 Durán, N., Marcato, P. D., De Souza, G. I. H., Alves, O. L. & Esposito, E. Antibacterial effect of silver nanoparticles produced by fungal process on textile fabrics and their effluent treatment. *Journal of Biomedical Nanotechnology* **3**, 203-208 (2007). 1550-7033
- 97 El-Rafie, M. H., Mohamed, A. A., Shaheen, T. I. & Hebeish, A. Antimicrobial effect of silver nanoparticles produced by fungal process on cotton fabrics. *Carbohydrate Polymers* **80**, 779-782 (2010). 0144-8617
- 98 Tripathi, A., Chandrasekaran, N., Raichur, A. M. & Mukherjee, A. Antibacterial Applications of Silver Nanoparticles Synthesized by Aqueous Extract of Azadirachta Indica (Neem) Leaves. *Journal of Biomedical Nanotechnology* **5**, 93-98 (2009)
- 99 Sathishkumar, M. *et al.* Cinnamon zeylanicum bark extract and powder mediated green synthesis of nano-crystalline silver particles and its bactericidal activity. *Colloids and surfaces. B, Biointerfaces* **73**, 332-338 (2009). 1873-4367 (Electronic), 0927-7765 (Linking)
- 100 Sathishkumar, M., Sneha, K. & Yun, Y.-S. Immobilization of silver nanoparticles synthesized using Curcuma longa tuber powder and extract on cotton cloth for bactericidal activity. *Bioresource Technology* **101**, 7958-7965 (2010). 0960-8524

- 101 Ravindra, S., Murali Mohan, Y., Narayana Reddy, N. & Mohana Raju, K. Fabrication of antibacterial cotton fibres loaded with silver nanoparticles via "Green Approach". *Colloids and Surfaces A: Physicochemical and Engineering Aspects* **367**, 31-40 (2010). 0927-7757
- 102 De Gusseme, B. *et al.* Virus Removal by Biogenic Cerium. *Environmental Science & Technology* **44**, 6350-6356 (2010). 0013-936X
- 103 De Gusseme, B. *et al.* Biogenic Silver for Disinfection of Water Contaminated with Viruses. *Applied and Environmental Microbiology* **76**, 1082-1087 (2010). 0099-2240
- 104 Musarrat, J. *et al.* Production of antimicrobial silver nanoparticles in water extracts of the fungus *Amylomyces rouxii* strain KSU-09. *Bioresource Technology* **101**, 8772-8776 (2010). 0960-8524
- 105 Sadhasivam, S., Shanmugam, P. & Yun, K. Biosynthesis of silver nanoparticles by *Streptomyces hygroscopicus* and antimicrobial activity against medically important pathogenic microorganisms. *Colloids and Surfaces B: Biointerfaces* **81**, 358-362 (2010). 0927-7765
- 106 Jaidev, L. R. & Narasimha, G. Fungal mediated biosynthesis of silver nanoparticles, characterization and antimicrobial activity. *Colloids and Surfaces B: Biointerfaces* **81**, 430-433 (2010). 0927-7765
- 107 Nabikhan, A., Kandasamy, K., Raj, A. & Alikunhi, N. M. Synthesis of antimicrobial silver nanoparticles by callus and leaf extracts from saltmarsh plant, *Sesuvium portulacastrum* L. *Colloids and Surfaces B: Biointerfaces* **79**, 488-493 (2010). 0927-7765
- 108 Gajbhiye, M., Kesharwani, J., Ingle, A., Gade, A. & Rai, M. Fungus-mediated synthesis of silver nanoparticles and their activity against pathogenic fungi in combination with fluconazole. *Nanomedicine: Nanotechnology, Biology and Medicine* **5**, 382-386 (2009). 1549-9634
- 109 Bankar, A., Joshi, B., Ravi Kumar, A. & Zinjarde, S. Banana peel extract mediated synthesis of gold nanoparticles. *Colloids and Surfaces B: Biointerfaces* **80**, 45-50 (2010). 0927-7765

- 110 Das, S. K., Das, A. R. & Guha, A. K. Gold nanoparticles: microbial synthesis and application in water hygiene management. *Langmuir* **25**, 8192-8199 (2009). 0743-7463 (Print), 0743-7463 (Linking)
- 111 Verma, V. C., Kharwar, R. N. & Gange, A. C. Biosynthesis of antimicrobial silver nanoparticles by the endophytic fungus *Aspergillus clavatus*. *Nanomedicine: Nanotechnology, Biology and Medicine* **5**, 33-40 (2010)
- 112 Govindaraju, K., Tamilselvan, S., Kiruthiga, V. & Singaravelu, G. Biogenic silver nanoparticles by *Solanum torvum* and their promising antimicrobial activity. *Journal of Biopesticides* **3**, 394-399 (2010)
- 113 Sun, R. W. Y. *et al.* Silver nanoparticles fabricated in Hepes buffer exhibit cytoprotective activities toward HIV-1 infected cells. *Chem. Commun.*, 5059-5061 (2005). 1359-7345
- 114 Shankar, S. S., Rai, A., Ahmad, A. & Sastry, M. Controlling the Optical Properties of Lemongrass Extract Synthesized Gold Nanotriangles and Potential Application in Infrared-Absorbing Optical Coatings. *Chemistry of Materials* **17**, 566-572 (2005). 0897-4756
- 115 Basha, K. S. *et al.* Phytochemical mediated gold nanoparticles and their PTP 1B inhibitory activity. *Colloids and Surfaces B: Biointerfaces* **75**, 405-409 (2010). 0927-7765
- 116 Moulton, M. C. *et al.* Synthesis, characterization and biocompatibility of "green" synthesized silver nanoparticles using tea polyphenols. *Nanoscale* **2**, 763-770 (2010). 2040-3364
- 117 Sun, J.-B. *et al.* Preparation and anti-tumor efficiency evaluation of doxorubicin-loaded bacterial magnetosomes: Magnetic nanoparticles as drug carriers isolated from *Magnetospirillum gryphiswaldense*. *Biotechnology and Bioengineering* **101**, 1313-1320 (2008). 1097-0290
- 118 Sundaramoorthi, C. *et al.* Biosynthesis of silver nanoparticles from *Aspergillus niger* and evaluation of its wound healing activity in experimental rat model. *International Journal of PharmTech Research* **1**, 1523-1529 (2009). 0974-4304

- 119 Zheng, B. *et al.* Gold nanoparticles-coated eggshell membrane with immobilized glucose oxidase for fabrication of glucose biosensor. *Sensors and Actuators B: Chemical* **152**, 49-55 (2011). 0925-4005
- 120 Raghunandan, D. *et al.* Anti-cancer studies of noble metal nanoparticles synthesized using different plant extracts. *Cancer Nanotechnology* **2**, 57-65 (2011). 1868-6958
- 121 Raghunandan, D. *et al.* Rapid biosynthesis of irregular shaped gold nanoparticles from macerated aqueous extracellular dried clove buds (*Syzygium aromaticum*) solution. *Colloids and Surfaces B: Biointerfaces* **79**, 235-240 (2010). 0927-7765
- 122 Satyavani, K., Gurudeeban, S., Ramanathan, T. & Balasubramanian, T. Biomedical potential of silver nanoparticles synthesized from calli cells of *Citrullus colocynthis* (L.) Schrad. *J Nanobiotechnology* **9**, 43 (2011). 1477-3155 (Electronic), 1477-3155 (Linking)
- 123 Jacob, S. J., Finub, J. S. & Narayanan, A. Synthesis of silver nanoparticles using Piper longum leaf extracts and its cytotoxic activity against Hep-2 cell line. *Colloids and surfaces. B, Biointerfaces* **91**, 212-214 (2012). 1873-4367 (Electronic), 0927-7765 (Linking)
- 124 Amarnath, K., Mathew, N., Nellore, J., Siddarth, C. & Kumar, J. Facile synthesis of biocompatible gold nanoparticles from <i>Vites vineferaCancer Nanotechnology **2**, 121-132 (2011). 1868-6958
- 125 Valodkar, M., Jadeja, R. N., Thounaojam, M. C., Devkar, R. V. & Thakore, S. Biocompatible synthesis of peptide capped copper nanoparticles and their biological effect on tumor cells. *Mater. Chem. Phys.* **128**, 83-89 (2011). 0254-0584
- 126 Venkatpurwar, V., Shiras, A. & Pokharkar, V. Porphyrin capped gold nanoparticles as a novel carrier for delivery of anticancer drug: In vitro cytotoxicity study. *International Journal of Pharmaceutics* **409**, 314-320 (2011). 0378-5173
- 127 Satyavani, K., Gurudeeban, S., Ramanathan, T. & Balasubramanian, T.. Biomedical potential of silver nanoparticles synthesized from calli cells of *Citrullus colocynthis* (L.) Schrad. *Journal of Nanobiotechnology* **9**, 43 (2011). 1477-3155

- 128 Li, X. *et al.* Purified and sterilized magnetosomes from *Magnetospirillum gryphiswaldense* MSR-1 were not toxic to mouse fibroblasts in vitro. *Letters in Applied Microbiology* **45**, 75-81 (2007). 1472-765X
- 129 Tonks, N. K. PTP1B: From the sidelines to the front lines! *FEBS Letters* **546**, 140-148 (2003). 0014-5793
- 130 Zheng, B. *et al.* Preparation of gold nanoparticles on eggshell membrane and their biosensing application. *Talanta* **82**, 177-183 (2010). 0039-9140
- 131 Kalishwaralal, K. *et al.* Biosynthesis of silver and gold nanoparticles using *Brevibacterium casei*. *Colloids and Surfaces B: Biointerfaces* **77**, 257-262 (2010). 0927-7765
- 132 Guo, S. & Wang, E. Synthesis and electrochemical applications of gold nanoparticles. *Analytica Chimica Acta* **598**, 181-192 (2007). 0003-2670
- 133 Nguyen, D. T., Kim, D. J. & Kim, K. S. Controlled synthesis and biomolecular probe application of gold nanoparticles. *Micron* **42**, 207-227 (2011). 1878-4291 (Electronic), 0968-4328 (Linking)
- 134 Jha, A. K. & Prasad, K. Ferroelectric BaTiO₃ nanoparticles: Biosynthesis and characterization. *Colloids and Surfaces B: Biointerfaces* **75**, 330-334 (2010). 0927-7765
- 135 Torres-Chavolla, E., Ranasinghe, R. J. & Alocilja, E. C. Characterization and Functionalization of Biogenic Gold Nanoparticles for Biosensing Enhancement. *Nanotechnology, IEEE Transactions on* **9**, 533-538 (2010). 1536-125X
- 136 Shilov, V., Voitenko, E., Marochko, L. & Podol'skaya, V. Electric characteristics of cellular structures containing colloidal silver. *Colloid Journal* **72**, 125-132 (2010). 1061-933X
- 137 Zheng, D., Hu, C., Gan, T., Dang, X. & Hu, S. Preparation and application of a novel vanillin sensor based on biosynthesis of Au-Ag alloy nanoparticles. *Sensors and Actuators B: Chemical* **148**, 247-252 (2010). 0925-4005
- 138 Pingarrón, J. M., Yáñez-Sedeño, P. & González-Cortés, A. Gold nanoparticle-based electrochemical biosensors. *Electrochimica Acta* **53**, 5848-5866 (2008). 0013-4686

- 139 Zheng, B. Z. *et al.* Gold nanoparticles-coated eggshell membrane with immobilized glucose oxidase for fabrication of glucose biosensor. *Sensor Actuat B-Chem* **152**, 49-55 (2011). 0925-4005
- 140 Sicard, C. *et al.* Nano-gold biosynthesis by silica-encapsulated micro-algae: a "living" bio-hybrid material. *Journal of Materials Chemistry* **20**, 9342-9347 (2010). 0959-9428
- 141 Wang, T., Yang, L., Zhang, B. & Liu, J. Extracellular biosynthesis and transformation of selenium nanoparticles and application in H₂O₂ biosensor. *Colloids and Surfaces B: Biointerfaces* **80**, 94-102 (2010). 0927-7765
- 142 Du, L., Jiang, H., Liu, X. & Wang, E. Biosynthesis of gold nanoparticles assisted by *Escherichia coli* DH5[α] and its application on direct electrochemistry of hemoglobin. *Electrochemistry Communications* **9**, 1165-1170 (2007). 1388-2481
- 143 Fayaz, M., Tiwary, C. S., Kalaichelvan, P. T. & Venkatesan, R. Blue orange light emission from biogenic synthesized silver nanoparticles using *Trichoderma viride*. *Colloid Surf. B-Biointerfaces* **75**, 175-178 (2010). 0927-7765
- 144 Sarkar, R., Kumbhakar, P. & Mlitra, A. K. Green synthesis of silver nanoparticles and its optical properties. *Digest Journal of Nanomaterials and Biostructures* **5**, 491 - 496 (2010). 1842 - 3582
- 145 Sathyavathi, R., Krishna, M. B., Rao, S. V., Saritha, R. & Rao, D. N. Biosynthesis of Silver Nanoparticles Using *Coriandrum Sativum* Leaf Extract and Their Application in Nonlinear Optics. *Advanced Science Letters* **3**, 138-143 (2010). 1936-6612
- 146 Liao, K.-S. *et al.* Strong nonlinear photonic responses from microbiologically synthesized tellurium nanocomposites. *Chemical Physics Letters* **484**, 242-246 (2010). 00092614
- 147 Fayaz, A. M., Girilal, M., Venkatesan, R. & Kalaichelvan, P. T. Biosynthesis of anisotropic gold nanoparticles using *Maduca longifolia* extract and their potential in infrared absorption. *Colloids and surfaces. B, Biointerfaces* **88**, 287-291 (2011). 1873-4367 (Electronic), 0927-7765 (Linking)
- 148 Bao, H., Hao, N., Yang, Y. & Zhao, D. Biosynthesis of biocompatible cadmium telluride quantum dots using yeast cells. *Nano Research* **3**, 481-489 (2010). 1998-0124, 1998-0000

- 149 Bao, H. *et al.* Extracellular microbial synthesis of biocompatible CdTe quantum dots. *Acta Biomater* **6**, 3534-3541 (2010). 1878-7568 (Electronic), 1742-7061 (Linking)
- 150 Kowshik, M. *et al.* Microbial synthesis of semiconductor CdS nanoparticles, their characterization, and their use in the fabrication of an ideal diode. *Biotechnology and Bioengineering* **78**, 583-588 (2002). 1097-0290
- 151 Pandian, S. R. K., Deepak, V., Kalishwaralal, K. & Gurunathan, S. Biologically synthesized fluorescent CdS NPs encapsulated by PHB. *Enzyme and Microbial Technology* **48**, 319-325 (2011). 0141-0229
- 152 Wang, Y., He, X., Wang, K., Zhang, X. & Tan, W. Barbated Skullcup herb extract-mediated biosynthesis of gold nanoparticles and its primary application in electrochemistry. *Colloids and Surfaces B: Biointerfaces* **73**, 75-79 (2009). 0927-7765
- 153 Ghoreishi, S. M., Behpour, M. & Khayat Kashani, M. Green synthesis of silver and gold nanoparticles using *Rosa damascena* and its primary application in electrochemistry. *Physica E: Low-dimensional Systems and Nanostructures* **44**, 97-104 (2011). 1386-9477
- 154 Sadhasivam, S., Shanmugam, P., Veerapandian, M., Subbiah, R. & Yun, K. Biogenic synthesis of multidimensional gold nanoparticles assisted by *Streptomyces hygroscopicus* and its electrochemical and antibacterial properties. *BioMetals*, 1-10 (2011). 0966-0844
- 155 Iskandar, F. Nanoparticle processing for optical applications - A review. *Advanced Powder Technology* **20**, 283-292 (2009). 0921-8831
- 156 Talapin, D. V., Lee, J.-S., Kovalenko, M. V. & Shevchenko, E. V. Prospects of Colloidal Nanocrystals for Electronic and Optoelectronic Applications. *Chemical Reviews* **110**, 389-458 (2009). 0009-2665
- 157 Safarik, I. & Safarikova, M. Magnetic nano- and microparticles in biotechnology. *Chemical Papers* **63**, 497-505 (2009). 0366-6352
- 158 Faivre, D. & Schüler, D. Magnetotactic Bacteria and Magnetosomes. *Chemical Reviews* **108**, 4875-4898 (2008). 0009-2665
- 159 Kundu, S., Kale, A. A., Banpurkar, A. G., Kulkarni, G. R. & Ogale, S. B. On the change in bacterial size and magnetosome features for *Magnetospirillum*

- magnetotacticum (MS-1) under high concentrations of zinc and nickel. *Biomaterials* **30**, 4211-4218 (2009). 0142-9612
- 160 Telling, N. D. *et al.* Remediation of Cr(VI) by biogenic magnetic nanoparticles: An x-ray magnetic circular dichroism study. *Applied Physics Letters* **95**, 163701-163703 (2009)
- 161 Cutting, R. S. *et al.* Optimizing Cr(VI) and Tc(VII) Remediation through Nanoscale Biomineral Engineering. *Environmental Science & Technology* **44**, 2577-2584 (2010). 0013-936X
- 162 Coker, V. S. *et al.* Microbial Engineering of Nanoheterostructures: Biological Synthesis of a Magnetically Recoverable Palladium Nanocatalyst. *ACS Nano* **4**, 2577-2584 (2010). 1936-0851
- 163 Moon, J.-W. *et al.* Large-scale production of magnetic nanoparticles using bacterial fermentation. *Journal of Industrial Microbiology & Biotechnology* **37**, 1023-1031 (2010). 1367-5435
- 164 Roh, Y., Vali, H., Phelps, T. J. & Moon, J. W. Extracellular synthesis of magnetite and metal-substituted magnetite nanoparticles. *Journal of Nanoscience and Nanotechnology* **6**, 3517-3520 (2006). 1533-4880
- 165 Staniland, S. *et al.* Controlled cobalt doping of magnetosomes in vivo. *Nat Nano* **3**, 158-162 (2008). 1748-3387
- 166 Zhu, H. *et al.* Biosynthesis of spherical Fe₃O₄/bacterial cellulose nanocomposites as adsorbents for heavy metal ions. *Carbohydrate Polymers* **86**, 1558-1564 (2011). 0144-8617
- 167 Coker, V. S. *et al.* Harnessing the Extracellular Bacterial Production of Nanoscale Cobalt Ferrite with Exploitable Magnetic Properties. *ACS Nano* **3**, 1922-1928 (2009). 1936-0851
- 168 Moon, J.-W. *et al.* Large-scale production of magnetic nanoparticles using bacterial fermentation. *Journal of Industrial Microbiology & Biotechnology* **37**, 1023-1031 (2010). 1367-5435
- 169 Yeary, L. W. *et al.* Magnetic properties of bio-synthesized zinc ferrite nanoparticles. *Journal of Magnetism and Magnetic Materials* **323**, 3043-3048 (2011). 0304-8853

- 170 Ahmad, A. *et al.* Fungus-Based Synthesis of Chemically Difficult-To-Synthesize Multifunctional Nanoparticles of CuAlO₂. *Advanced Materials* **19**, 3295-3299 (2007). 1521-4095
- 171 Ankamwar, B., Damle, C., Ahmad, A. & Sastry, M. Biosynthesis of Gold and Silver Nanoparticles Using Emblica Officinalis Fruit Extract, Their Phase Transfer and Transmetallation in an Organic Solution. *Journal of Nanoscience and Nanotechnology* **5**, 1665-1671 (2005). 1533-4880
- 172 Ankamwar, B., Chaudhary, M. & Sastry, M. Gold Nanotriangles Biologically Synthesized using Tamarind Leaf Extract and Potential Application in Vapor Sensing. *Synthesis and Reactivity in Inorganic, Metal-Organic, and Nano-Metal Chemistry* **35**, 19 - 26 (2005). 1553-3174
- 173 Haverkamp, R., Marshall, A. & Agterveld, D. Pick your carats: nanoparticles of goldsilvercopper alloy produced in vivo. *Journal of Nanoparticle Research* **9**, 697-700 (2007)
- 174 Zhou, H. *et al.* Bacteria-based controlled assembly of metal chalcogenide hollow nanostructures with enhanced light-harvesting and photocatalytic properties. *Nanotechnology* **20**, 085603 (2009). 0957-4484
- 175 Xie, J., Lee, J. Y., Wang, D. I. C. & Ting, Y. P. Silver Nanoplates: From Biological to Biomimetic Synthesis. *ACS Nano* **1**, 429-439 (2007). 1936-0851
- 176 Senapati, S., Ahmad, A., Khan, M. I., Sastry, M. & Kumar, R. Extracellular Biosynthesis of Bimetallic Au–Ag Alloy Nanoparticles. *Small* **1**, 517-520 (2005). 1613-6829
- 177 Sawle, B. D. *et al.* Biosynthesis and stabilization of Au and Au–Ag alloy nanoparticles by fungus, *Fusarium semitectum*. *Science and Technology of Advanced Materials* **9**, 035012 (2008). 1468-6996
- 178 van den Hoek, C., Mann, D. & Jahns, H. *Algae - An Introduction to Phycology*. (Cambridge University Press 1995). 9780521729833
- 179 Volcani, B. in *Silicon and siliceous structures in biological systems* (eds TL Simpson & BE Volcani) 157-200 (Springer-Verlag, 1981). 0387905928
- 180 Hildebrand, M. Biological processing of nanostructured silica in diatoms. *Progress in Organic Coatings* **47**, 256-266 (2003). 0300-9440

- 181 Foo, C. W. P., Huang, J. & Kaplan, D. L. Lessons from seashells: silica mineralization via protein templating. *Trends in Biotechnology* **22**, 577-585 (2004). 0167-7799
- 182 Kröger, N., Bergsdorf, C. & Sumper, M. Frustulins: Domain Conservation in a Protein Family Associated with Diatom Cell Walls. *European Journal of Biochemistry* **239**, 259-264 (1996). 1432-1033
- 183 van de Poll, W. H., Vrieling, E. G. & Gieskes, W. W. C. Location and expression of frustulins in the pennate diatoms *Cylindrotheca fusiformis*, *Navicula pelliculosa*, and *Navicula salinarum* (Bacillariophyceae). *Journal of Phycology* **35**, 1044-1053 (1999). 0022-3646
- 184 El Rassy, H., Belamie, E., Livage, J. & Coradin, T. Onion phases as biomimetic confined media for silica nanoparticle growth. *Langmuir* **21**, 8584-8587 (2005). 0743-7463
- 185 Hildebrand, M. Prospects of manipulating diatom silica nanostructure. *Journal of Nanoscience and Nanotechnology* **5**, 146-157 (2005). 1533-4880
- 186 Krpetic, Z., Scari, G., Caneva, E., Speranza, G. & Porta, F. Gold Nanoparticles Prepared Using Cape Aloe Active Components. *Langmuir* **25**, 7217-7221 (2009). 0743-7463
- 187 Guillard, R. R. L. & Lorenzen, C. J. Yellow-Green Algae With Chlorophyllide c. *Journal of Phycology* **8**, 10-14 (1972). 1529-8817
- 188 Kelly, K. L., Coronado, E., Zhao, L. L. & Schatz, G. C. The optical properties of metal nanoparticles: The influence of size, shape, and dielectric environment. *Journal of Physical Chemistry B* **107**, 668-677 (2003). 1520-6106
- 189 Massart, R. Preparation of aqueous magnetic liquids in alkaline and acidic media *Ieee Transactions on Magnetics* **17**, 1247-1248 (1981). 0018-9464
- 190 Šafaříková, M., Ptáčková, L., Kibriková, I. & Šafařík, I. Biosorption of water-soluble dyes on magnetically modified *Saccharomyces cerevisiae* subsp. *uvarum* cells. *Chemosphere* **59**, 831-835 (2005). 0045-6535
- 191 Holesova, S., Valaskova, M., Plevova, E., Pazdziora, E. & Matejova, K. Preparation of novel organovermiculites with antibacterial activity using chlorhexidine diacetate. *Journal of Colloid and Interface Science* **342**, 593-597 (2010). 0021-9797

- 192 Andrews, J. M. Determination of minimum inhibitory concentrations. *Journal of Antimicrobial Chemotherapy* **48**, 5-16 (2001)
- 193 Lengke, M. F., Fleet, M. E. & Southam, G. Morphology of gold nanoparticles synthesized by filamentous cyanobacteria from gold(I)-thiosulfate and gold(III)-chloride complexes. *Langmuir* **22**, 2780-2787 (2006). 0743-7463
- 194 Lengke, M. F., Fleet, M. E. & Southam, G. Biosynthesis of silver nanoparticles by filamentous cyanobacteria from a silver(I) nitrate complex. *Langmuir* **23**, 2694-2699 (2007). 0743-7463
- 195 Lengke, M. & Southam, G. Bioaccumulation of gold by sulfate-reducing bacteria cultured in the presence of gold(I)-thio sulfate complex. *Geochimica Et Cosmochimica Acta* **70**, 3646-3661 (2006). 0016-7037
- 196 Vijayakumar, P. S. & Prasad, B. L. V. Intracellular Biogenic Silver Nanoparticles for the Generation of Carbon Supported Antiviral and Sustained Bactericidal Agents. *Langmuir* **25**, 11741-11747 (2009). 0743-7463
- 197 Brayner, R. *et al.* Cyanobacteria as Bioreactors for the synthesis of Au, Ag, Pd, and Pt nanoparticles via an enzyme-mediated route. *Journal of Nanoscience and Nanotechnology* **7**, 2696-2708 (2007). 1533-4880
- 198 Lengke, M. F. *et al.* Precipitation of gold by the reaction of aqueous gold(III) chloride with cyanobacteria at 25-80 degrees C - Studied by X-ray absorption spectroscopy. *Canadian Journal of Chemistry-Revue Canadienne De Chimie* **85**, 651-659 (2007). 0008-4042
- 199 Allabashi, R., Stach, W., de la Escosura-Muñiz, A., Liste-Calleja, L. & Merkoçi, A. ICP-MS: a powerful technique for quantitative determination of gold nanoparticles without previous dissolving. *Journal of Nanoparticle Research* **11**, 2003-2011 (2009). 1388-0764
- 200 Gallardo, O. A. D. *et al.* Silver oxide particles/silver nanoparticles interconversion: susceptibility of forward/backward reactions to the chemical environment at room temperature. *RSC Advances* (2012)
- 201 Mosiniewicz-Szablewska, E., Safarikova, M. & Safarik, I. Magnetic Studies of Ferrofluid-Modified Microbial Cells. *Journal of Nanoscience and Nanotechnology* **10**, 2531-2536 (2010). 1533-4880

- 202 Vieira, A. *et al.* Adsorption of cysteine on hematite, magnetite and ferrihydrite: FT-IR, Mössbauer, EPR spectroscopy and X-ray diffractometry studies. *Amino Acids* **40**, 205-214 (2011). 0939-4451
- 203 Schröfel, A., Kratošová, G., Bohunická, M., Dobročka, E. & Vávra, I. Biosynthesis of gold nanoparticles using diatoms—silica-gold and EPS-gold bionanocomposite formation. *Journal of Nanoparticle Research* **13**, 3207-3216 (2011). 1388-0764
- 204 Lengke, M. F., Fleet, M. E. & Southam, G. Bioaccumulation of gold by filamentous cyanobacteria between 25 and 200 degrees C. *Geomicrobiology Journal* **23**, 591-597 (2006). 0149-0451
- 205 Ben-Ari, E. T. Not just slime - Beneath the slippery exterior of a microbial biofilm lies a remarkably organized community of organisms. *Bioscience* **49**, 689-695 (1999). 0006-3568
- 206 Allison, D. G., Gilbert, P., Lappin-Scott, H. M. & Wilson, M. *Community Structure and Co-operation in Biofilms*. (Cambridge University Press, 2000). 9780511754814
- 207 Flemming H. C., W. J., Mayer C., Kurstgens V., Borchard W. in *Community Structure and Co-operation in Biofilms* (ed P. Gilbert David G. Allison, H. M. Lappin-Scott, M. Wilson) (Cambridge University Press, 2000).
- 208 Flemming, H. C. & Wingender, J. Relevance of microbial extracellular polymeric substances (EPSs) - Part I: Structural and ecological aspects. *Water Science and Technology* **43**, 1-8 (2001). 0273-1223
- 209 Wimpenny, J. in *Community Structure and Co-operation in Biofilms* (ed P. Gilbert David G. Allison, H. M. Lappin-Scott, M. Wilson) (Cambridge University Press, 2000). 9780511754814
- 210 Sutherland, I. W. Biofilm exopolysaccharides: a strong and sticky framework. *Microbiology* **147**, 3-9 (2001)
- 211 Sutherland, I. W. The biofilm matrix – an immobilized but dynamic microbial environment. *Trends in Microbiology* **9**, 222-227 (2001). 0966-842X
- 212 Bhattacharya, D. & Gupta, R. K. Nanotechnology and potential of microorganisms. *Critical Reviews in Biotechnology* **25**, 199-204 (2005). 0738-8551
- 213 Kuyucak, N. & Volesky, B. Accumulation of gold by algal biosorbent . *Biorecovery* **1**, 189-204 (1989). 0269-7572

- 214 Greene, B. *et al.* Interaction of gold(I) and gold(III) complexes with algal biomass. *Environmental Science & Technology* **20**, 627-632 (1986). 0013-936X
- 215 Davis, T. A., Volesky, B. & Mucci, A. A review of the biochemistry of heavy metal biosorption by brown algae. *Water Research* **37**, 4311-4330 (2003). 0043-1354
- 216 Kröger, N., Deutzmann, R. & Sumper, M. Polycationic Peptides from Diatom Biosilica That Direct Silica Nanosphere Formation. *Science* **286**, 1129-1132 (1999)
- 217 Kroger, N., Lorenz, S., Brunner, E. & Sumper, M. Self-assembly of highly phosphorylated silaffins and their function in biosilica morphogenesis. *Science* **298**, 584-586 (2002). 0036-8075
- 218 Kroger, N., Deutzmann, R. & Sumper, M. Silica-precipitating peptides from diatoms - The chemical structure of silaffin-1A from *Cylindrotheca fusiformis*. *Journal of Biological Chemistry* **276**, 26066-26070 (2001). 0021-9258
- 219 Nam, D. H., Won, K., Kim, Y. H. & Sang, B. I. A Novel Route for Immobilization of Proteins to Silica Particles Incorporating Silaffin Domains. *Biotechnol. Prog.* **25**, 1643-1649 (2009). 8756-7938
- 220 Georgia C, P. Nanoparticle magnetism. *Nano Today* **4**, 438-447 (2009). 1748-0132
- 221 Alibeigi, S. & Vaezi, M. R. Phase Transformation of Iron Oxide Nanoparticles by Varying the Molar Ratio of Fe²⁺:Fe³⁺. *Chemical Engineering & Technology* **31**, 1591-1596 (2008). 1521-4125
- 222 Kuroda, K., Ishida, T. & Haruta, M. Reduction of 4-nitrophenol to 4-aminophenol over Au nanoparticles deposited on PMMA. *Journal of Molecular Catalysis a-Chemical* **298**, 7-11 (2009). 1381-1169
- 223 Pradhan, N., Pal, A. & Pal, T. Silver nanoparticle catalyzed reduction of aromatic nitro compounds. *Colloids and Surfaces A: Physicochemical and Engineering Aspects* **196**, 247-257 (2002). 0927-7757
- 224 Narayanan, K. B. & Sakthivel, N. Synthesis and characterization of nano-gold composite using *Cylindrocylindrium floridanum* and its heterogeneous catalysis in the degradation of 4-nitrophenol. *J. Hazard. Mater.* **189**, 519-525 (2011). 0304-3894
- 225 Lara, H., Ayala-Núñez, N., Ixtapan Turrent, L. & Rodríguez Padilla, C. Bactericidal effect of silver nanoparticles against multidrug-resistant bacteria. *World Journal of Microbiology and Biotechnology* **26**, 615-621 (2010). 0959-3993

- 226 Schröfel, A. & Kratošová, G. Vol. 5 *Fundamental Biomedical Technologies* (ed Aleš Prokop) 373-409 (Springer Netherlands, 2011). 978-94-007-1248-5

I) AUTHORS PUBLICATIONS:

Kratošová, G., **Schröfel, A.**, Seidlerová, J., Křištofová, J.: Adaptation of *Acidithiobacillus* bacteria to metallurgical wastes and its potential environmental risks, *Waste Management & Research*. 30(3): 295–301, 2012

Schröfel A., Kratošová G.: Biosynthesis of metallic nanoparticles and their application, In: Intracellular Delivery: Fundamentals and Applications (Ed: Aleš Prokop), Springer Verlag, 2011

Schröfel, A., Kratošová, G., Krautová, M., Dobročka, E., Vávra, I.: Biosynthesis of gold nanoparticles using diatoms – silica-gold and EPS-gold bionanocomposite formation, *Journal of Nanoparticle research*, 13 (8): 3207-3216, 2011, DOI: 10.1007/s11051-011-0221-6

Gardian, Z., Bumba, L., **Schröfel, A.**, Herbstová, M., Nebesářová, J., Vácha, F.: Organisation on Photosystem I and Photosystem II in red alga *Cyanidium caldarium*: encounter of cyanobacterial and higher plant concepts. *BBA-Bioenergetics*. 1767: 725-731, 2007.